

Chromosome dynamics during cell divisions in
Drosophila melanogaster:
The role of Rad21 in meiotic cohesion and dynamic
analysis of the condensin subunit CapG in early
embryonic mitotic divisions

Dissertation

zur Erlangung des Grades eines
-Doktors der Naturwissenschaften-

-Dr. rer. nat.-

der Fakultät für Biologie, Chemie und Geowissenschaften
der Universität Bayreuth

vorgelegt von

Sonal Nagarkar

Bayreuth 2010

Die vorliegende Arbeit wurde in der Zeit von Februar 2006 bis Juni 2010 an der Universität Bayreuth am Lehrstuhl für Genetik, unter der Betreuung von PD Dr. Stefan Heidmann angefertigt.

Promotionsgesuch eingereicht am: 30.07.2010

Tag des wissenschaftlichen Kolloquiums:09.12.2010

Erstgutachter: PD. Dr. Stefan Heidmann

Zweitgutachter: Prof. Dr. K.H. Hoffmann

*To,
my
Dear father*

ACKNOWLEDGEMENTS

My stay in Germany was a wonderful experience. It has been a long tumultuous journey, all during the course of this, I have been accompanied and supported by a number of people. It is a pleasure now to have the opportunity to express my gratitude to all of them.

Firstly, I would like to thank my thesis supervisor PD Dr. Stefan Heidmann, whose encouragement and guidance from the initial to the final level enabled me to develop an understanding of the subject. He has provided me with the support and freedom to explore and carry out the work presented here. I have also received many valuable criticisms from him. All the way through my graduate studies, he has been extremely helpful and motivating.

Thanks are due to Prof. Dr. Christian F. Lehner and Prof. Dr. Olaf Stemmann for their critical views and fruitful advises on my experiments. The inputs they provided at various phases of this work were very valuable. I am thankful to Doris for her constructive suggestions and support in performing some critical experiments.

I would like to thank Brigitte, Jutta and Marion for technical help in my experiments, and Petra for the delicious food supply that my flies loved. I am thankful to Margit and Petra who I always bothered whenever I had a bureaucratic problem and always helped me solving it. I am especially grateful to Sina for the critical reading of my thesis manuscript.

Sabine is a great companion in the lab, her personal and professional support during the time I stayed there was incredible. I thank her for listening to my problems and complaints, and of course for her unlimited care. Johannes, Fabian and Christian are affectionately acknowledged for scientific and non scientific discussions, and for many of our gala times. Things were always smooth and comfortable for me when they were around. Tina, Marion, Quynh Anh, Kerstin, Ayan and Evelin have been all

time pals for food and fun. I thank them all for the support and friendship that made my stay here in Germany so fantastic.

In addition, I am grateful to the members of Stemmann lab for their co-operation, helpful discussions and providing a pleasant working environment. In particular, discussions with Bernd and Mo were always enjoyable and fruitful.

Finally, I wish to express my love and gratitude to my family and friends. Shweta, Suvarna, Ashima, Madhav and above all Piyush have always been a constant source of encouragement and provided me with moral strength. I am heartily thankful to my family and in-laws for their ever-loving support, encouragement and understanding during the years of my studies and work. My parents had more faith in me than could ever be described. Their love, support and patience are the powers that drive me. My sisters Deepti and Rachana, and my brother Shivansh are my best pals and they have always shielded me from the general worries so that I could be free to focus on my work. Pratap, my brother-in-law, has always been a great source of inspiration. Special acknowledgement is also due to Manish, my husband, for his love and support and untiring encouragement. No words can express my appreciations and gratitude towards him.

I am extremely thankful to everybody who has helped me one way or the other during all this time.

Table of Contents

Summary	10
Zusammenfassung	12
Chapter I Introduction	14
1 The eukaryotic cell cycle	14
1.1 The chromosome cycle.....	17
1.1.1 DNA replication	18
1.1.2 Sister chromatid cohesion	19
1.1.2.1 The cohesin complexes in mitosis and meiosis.....	20
1.1.2.2 The molecular mechanisms of sister chromatid cohesion.....	23
1.1.2.3 Establishment of the sister chromatid cohesion.....	25
1.1.2.4 Other functions of the cohesin complex.....	26
1.1.3 Chromosome condensation	28
1.1.3.1 The condensin complexes.....	30
1.1.3.2 Localization of the condensin complexes.....	32
1.1.3.3 Regulation of the condensin complexes.....	33
1.1.3.4 Other biological functions of condensins.....	35
1.1.4 Chromosome segregation	36
1.1.4.1 Dissolution of the cohesin complex.....	36
1.1.4.2 Role of the condensin I complex in sister chromatid segregation.....	40
Aims of the thesis	41
Chapter II Results	42
2.1 Localization and dynamic analysis of the condensin I subunit CapG	42
2.1.1 Characterization of CapG-EGFP transgenic lines.....	42
2.1.2 CapG-EGFP is a biologically functional protein.....	44
2.1.3 Chromatin association profile of CapG-EGFP during mitosis.....	46
2.1.4 CapG-EGFP loading initiates at centromeres.....	49
2.1.5 CapG-EGFP shows stable association with chromatin.....	52

2.2 Analysis of a potential cohesive role for Rad21 and redundancy between Rad21 and C(2)M during female meiosis.....	54
2.2.1 Generation of <i>Rad21^{ex8}</i> and <i>c(2)M^{EP};Rad21^{ex8}</i> mutant oocytes	54
2.2.2 The Rad21-3TEV(271)-myc protein is efficiently cleaved in oocytes.....	60
2.2.3 Rad21 cleavage causes disassembly of the synaptonemal complex.....	62
2.2.4 Chromosomal localization of Smc1 in oocyte nuclei is abolished after Rad21 cleavage.....	64
2.2.5 Rad21 cleavage causes loss of cohesion between homologue chromosomes during prophase I.....	66
2.2.6 Rad21 cleavage causes homologue nondisjunction and premature sister chromatid segregation during meiosis I.....	66
2.3 Analysis of a cohesive role of C(2)M during female meiosis.....	71
2.3.1 Generation of TEV cleavable genomic C(2)M transgenic lines.....	71
2.3.2 Transgene expression and <i>in-vitro</i> cleavage of C(2)M-3TEV (191/250/339)-HA.....	72
2.3.3 Localization of C(2)M-HA and C(2)M-3TEV (191/250/339)-HA.....	73
2.3.4 The TEV cleavable C(2)M-HA variants are not biologically functional.....	74
Chapter III Discussion.....	78
Chapter IV Materials and methods.....	85
4.1 <i>Drosophila</i> lines.....	85
4.2 Quantitative analysis of loading of CapG-EGFP onto the chromatin	88
4.3 Quantitative analysis of dynamic association of fluorescently labeled condensin subunits with chromatin.....	89
4.4 Protein extraction and western blotting.....	89
4.4.1 Protein preparation from embryos.....	89
4.4.2 Protein preparation from embryos of different phases of mitosis 14.....	90
4.4.3 Protein preparation from stage 6 to stage 10 egg chambers /ovaries.....	90
4.4.4 Sample preparation and western blotting.....	90
4.5 <i>In vitro</i> cleavage assay using purified TEV protease.....	91
4.6 Mass isolation of S14 oocytes.....	91
4.7 <i>In vitro</i> activation of S14 oocytes.....	91
4.8 Cytological analysis and immunofluorescence.....	92

4.8.1 Immunostaining of embryos.....	92
4.8.2 Immunostaining of ovarioles.....	93
4.8.3 Immunostaining of S14 oocytes.....	93
4.9 Fluorescent in situ hybridization on S14 oocytes.....	94
4.10 Genomic DNA preparation from single flies.....	95
4.11 Cloning.....	95
4.12 Construction of HA tagged TEV protease cleavable <i>c(2)M</i> transgenes.....	96
4.13 Construction of UASP1-TEV-V5 strains.....	98
4.14 Inverse PCR.....	98
4.15 DNA isolation from agarose gel with DEAE membrane.....	99
4.16 Microscopy and Image processing.....	100
4.17 Solutions.....	100
4.18 Antibodies.....	103
4.19 Primers	104
Chapter V Abbreviations.....	106
Chapter VI References.....	109
<i>Curriculum vitae</i>.....	128

Summary

Faithful segregation of genetic material is an essential hallmark of cell division. In eukaryotic cells, the DNA is replicated during S phase into two identical copies, which reside intimately paired (cohesed) in the nucleus as dispersed and entangled interphase chromatin fibers. At the onset of mitosis, the chromatin fibers start to resolve and by the end of metaphase they are compacted and individualized into a pair of cylindrical structures called sister chromatids, which remain connected until anaphase onset by residual sister chromatid cohesion in their centromeric regions. The compaction process is known as chromosome condensation, which is a prerequisite for accurate segregation of sister chromatids in anaphase. Chromosome condensation and sister chromatid cohesion require multisubunit protein complexes, the condensin and the cohesin complexes, respectively. Both complexes are composed of two core SMC subunits and a set of non-SMC subunits, which are conserved among most eukaryotes.

In the first part of my thesis, I have analyzed the localization and dynamic behavior of a functional, EGFP-fused variant of CapG, one of the non-SMC subunits of the condensin I complex in *Drosophila melanogaster*. *In vivo* fluorescence microscopy of early embryonic mitotic divisions revealed that CapG-EGFP is mainly nuclear during interphase and that it starts to enrich at centromeric proximal regions in late interphase. Thereafter, CapG-EGFP spreads onto the chromosome arms concomitantly with the initiation of chromosome condensation (ICC) and loading is complete already in prophase at the time of nuclear envelope breakdown. Furthermore, FRAP analyses revealed that a major proportion of CapG-EGFP is stably bound to chromatin during metaphase and only a minor fraction shows a dynamic association with chromatin. These results are similar, but not identical, to findings previously obtained for another non-SMC subunit, CapH/Barren, suggesting interactions of the individual non-SMC subunits with chromatin outside a *bona fide* condensin complex.

Since a non-SMC cohesin subunit homologous to the typical meiotic Rec8 protein found in other eukaryotes appears to be missing in *Drosophila*, I have assessed in the second part of my thesis a possible cohesive role for the mitotic subunit Rad21 during female meiosis. Furthermore, a potential redundancy during oogenesis between Rad21 and another candidate cohesin subunit, C(2)M, was analyzed. Forced proteolysis of

Rad21 during oogenesis resulted in delocalization of the canonical cohesin core subunit Smc1 from oocyte chromatin. Furthermore, immunofluorescence and fluorescence *in situ* hybridization analyses revealed a high proportion of premature homolog disjunction and premature sister chromatid separation in the developing mutant oocytes and also during the meiotic divisions. Moreover, it was established that Rad21 has a role in the maintenance of the synaptonemal complex (SC), as shown by delocalization of the transversal SC component C(3)G. Taken together, these results suggest that Rad21 is indeed involved in sister chromatid cohesion during female meiosis in *D. melanogaster*. Since in the absence of Rad21 and the concomitant presence of C(2)M meiotic sister chromatid cohesion is compromised, Rad21 appears to play the major role in meiotic sister chromatid cohesion in *D. melanogaster* and a functional redundancy between C(2)M and Rad21 is unlikely.

Zusammenfassung

Die akkurate Verteilung des genetischen Materials ist ein wesentliches Merkmal der Zellteilung. In eukaryontischen Zellen werden während der DNA Replikation zwei identische Kopien der DNA erzeugt, die zunächst in der Interphase eng gepaart als dekondensierte und miteinander verwickelte Chromatinfasern vorliegen. Zu Beginn der Mitose werden die Chromatinfasern entwirrt und kondensiert, bis sie am Ende der Metaphase als individualisierte zylindrische Strukturen vorliegen, die bei höheren Eukaryonten als so genannte Schwesterchromatiden lichtmikroskopisch sichtbar werden. Lediglich im Zentromerbereich werden sie noch durch Schwesterchromatiden-Kohäsion zusammen gehalten. Der Prozess der Chromosomenkondensation ist eine Voraussetzung für die korrekte Segregation der Schwesterchromatiden in der folgenden Anaphase. Chromosomenkondensation und Schwesterchromatiden-Kohäsion beruhen auf der Aktivität der Multiproteinkomplexe Kondensin und Kohäsin. Beide Komplexe bestehen aus je zwei Kern-SMC Untereinheiten und einer Gruppe von nicht-SMC Untereinheiten, die innerhalb der meisten Eukaryonten konserviert sind.

Im ersten Teil meiner Arbeit habe ich die Lokalisation und das dynamische Verhalten einer biologisch funktionellen EGFP-markierten Variante von CapG untersucht, einer nicht-SMC Untereinheit des Kondensin I-Komplexes aus *Drosophila melanogaster*. Fluoreszenzmikroskopische Analysen von frühen mitotischen Teilungen in *Drosophila*- Embryonen zeigten, dass CapG-EGFP in der Interphase nukleär angereichert ist und in der späten Interphase anfängt, präferentiell an zentromere Bereiche zu lokalisieren. Mit dem Beginn der Chromosomenkondensation breitet sich CapG-EGFP entlang der Chromosomenarme aus, und die maximale Chromatinassoziation ist bereits in der Prophase zum Zeitpunkt der Auflösung der Kernhülle erreicht. Weiterhin ergaben FRAP-Analysen, dass während der Metaphase ein großer Anteil des CapG-EGFP stabil ans Chromatin gebunden ist, und nur ein kleiner Teil dynamisch mit dem Chromatin assoziiert ist. Diese Ergebnisse sind ähnlich, wenn auch nicht identisch, wie Resultate einer früheren Studie zur Lokalisation und Dynamik einer andern nicht-SMC Kondensin I Untereinheit (CapH/Barren). Dieser Sachverhalt legt Interaktionen der einzelnen nicht-SMC

Untereinheiten mit dem Chromatin außerhalb eines kanonischen Kondensin-Komplexes nahe.

In *Drosophila* ist bisher kein Homolog zu der meiotischen nicht-SMC Kohäsion-Untereinheit Rec8 identifiziert worden, während in anderen Eukaryonten solche Homologe in den meisten Fällen beschrieben wurden. Deswegen habe ich im zweiten Teil meiner Arbeit eine mögliche Rolle der mitotischen nicht-SMC Kohäsion-Untereinheit Rad21 in der Schwesterchromatiden-Kohäsion während der weiblichen Meiose untersucht. Zusätzlich wurde eine mögliche funktionelle Redundanz zwischen Rad21 und C(2)M abgeklärt, welches als weiteres Kandidatenprotein für eine meiotische Kohäsion-Untereinheit diskutiert wird. Erzwungene Proteolyse von Rad21 während der Oogenese hat eine Delokalisation der kanonischen Kern-Kohäsion-Untereinheit Smc1 vom Chromatin der Oozyte zur Folge. Weiterhin zeigten Immunfluoreszenzanalysen und Fluoreszenz in situ-Hybridisierungs-Experimente einen hohen Anteil von frühzeitiger Trennung der homologen Chromosomen und frühzeitiger Schwesterchromatidentrennung in der sich entwickelnden Oozyte sowie während der meiotischen Teilungen. Darüber hinaus deutet die Delokalisation von C(3)G, einer transversalen Komponente des synaptonemalen Komplexes, auf eine Rolle von Rad21 bei der Aufrechterhaltung des synaptonemalen Komplexes hin. Zusammengefasst legen die Ergebnisse nahe, dass Rad21 in der Tat bei der Schwesterchromatiden-Kohäsion während der Meiose in *D. melanogaster* Weibchen eine wesentliche Rolle spielt. Dagegen scheint Rad21 nicht redundant mit C(2)M zu sein, da die Abwesenheit von Rad21 auch in der Präsenz von C(2)M zu klaren Kohäsionsdefekten führt.

Chapter I Introduction

1. The eukaryotic cell cycle

Every cell, except terminally differentiated ones, undergoes cell division and gives rise to two genetically identical daughter cells. The cell cycle is a series of events in which a cell grows, duplicates its genetic material and this genetic material is then partitioned into two newly formed daughter cells. Precise regulation of the chromosome cycle is critical since mistakes may lead to aneuploidy which can result in cancer in multicellular organisms. The eukaryotic cell cycle can be divided into two major functional phases, S and M phase, and two preparatory gap phases G₁ and G₂. In S phase a cell replicates its genomic DNA into two identical copies; subsequently these fully replicated chromosomes are segregated to each of the two daughter nuclei during M phase. The G₁ phase precedes S phase, whereas G₂ phase precedes M phase. G₁ and G₂ provide the time required for growth of the cell and synthesis of all cellular components needed to support the following phase. The G₁, S and G₂ phases together are referred to as interphase. The M phase is itself composed of two tightly coupled events, mitosis and cytokinesis.

Mitosis is the process by which all somatic cells of a multicellular organism multiply; it distributes duplicated chromosomes into daughter nuclei. Mitosis can be divided into five distinct sub-phases; prophase, prometaphase, metaphase, anaphase and telophase (Fig 1.1). In interphase, chromosomes are dispersed in the nucleus as morphologically indistinguishable chromatin fibers. During prophase these chromatin fibers begin to condense, and in late prophase each chromosome forms two identical coiled filaments (sister chromatids). Both sister chromatids are joined throughout their length and contain a constricted region, the centromere. The centrioles migrate to opposite poles and at the same time the assembly of the mitotic spindle is initiated by formation of asters of microtubules around centrosomes. Centrosomes are specialized organelles that constitute the microtubule organizing centers (MTOCs) in animal cells). In higher eukaryotes, nuclear envelope breakdown (NEBD) marks the end of prophase and entry into prometaphase. In this phase, the mitotic spindle is fully assembled and captures the chromosomes at the outer surface of the kinetochore (a protein complex that assembles on centromeric DNA). The chromosomes initially

attach to the spindle fibres from a single pole (mono-orientation) and then the sister chromatids become attached to microtubules emanating from opposite poles (bi-orientation). When all the chromosomes are attached to the spindle, they start to move towards the center and align on the equatorial plane of the cell during metaphase.

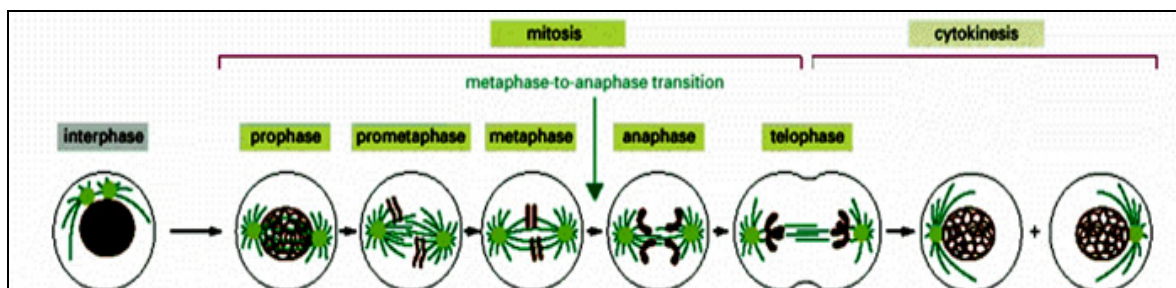


Figure 1.1 Schematic representation of different phases of the eukaryotic cell cycle. G₁, S and G₂ phase are referred to as interphase. During interphase chromatin is decondensed, in prophase chromosomes start to condense and centrosomes move towards the opposite poles. In prometaphase nuclear envelope breakdown and chromosomes are captured by microtubules. All the chromosomes are aligned at the metaphase plate during metaphase takes place. At the onset of anaphase sister chromatids separate and migrate to the opposite poles. At the end of mitosis (telophase), the chromatin starts to decondense, the mitotic spindle disassembles and the nuclear membrane re-forms around each of the daughter nuclei. Subsequently the cell divides into two daughter cells by cytokinesis. Chromatin is shown in brown, microtubules in dark green and centrosomes in light green (Adapted from Alberts et al., 2002).

Once all the chromosomes are aligned at the metaphase plate and all sister kinetochores are attached to the spindle from opposite poles, the two sister chromatids of all chromosomes start to separate simultaneously. Segregation of sister chromatids occurs in anaphase, when the spindle fibres from opposite poles pull the individual sister chromatids towards the spindle pole which they face. In telophase the sister chromatids reach the opposite poles and decondense, the mitotic spindle disassembles, and the nuclear envelope begins to form around each set of sister chromatids, resulting in two daughter nuclei (fig. 1.1). During the last stages of mitosis a cleavage furrow starts to appear on the cell surface. It is a contractile ring composed of actin filaments, myosin II, and many structural and regulatory proteins. The furrow rapidly deepens and completely divides the cell into two new daughter cells during cytokinesis (fig. 1.1).

In contrast to mitosis by which a somatic cell divides, meiosis is a specialized kind of process by which one diploid cell divides twice and forms four haploid daughter

cells. In multicellular organisms meiosis is restricted to the germ cells. The reduction in ploidy is achieved by a single round of DNA replication followed by two rounds of nuclear division (meiosis I and II). In meiosis I the homologue chromosomes form pairs and then segregate into two daughter cells, while in meiosis II the two sister chromatids separate from each other. Each meiotic division can be divided in four phases; prophase, metaphase, anaphase and telophase.

The first meiotic division (meiosis I) starts once pre meiotic DNA replication is complete. It begins with a long prophase, which can be sub-divided into five distinct stages; leptotene, zygotene, pachytene, diplotene, and diakinesis, on the basis of chromosome morphology. The chromosomes are visible as thin threads during the leptotene and side by side pairing of homologue chromosomes starts during zygotene. After pairing, the homologues are tightly linked at the sites of recombination by a process called synapsis. During synapsis a ribbon shaped protein scaffold, called the synaptonemal complex (SC) forms along the entire length of the paired chromosomes (Fawcett, 1956; Moses, 1956). The SC is composed of one central element, two lateral/axial elements and several transverse filaments (Schmekel et al., 1993). The main function of the SC is to keep the homologues in juxtaposition during chromosome pairing. It is also involved in homologous recombination and the proper segregation of chromosomes (Egel, 1995; Sym and Roeder, 1994; von Wettstein, 1984). At pachytene the homologues are fully synapsed and they begin to condense. Several cross-overs form during this stage to facilitate the exchange of genetic material whereby double strand breaks (DSB) are introduced into the two juxtaposed chromatids of the homologous chromosomes and the chromatids are re-joined in a cross wise fashion with their paired partners. By the end of diplotene, recombination between homologues is completed. The SC starts to disassemble, leaving the chromosomes linked at the specific sites of crossing over called chiasmata. At diakinesis, chromosomes become fully condensed, the nuclear envelope disappears, the spindle forms and the chromosomes migrate to the center of the cell to form the metaphase plate. In metaphase I all chromosomes align at the metaphase plate. The homologues orient in opposite direction, while the two sister chromatids remain mono-oriented. At anaphase I, chiasmata resolve and the homologues separate but the sister chromatids remain associated at their centromeres.

By the end of telophase I, the homologues reach opposite poles and start to decondense. Meiosis II starts after a brief interkinesis, during which the chromosomes elongate and decondense, and the nuclear membrane re-forms. Meiosis II resembles mitosis. In prophase II chromosomes condense again and migrate towards the center of the cell. At metaphase II, the sister chromatids bi-orient and align at the metaphase plate. At anaphase II, the two sister chromatids separate followed by telophase II and cytokinesis, which results in the formation of four haploid cells. In some organisms meiosis is specifically modified. For example in mammals, the number of gametes obtained from meiosis differs between males and females. In males, four haploid spermatids of similar size are produced during meiotic divisions while in females, the meiotic cytoplasmic divisions are very asymmetric. As a consequence, only one functional oocyte is obtained from each female meiotic event. The other three haploid cells are pinched off from the oocyte as polar bodies. Moreover, in many animal species, oocytes arrest in either metaphase I or II as a common and unique feature. In *Drosophila*, mature oocytes arrest in metaphase-I until fertilization takes place.

1.1 The chromosome cycle

Eukaryotic cells inherit their genome in the form of chromosomes. The fundamental aspect of cell division is to accurately pass all the genetic information, stored in DNA, to the daughter cells. During the cell cycle, the chromosomes undergo a series of dynamic structural and functional changes, which permit faithful duplication of the genome and its stable inheritance. The chromosome cycle involves four major stages; DNA replication, sister chromatid cohesion, chromosome condensation and chromosome segregation. These events are coordinated with each other to achieve the highly regulated and faithful duplication and segregation of the genetic information. During G1, the cell is transcriptionally very active and synthesizes many structural proteins and enzymes required for DNA replication. Therefore, during this phase chromosomes are present as dispersed chromatin fibers. After G1, the cell enters S phase, in which DNA is replicated concomitantly with establishment of cohesion between the two newly synthesized sister chromatids. In M phase, chromosome condensation starts in prophase and finally the two sister chromatids are accurately segregated to the two daughter cells in anaphase.

1.1.1 DNA Replication

During S phase, the entire genome of a cell is duplicated. Accurate replication of DNA is essential for maintaining viability and genetic integrity of the cell. DNA replication occurs in a semiconservative way in which each of the two DNA strands serves as a template for the formation of the two new strands and each of the two daughter cells inherits one new DNA strand and one old DNA strand organized in a double helix. Replication starts at replication origins. In the unicellular eukaryote *Saccharomyces cerevisiae*, these replication origins are specific consensus sequences called autonomously replicating sequences (ARS) (Brewer and Fangman, 1987; Stinchcomb et al., 1979). In higher eukaryotes, there are no defined consensus sequences reported, although origins are often found to be located in promoter regions. (Cadoret et al., 2008; Sequeira-Mendes et al., 2009).

For preparation of DNA replication, the so called prereplicative complex (pre-RC) is assembled at a replication origin during G1. The assembly of pre-RC starts when the origin bound, six -subunit protein complex ORC (Origin Recognition Complex) (Bell and Stillman, 1992) recruits Cdc6 (Cell division cycle 6) and Cdt1 (chromatin licensing and DNA replication factor 1) to the origin. Once the ORC-Cdc6-Cdt1 complex has formed at the origin, it recruits the Mcm2–7 complex. The Mcm2–7 complex is a heterohexamer of six related ‘minichromosome maintenance’ proteins (Bowers et al., 2004; Donovan et al., 1997; Nishitani et al., 2000; Randell et al., 2006; Tanaka et al., 1997). The Mcm2–7 complex unravels the DNA helix at the replication origin and then travels along with the replication machinery to unwind DNA at the replication fork (Ishimi, 1997; Labib et al., 2000). After unwinding, the separated DNA strands are then captured by replication protein A, a single strand binding protein, which prevents reannealing of the two strands. Each strand is then primed for replication by primase. Because two template DNA strands run in opposite directions, the elongation process is different for the 5'-3' and 3'-5' template. One strand (the leading strand) is synthesized continuously in the direction of progression of replication fork, and the other strand is synthesized discontinuously in short DNA fragments (Okazaki fragments), which are later joined by the DNA ligase. The Mcm2–7 complex disassembles when one replication fork encounters another replication fork heading towards it, which results in termination of the replication.

For maintaining genomic stability DNA replication should occur only once per cell cycle, which is achieved by preventing the replicated DNA from becoming re-licensed. To prevent re-licensing, the loading of new Mcm2–7 complex is inhibited during late G1, S, G2 and early M phase by down regulating the activity of the ORC–Cdc6–Cdt1 complex. During S phase, activated Cyclin-dependent-kinases (cdks) cause phosphorylation of Cdc6, Cdt1 and ORC, which targets them for ubiquitylation and subsequent proteolysis, thereby preventing assembly of the pre-RC (Drury et al., 1997; Nguyen et al., 2001; Weinreich et al., 2001; Li et al., 2004). In budding yeast, Cdk dependent phosphorylation leads to nuclear export of Mcm2-7 and Cdt1, which prevents these proteins to gain access to DNA (Labib et al., 1999; Tanaka and Diffley, 2002).

1.1.2 Sister chromatid cohesion

During S phase the cell synthesizes two copies of each chromosome which are only later distributed into daughter cells during cell division. Synthesis of the two copies in S phase and their distribution in M phase is separated by a considerably long G2 phase, during which they should be prevented from drifting away from each other. For this purpose the replicated sister chromatids are maintained tightly paired, from the time of their synthesis in S phase until the onset of anaphase in mitosis or meiosis II. This interaction is called sister chromatid cohesion. It is essential for the mechanism that orients the two sister kinetochores of the two sister chromatids such that they segregate to opposite poles of the cell during anaphase. Two mechanisms are known to be involved in sister chromatid cohesion. The first, DNA catenation, is the intertwining of duplicated DNA molecules which occur during S phase when two adjacent replication forks encounter during replication (Murray and Szostak, 1985; Sundin and Varshavsky, 1980). However, it is highly unlikely that DNA catenation alone holds the two sister chromatids together as most of the DNA catenation is resolved by the enzyme Topoisomerase II by the time metaphase takes place, so it has only a small contribution to the sister chromatid cohesion after this point (DiNardo et al., 1984). It has also been shown in yeast that the cohesion between sister minichromosomes is maintained even in the absence of DNA catenation (Koshland and Hartwell, 1987). The second mechanism, by which sister chromatid cohesion is maintained, involves a

multisubunit protein complex called the cohesin complex. The cohesin complex can mediate cohesion even in the absence of catenation (Ivanov and Nasmyth, 2007). Numerous studies have also shown that the cohesin complex is the key player of sister-chromatid cohesion and is essential for chromosome segregation (Guacci et al., 1997; Losada et al., 1998; Michaelis et al., 1997).

1.1.2.1 The Cohesin complexes in mitosis and meiosis

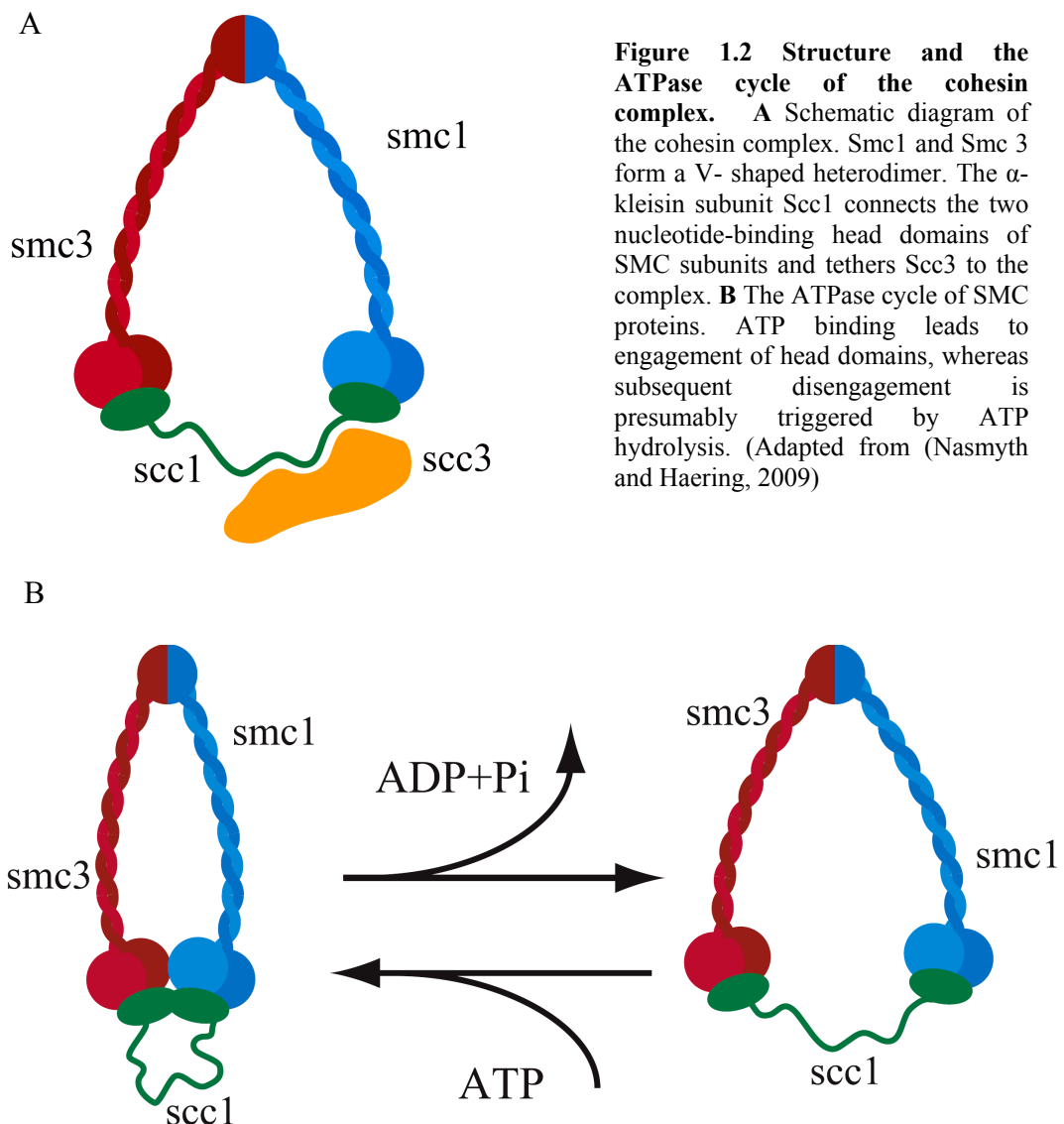
It is well established that the DNA catenation is not sufficient for sister chromatid cohesion and that is solely mediated by the cohesin complex. Cohesin is a heterotetrameric complex, consisting of Smc1, Smc3, Scc1 (Rad21/Mcd1) and Scc3. These subunits were first identified in *S. cerevisiae* by several genetic screens for mutants that show precocious sister chromatid segregation. In a genetic study in *S. cerevisiae*, it was shown that the Smc1 protein is required for proper segregation of chromosomes (Strunnikov et al., 1993). In another genetic screen, mutants of a gene called *mcd1* were identified. These mutants were defective in sister chromatid cohesion and chromosome condensation (Guacci et al., 1997). An independent screen revealed three chromosomal proteins Smc1p, Smc3p and Scc1p (identical to Mcd1) which were essential for sister chromatid cohesion: (Michaelis et al., 1997). Further physical and genetic interactions were shown between Smc1p and Mcd1 (Rad21/Scc1) (Guacci et al., 1997). Orthologs of all four subunits have been found in many eukaryotes and most of them have been shown to be involved in sister chromatid cohesion (Losada et al., 1998; Pasierbek et al., 2001; Sonoda et al., 2001).

The structure and topology of these subunits have been best characterized in budding yeast (Haering et al., 2002; Haering et al., 2004). The two core Smc subunits, Smc1 and Smc3 belong to the “Structural Maintenance of Chromosomes” (SMC) family of proteins. Proteins of the SMC family are highly conserved in all organisms including both bacteria and archaea (Losada and Hirano, 2005; Soppa, 2001). The SMC proteins are large polypeptides (900 – 1,300 amino acids) with a unique domain structure. Each N and C terminal domains contains a nucleotide-binding motif, known as the Walker A and Walker B motifs respectively. The terminal domains are separated by two long coiled coil segments connected by a non helical sequence. The two 45 nm long coiled coil segments fold back onto themselves through antiparallel

coiled-coil interactions, forming a central “hinge” domain at one end and a globular “head” domain composed of N- and C-terminal domains at the other end (Melby et al., 1998; Saitoh et al., 1994). In the globular head domain, the Walker A motif of the N-terminal domain and Walker B motif of the C-terminal domain form a functional ATPase of the ABC (ATP binding cassette) family (Lowe et al., 2001). Two monomers of SMC proteins associate with each other at the hinge domain and form a V-shaped dimer (Anderson et al., 2002; Haering et al., 2002) (fig. 1.2). In prokaryotes, the SMC proteins form homodimers. In eukaryotes, different SMC proteins form heterodimers, as in case of cohesin, which contains a Smc1/Smc3 heterodimer (Haering et al., 2002), and condensin, which contains a Smc2/Smc4 heterodimer (Hirano et al., 1997) (see chapter 2.3.1). The third cohesin subunit Scc1 (Sister-chromatid cohesion1)/Rad21/Mcd1 is a member of the α -kleisin family of proteins (Schleiffer et al., 2003). It bridges the ATPase heads of Smc1 and Smc3 (Fig. 1.2 A). The N terminus of Scc1 binds to the ATPase head domain of Smc3 and the C terminus binds to the ATPase head domain of Smc1, forming a large triangular ring of 35 nm diameter (Gruber et al., 2003). A fourth subunit of the cohesin complex, called Scc3 (Sister-chromatid cohesion3) is further associated with Scc1 (fig. 1.2 A). Scc3 is a HEAT (Huntingtin, Elongation factor 3, the A subunit of protein phosphatase 2A, TOR lipid kinase) repeats containing protein (Neuwald and Hirano, 2000). These repeats are involved in protein-protein interactions. Higher eukaryotes contain two closely related mitotic Scc3 homologues, called stromalin antigens 1 and 2 (SA1 and SA2), which are expressed in a mutually exclusive manner (Carramolino et al., 1997; Losada et al., 2000; Sumara et al., 2000). Although the role of Scc3 is not clear, it could be involved in regulating the ring’s opening and/or its persistence.

In somatic cells, the cohesin complex consists of the four canonical subunits mentioned above, but in germ cells, distinct meiosis-specific subunits have been characterized in various organisms. Studies in budding and fission yeast have shown that during meiosis, Scc1 is replaced by a meiosis-specific α -kleisin paralog called Rec8 (Klein et al., 1999; Watanabe and Nurse, 1999). Orthologs of Rec8 have been characterized in several organisms (Cai et al., 2003; Pasierbek et al., 2001; Xu et al., 2005).

Meiotic isoforms of other cohesin subunits have also been characterized in various organisms. In mammals, paralogs of Smc1, Scc1/Rad21/Mcd1 and SA1/SA2 are called Smc1 β , Rec8 and STAG3, respectively (Parisi et al., 1999; Pezzi et al., 2000; Revenkova et al., 2001). In fission yeast meiotic cells, two orthologs of Scc3, Psc3 and Rec11 have been found, (Kitajima et al., 2003).



The *Drosophila* genome appears to lack a clear Rec8 homolog. A refined bioinformatics analysis revealed the synaptonemal complex (SC) protein C(2)M as a member of the α -kleisin family (Schleiffer et al., 2003). It associates with lateral

elements of the SC and promotes the normal organization of the transversal synaptonemal complex component C(3)G during female meiotic prophase (Manheim and McKim, 2003). Since C(2)M is expressed in the female germline and C(2)M mutants exhibit an elevated rate of non-disjunction events, C(2)M is an attractive candidate for the Rec8 homolog in *Drosophila*, despite its low level of conservation. Furthermore, C(2)M was shown to be associated with SMC3 (Heidmann et al., 2004). However, C(2)M protein does not localize to meiotic chromatin early enough and disappears from chromosomes long before the first meiotic division. Moreover, inactivation of C(2)M causes less severe defects during meiosis than Rec8 deletion in yeast and *C. elegans*. These observations suggest that C(2)M might not be the one and only functional Rec8 homologue involved in sister chromatid cohesion during meiosis (Heidmann et al., 2004).

This conclusion allows the formation of three hypotheses, one postulating that Rad21, which is the *Drosophila* homologue of Scc1/Mcd1, might be responsible for sister chromatid cohesion during meiosis or a partial redundancy exists between C(2)M and Rad21, which some other organisms exhibit at low levels during meiosis (Parra et al., 2004; Prieto et al., 2002; Xu et al., 2004). Alternatively, as a 3rd hypothesis, a completely different protein is involved. From now on, Scc1/Rad21/Mcd1 will be referred to as just Rad21.

1.1.2.2 The molecular mechanism of sister chromatid cohesion

After the discovery of the cohesin complex, the ring or embrace model was proposed for sister chromatid cohesion. According to this model, the interaction between DNA and cohesin is topological and the cohesin complex holds one or both sister chromatids inside the ring (Gruber et al., 2003; Haering et al., 2002; Ivanov and Nasmyth, 2007). Based on the ring model, three models have been proposed for sister chromatid cohesion: The one cohesin ring model, the handcuff model and the bracelet model. The **one cohesin ring model** is the most accepted model. It suggests that only one cohesin ring traps the two sister chromatids inside (fig. 1.3 A). The cohesin ring has a diameter of around 35 nm: this size is large enough for encircling two sister chromatids as 10-nm nucleosomal chromatin fibers.

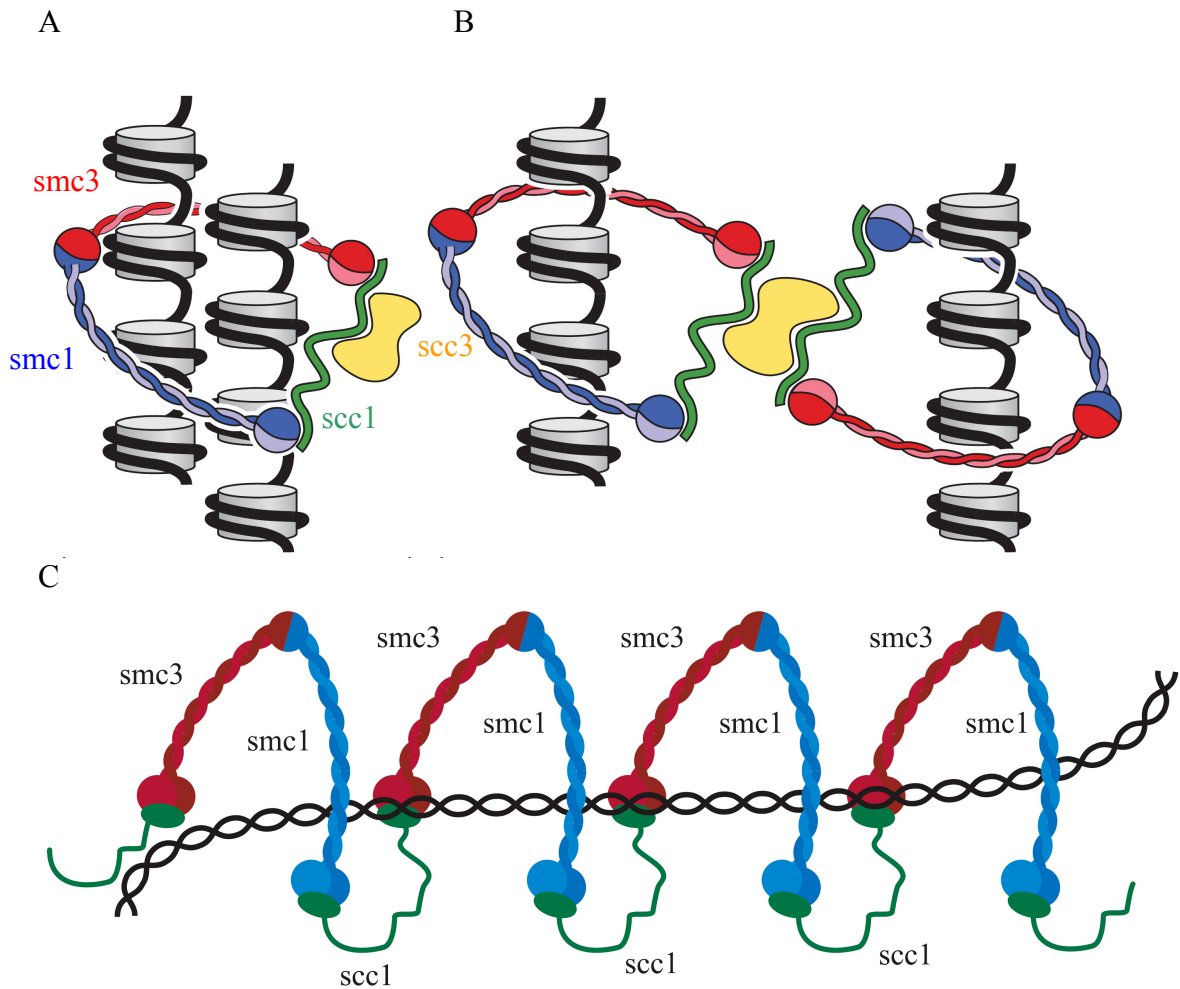


Figure 1.3 Models for sister chromatid cohesion. The one cohesin ring model (A), in which a single ring of cohesin complex topologically entraps the sister chromatids inside. B The handcuff model, involving association of two tripartite Smc1/Smc3/Scc1 rings by a single Scc3 subunit and C The bracelet model which suggest that chromatin-bound cohesins form oligomeric filaments which entrap the sister chromatids. (Adapted from Nasmyth and Haering, 2009)

The model also proposed that after ATP hydrolysis, the head domains of Smc1 and Smc3 disengage which might cause opening of the ring (fig. 1.2 B). This opening of the ring allows the two sister chromatids to enter the ring. The ring would re-close upon binding of a new ATP molecule, which leads to engagement of head domains (Gruber et al., 2003; Haering et al., 2002). However two recent reports, the first presenting biochemical studies using bacterial SMC proteins (Hirano and Hirano,

2006) and a second of work in yeast (Gruber et al., 2006) showed that it is the hinge domain which mediates the entrapment of DNA. It has also been proposed that the energy created either by ATP hydrolysis or by binding to the head domains might be used to open the hinge, for review see (Nasmyth and Haering, 2009).

According to **the handcuff model**, the holo-cohesin complex contains two single cohesin rings. Each Smc1-Smc3 heterodimer of the two rings embraces one of the two sister chromatids and the Scc3 protein connects the two SMC heterodimers by which individual cohesin complexes become paired (fig. 1.3 B). The embracement of sister chromatids takes place during DNA replication (Chang et al., 2005; Huang and Moazed, 2006; Milutinovich and Koshland, 2003; Zhang et al., 2008b).

In the **bracelet model**, sister chromatid cohesion is mediated by several cohesin complexes arranged in a filament like structure (bracelet) (fig. 1.3 C). The head domains of two different Smc heterodimers interact via Scc1/Rad21/Mcd1, forming multimeric filaments which entrap the sister chromatids (Huang et al., 2005). Although several observations are consistent with this model, definitive experimental evidence supporting the bracelet model is lacking.

1.1.2.3 Establishment of sister chromatid cohesion

Several studies reveal that in vertebrates, the loading of cohesin starts at the end of telophase (Darwiche et al., 1999; Gerlich et al., 2006b; Losada et al., 1998), while in yeast, cohesin starts to load in late G1 phase (Guacci et al., 1997; Michaelis et al., 1997). Chromatin immunoprecipitation (ChIP) experiments indicated that loading of cohesin starts at specific sites on chromosome arms called cohesin attachment regions (CARs) (Blat and Kleckner, 1999; Tanaka et al., 1999) and at pericentromeric regions (Megee and Koshland, 1999; Tanaka et al., 1999). Although loading of cohesin continues until anaphase, sister chromatid cohesion is established only in S phase, following DNA replication (Lengronne et al., 2006; Uhlmann and Nasmyth, 1998). Cohesin loading is a highly regulated process, which involves several factors. Studies in *S. cerevisiae* (Ciosk et al., 2000), *Drosophila* (Gause et al., 2008), *Xenopus* egg extracts (Gillespie and Hirano, 2004) and in mammalian cells (Watrin et al., 2006) suggest that the Scc2/Scc4 complex is an important protein complex for the loading of

cohesin complex on chromatin. However, how this complex promotes the loading of the cohesin complex is unclear. It might act by stimulating the ATPase activity of cohesin, which allows opening of the hinge domain. Loading of the cohesin complex also depends on the formation of the prereplicative complex. The Scc2/Scc4 complex is recruited by Cdc7/Drf1 kinase at the prereplicative complex (Takahashi et al., 2008; Takahashi et al., 2004). Once Scc2/Scc4 is recruited to the chromatin, it in turn recruits the cohesin complex (Takahashi et al., 2004). After the loading of cohesin onto chromatin, an acetyl transferase, Eco1 stabilizes the cohesin complex in most of the eukaryotes until its dissolution in anaphase (Horsfield et al., 2007; Ivanov et al., 2002; Toth et al., 1999). Eco1 is recruited to replication forks, probably through an interaction with the DNA polymerase processivity factor PCNA (Moldovan et al., 2006). Eco1 acetylates two evolutionary conserved lysine residues within the head domain of the cohesin subunit Smc3 during DNA replication when the fork passes the cohesin binding sites (Rolef Ben-Shahar et al., 2008; Rowland et al., 2009; Unal et al., 2008; Zhang et al., 2008a). Smc3 acetylation remains high throughout G2 and mid M phase, and starts to decrease at the end of anaphase (Rolef Ben-Shahar et al., 2008). These studies indicate that cohesin establishment depends on Smc3 acetylation during DNA replication. This suggests that newly produced cohesin subunits cannot be acetylated during G2 and M phases and thus cannot establish sister chromatid cohesion. This is the reason why sister chromatid cohesion is established only during S phase.

1.1.2.4 Other functions of the cohesin complex

Cohesin, beside its role in sister chromatid cohesion, is implicated in many other biological functions like double stranded break (DSB) repair in meiosis and mitosis, mono-orientation of the sister kinetochores in meiosis I and transcriptional regulation of many genes in several organisms. The role of the cohesin complex in DNA damage repair was first discovered in *Schizosaccharomyces pombe*. Rad21 mutants showed sensitivity to radiation and defects in DSB repair (Birkenbihl and Subramani, 1992). Several other studies showed that mutations in cohesin subunits cause a greater sensitivity to radiation and DNA damaging agents (Kim et al., 2002; Schar et al., 2004). These findings suggested that cohesin is involved in the repair of DSBs in

mitosis (Sjogren and Nasmyth, 2001) and in meiosis (Ellermeier and Smith, 2005; Klein et al., 1999). Genetic experiments in budding yeast also showed that proteins, which are required for loading and establishment of cohesion, are also required for DNA damage repair (Sjogren and Nasmyth, 2001; Strom et al., 2004; Unal et al., 2004). For example in Eco1/Ctf7 mutants, which are defective in DSB repair, the assembly of the cohesin complex is normal (Unal et al., 2007). This observation implies that requirement of cohesin in DNA repair depends on its ability to establish sister chromatid cohesion. Based on these observations it was proposed that the cohesion complex holds the two sister chromatids in close proximity, thus enabling the broken DNA ends to find and invade their sister sequences, thereby allowing homologous recombination (Sjogren and Nasmyth, 2001). Furthermore, the involvement of cohesin complex in the SC assembly has also been reported in many organisms (Bannister et al., 2004; Eijpe et al., 2000; Klein et al., 1999; Molnar et al., 1995; Revenkova et al., 2004).

Analysis of Rec8 mutants in *S. pombe* (Watanabe and Nurse, 1999), in maize (Yu and Dawe, 2000) and *Arabidopsis* (Chelysheva et al., 2005) revealed equational division in meiosis I instead of reductional division. These studies indicated a role of the cohesin complex in mono-orientation of the sister kinetochores in meiosis I. It has also been shown that the mitotic cohesin localizes mainly to regions close to the centromere but not at the core centromere, while in meiosis, the cohesin complex localizes to the core centromere as well (Pidoux and Allshire, 2004). Based on this observation, a model was proposed according to which cohesion present at the core centromere and at the pericentromeric regions play distinct roles in defining the orientation of kinetochores. Cohesion established at the core centromere joins the two sister kinetochores together, allowing them to orient towards the same pole (mono-orientation) (Sakuno and Watanabe, 2009), while cohesin localization to the pericentromeric regions allows flexibility for biorientation of the kinetochores.

Cohesion's role in transcription regulation and development has also been studied in different organisms from yeast to human. The first indication of cohesin being involved in gene regulation came from genetic studies in budding yeast. In *S. cerevisiae*, Smc1 and Smc3 act as boundary elements and are essential to limit the spreading of the transcriptionally silent HMR mating type locus (Donze et al., 1999).

In zebrafish, the Smc3 and Scc1 subunits control the expression of the *runx1* gene during early embryonic development (Horsfield et al., 2007). In *Drosophila*, inactivation of the cohesin complex in mushroom-body γ -neurons causes defects in axon pruning due to reduction in expression of EcR-B1 within γ -neurons (Pauli et al., 2008). In human cells, the SA2 (Scc3) subunit acts as a transcriptional co-activator. It activates the multimeric NF-kappa B transcription factor by enhancing the expression of the transactivation domain of p65/RelA (Lara-Pezzi et al., 2004).

1.1.3 Chromosome condensation

For equal segregation of genetic material into two daughter cells, DNA present in interphase nuclei undergoes a highly dynamic process called chromosome condensation. It is an essential process in which dispersed and entangled interphase chromatin fibers are resolved and compacted into morphologically distinguishable compact structures, the mitotic chromosomes with individualized sister chromatids.

Eukaryotic genomic DNA is packaged into nucleosomes, which are composed of DNA and two molecules each of the four histones (H2A, H2B, H3, and H4) assembled into an octamer (Eickbush and Moudrianakis, 1978). Approximately 1.65 turns of DNA wrap around the exterior of the histone octamer to form the nucleosomal core particle. This packaging of DNA into nucleosomes creates a 10-nm chromatin fiber (Richmond et al., 1984). Further binding of a fifth histone (H1) to the nucleosome gives rise to a more condensed and higher-order structure, the 30-nm fiber (Oudet et al., 1975; Suau et al., 1979), but the relevance of the 30-nm fiber is still controversial (Robinson et al., 2006; van Holde and Zlatanova, 1995). Moreover histone H1 was found to be hyperphosphorylated during mitosis (Boggs et al., 2000; Fischer and Laemmli, 1980). After these two discoveries, it was thought that histone H1 has an important role in chromosome condensation. However, later it was shown that the chromosomes can condense even in the absence of H1 hyperphosphorylation (Guo et al., 1995). Furthermore, when histone H1 is depleted from *Xenopus* egg extract (Ohsumi et al., 1993), or when the H1 gene is disrupted in *Tetrahymena* (Shen et al., 1995), mitotic condensation was unperturbed. These pieces of evidence argue against a role of H1 in chromosome reorganization and condensation, however, in a recent report, it was shown that the core histone amino termini appear to play a critical role in

chromosome condensation (de la Barre et al., 2000), which supports the role of histone H1 in chromosome condensation.

As the cell progress further into mitosis, the 30 nm fiber again compacts another 200- 500 fold to achieve the final 10,000-20,000 fold compaction of a metaphase chromosome. Two models have been suggested for higher organization of chromosomes; the coiled/radial loop model and the hierarchical folding model. According to **coiled/radial loop model**, radially organized 30-nm chromatin fibers anchor to an axial chromosome scaffold (Marsden and Laemmli, 1979; Paulson and Laemmli, 1977). This scaffold is formed by several nonhistone proteins, including topoisomerase II (Earnshaw and Heck, 1985; Gasser et al., 1986; Lewis and Laemmli, 1982) and the protein Smc2 (Lewis and Laemmli, 1982; Saitoh et al., 1994), which is a core subunit of the condensin complexes. Moreover, it was shown that the anchoring of these loops to the chromosome scaffold occurs at specific AT rich DNA sequences, called scaffold associated region (SAR) DNA sequences (Mirkovitch et al., 1984; Razin, 1996). Later *in-vivo* studies revealed that the two scaffold proteins topoisomerase II and Smc2 did not localize to the axis of chromatin until late prophase, when chromosome compaction was nearly complete (Kireeva et al., 2004; Maeshima and Laemmli, 2003). Furthermore, experiments indicated that even after the depletion/knockdown of topoisomerase II (Carpenter and Porter, 2004; Sakaguchi and Kikuchi, 2004) and Smc2 (Hudson et al., 2003) chromosomes apparently condense normally. These observations argue against the coiled/radial loop model, in which a core protein scaffold supports the chromosomal mechanical properties.

The second model is the **hierarchical folding model**, in which the 10-nm and 30-nm chromatin fibers are proposed to fold either regularly or irregularly into distinct 100nm fibers folding motifs (Sedat and Manuelidis, 1978; Zatsepina et al., 1983) (Belmont et al., 1987). These motifs are then helically coiled to form the metaphase chromosomes. In contrast to the coiled/radial loop model, in the hierarchical model, chromosome condensation does not depend on formation of a core protein scaffold (Belmont and Bruce, 1994; Belmont et al., 1987; Sedat and Manuelidis, 1978; Zatsepina et al., 1983).

Based on the discovery that chromosome compaction is a gradual process and many intermediate stages of condensed chromosomes can exist until chromosomes are completely condensed another model, the **hierarchical folding axial glue model** of

chromosome structure was proposed. According to this model, the hierarchical folding of chromatin drives the compaction in early mitosis, whereas in later mitosis the shape and compaction of the chromosomes are stabilized by condensins and other proteins (Kireeva et al., 2004).

1.1.3.1 The condensin complexes

The mitotic chromosomes are composed of approximately equal masses of DNA, histones and non histone proteins. An earlier study has shown that after the extraction of the histone fraction from the mitotic chromosomes, a non soluble protein fraction called chromosome scaffold proteins can still maintain the structure of mitotic chromosomes (Adolph et al., 1977). In the chromosome scaffold fraction, one of the most abundant proteins found was Smc2 (Lewis and Laemmli, 1982; Saitoh et al., 1994). Moreover, immunofluorescence analysis showed that the Smc2 protein localizes to mitotic chromosomes (Kireeva et al., 2004; Maeshima and Laemmli, 2003). These observations suggested that the Smc2 protein might provide a structural backbone within the chromosome. Further biochemical studies in *Xenopus* egg extract indicated that immunodepletion of XCAP-C and XCAP-E (*Xenopus* chromosome associated proteins C and E, later termed as Smc4 and Smc2, respectively) caused defects in chromosome condensation (Hirano and Mitchison, 1994). In agreement with this, genetic studies in yeast also suggested that the SMC proteins are essential for mitotic chromosome dynamics *in vivo* (Saka et al., 1994; Strunnikov et al., 1995). A subsequent biochemical study revealed that the two proteins XCAP-C and XCAP-E form a pentameric complex with three other XCAP subunits: XCAP-D2, XCAP-G and XCAP-H (Hirano et al., 1997). As this complex was able to promote chromosome condensation *in vitro*, it was termed as “**condensin complex**”. The condensin complex is able to introduce positive supercoils into DNA in an ATP hydrolysis-dependent manner in the presence of topoisomerase I (Kimura and Hirano, 1997) and topoisomerase II (Kimura et al., 1999). Moreover, an *in vitro* electron spectroscopic imaging (ESI) study indicated that a single condensin complex is sufficient to introduce two or more supercoils into protein free DNA (Bazett-Jones et al., 2002) which further supported an instrumental role of condensin in chromosome condensation.

The canonical condensin complex, **condensin I** was isolated from *Xenopus* egg extracts (Hirano et al., 1997). Soon after the discovery of the condensin I complex, a second condensin complex, **condensin II** was identified in HeLa cells (Ono et al., 2003). The condensin II complex shares the same SMC core subunits (Smc2/Smc4) with condensin I, but contains three different non-SMC subunits Cap-D3, Cap-G2 and Cap-H2 (Fig 1.4). The two core SMC proteins are ATPases (Hirano, 2006; Hirano and Mitchison, 1994; Strunnikov et al., 1995) and their activity is essential for condensin function (Hudson et al., 2008; Stray and Lindsley, 2003). Two of the non SMC subunits of each complex, Cap-D2/D3 and Cap-G/G2 contain HEAT repeats (Neuwald and Hirano, 2000) and the third non SMC subunit Cap-H/H2, belong to the kleisin family of proteins (Schleiffer et al., 2003). Depletion of subunits of both the complexes in *Xenopus* and HeLa cells causes distinct morphological defects, suggesting that these complexes may contribute differently to mitotic chromosome architecture (Ono et al., 2003).

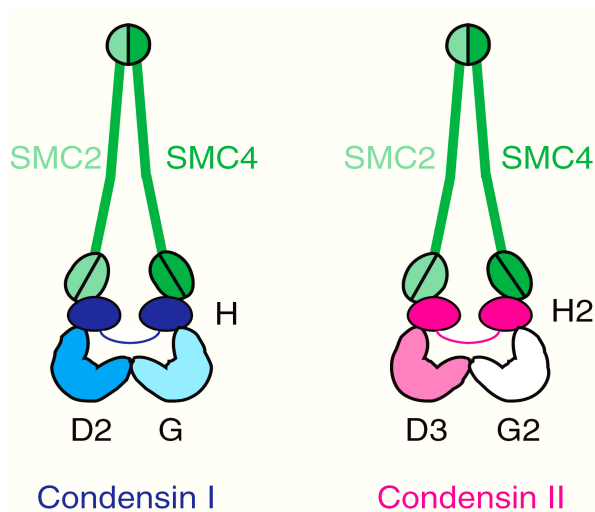


Figure 1.4 Architecture of the condensin complexes. Condensin complexes are composed of two core SMC subunits Smc2 and Smc4 and a set of three non SMC subunits CapD2, CapG and CapH in condensin I and CapD3, CapG2 and CapH2 in condensin II. Adapted from (Hirano, 2005)

In most higher eukaryotes both condensin complexes have been reported (Ono et al., 2003; Yeong et al., 2003), whereas yeast contains only condensin I. In *Drosophila*, condensin I has been reported, and homologues for Cap-D3 and Cap-H2 have also

been found but no homologue of Cap-G2 has been identified so far. A third condensin like complex known as **dosage compensation complex** (DCC) has been reported only in nematodes. It is involved in the reduction of transcription of X-linked genes during dosage compensation in hermaphrodites (Lieb et al., 1998). The DCC is composed of an Smc2 homologue, an Smc4 variant called DPY-27 and two closely related non SMC variants (Chuang et al., 1994; Hagstrom et al., 2002).

Previous studies have revealed that the Smc2 and Smc4 subunits form a heterodimer, which adopts a closed- arm “lollipop” like conformation (Anderson et al., 2002; Yoshimura et al., 2002). The non SMC subunits Cap-H and Cap-H2 link the ATPase head domains of both SMC subunits to each other and to both non SMC subunits (Onn et al., 2007). Although the architecture of condensin complex is now well studied, the topology of condensin interaction with chromosomes is still unknown.

The initial characterization of condensin complexes in yeast (Freeman et al., 2000; Lavoie et al., 2000; Saka et al., 1994; Strunnikov et al., 1995), *Xenopus* (Hirano et al., 1997) and vertebrate cells (Hirota et al., 2004) has shown that condensin complexes play a crucial role in mitotic chromosome organization. However, studies in several multicellular organisms and tissue culture cells revealed that chromosome compaction was almost normal in the absence of condensin subunits. Studies in *Drosophila* revealed that the condensin mutants and RNAi treated S2 cells achieve normal levels of chromosome compaction during mitosis, but they display strong defects in chromosome segregation during anaphase (Bhat et al., 1996; Coelho et al., 2003; Dej et al., 2004; Jager et al., 2005; Oliveira et al., 2005; Savvidou et al., 2005; Steffensen et al., 2001). Similarly in *C.elegans*, depletion of condensin subunits does not lead to any chromosome condensation defects during metaphase (Hagstrom et al., 2002). This suggests the existence of an alternate mechanism which ensures chromosome condensation prior to metaphase.

1.1.3.2 Localization of the condensin complexes

Spatial and temporal distribution of the two condensin complexes during the cell cycle has been shown to vary among different eukaryotes. In *S. cerevisiae*, the single

condensin complex is constitutively nuclear throughout the cell cycle (Bhalla et al., 2002; Freeman et al., 2000). However, in *S. pombe*, the condensin subunits are cytoplasmic during interphase, and transported into the nucleus during mitosis in a mitosis-specific phosphorylation dependent manner (Sutani et al., 1999). In *Drosophila*, different condensin I subunits behave differently. The core SMC subunit Smc4, was shown to be both nuclear and cytoplasmic during interphase (Steffensen et al., 2001), while the non SMC subunit Barren (Cap-H), is mainly cytoplasmic during interphase (Oliveira et al., 2007). Both subunits start to concentrate on chromatin during prophase, localize to the axial core of chromosomes during metaphase and anaphase and delocalize from chromatin in telophase (Oliveira et al., 2007; Steffensen et al., 2001). The non SMC subunit Cap-D2, is nuclear throughout interphase. It was found to be present on chromosome axes during mitosis and it remains associated with chromosomes as they decondense late in mitosis similar to Cap-H/ Barren and Smc4 (Savvidou et al., 2005). Studies in vertebrate cells showed that condensin I can mainly be found in the cytoplasm, whereas condensin II is nuclear during interphase. Condensin I gains access to the chromosomes only after nuclear envelope break down (NEBD) in prometaphase, while condensin II associates with chromatin during early prophase (Hirota et al., 2004; Ono et al., 2004). Both condensin complexes were found to be present at centromeres and axially along chromosome arms during metaphase, and have distinct alternating patterns as well as some regions of overlap along the chromosome arms (Ono et al., 2003). Similar to vertebrate cells, in plants it was found that condensin I is mainly located in the cytoplasm, whereas condensin II was in the nucleus during interphase (Fujimoto et al., 2005). Based on these observations it was proposed that the two condensin complexes might contribute in a mechanistically distinct fashion to mitotic chromosome architecture.

1.1.3.3 Regulation of the condensin complexes

During the cell cycle, chromosomal targeting and the assembly of condensin complexes are regulated by different factors. Initial studies in *Xenopus* egg extracts revealed that the non SMC subunits of condensin I are hyper-phosphorylated by Cdc2/Cdk1 in a mitosis specific manner and this phosphorylation is required for the supercoiling of DNA, as well as for the condensation of mitotic chromosomes *in vitro*

(Hirano et al., 1997; Kimura et al., 1998). Further *in vitro* experiments have shown that treatment with kinase inhibitors compromises condensin loading in mitotic extracts, whereas phosphatase inhibitors enhance condensin loading in interphase extracts (Hirano et al., 1997). In *S. pombe* the acid residue T19 of Cut3 (Smc4 homologue) is phosphorylated by Cdc2 kinase and this phosphorylation is required for mitotic accumulation of condensin components in the nucleus (Sutani et al., 1999). The human condensin I complex, however, remains phosphorylated throughout the cell cycle (Takemoto et al., 2004). In HeLa cells, Smc4, and all three non SMC subunits showed similar levels of phosphorylation in mitotic and non-mitotic cells. Phospho-epitope mapping revealed that different phosphorylation sites are used in interphase and mitosis (Takemoto et al., 2006; Takemoto et al., 2004). *In-vitro* studies also showed that human condensin I is phosphorylated by Cdc2/Cdk1 in mitosis (Kimura et al., 2001) and by CK2 in interphase (Takemoto et al., 2006). This phosphorylation by CK2 suppresses DNA supercoiling activity, which indicates that condensin I is negatively regulated by CK2 (Takemoto et al., 2006). Earlier studies revealed that the regulatory subunit of phosphatase 2A (PP2A) interacts with the condensin II subunit hHCP-6/hCap-D3 (Takemoto et al., 2009; Yeong et al., 2003) and targets the condensin II complex to chromosomes (Takemoto et al., 2009). When the cells progress further through anaphase, PP2A dephosphorylates hCap-D3, thereby regulating the condensin II complex (Takemoto et al., 2009). Taken together these observations suggest that the chromosomal targeting and loading of condensins could be regulated by kinases/phosphatases.

In addition to Cdk1 and CK2, Aurora B kinase has also been shown to play an important role in recruitment of condensin complexes in some organisms. In *Drosophila*, depletion of aurora B leads to failure in targeting of Barren (Cap-H) to the chromatin (Giet and Glover, 2001). Similarly in *C. elegans*, depletion of aurora B kinase prevents the association of core subunits of condensin complexes Mix1 (Smc2) and Smc4 with chromatin (Hagstrom et al., 2002). In vertebrates, aurora B kinase regulates the association of condensin I, but not condensin II, with chromatin (Lipp et al., 2007). A study in *Drosophila* revealed that the histone kinase Nhk1 is required for the loading of condensin onto meiotic chromosomes in oocytes (Ivanovska et al., 2005). Though so far, it is not known whether these kinases directly phosphorylate

one of the condensin subunits, or whether their action on a different substrate is a prerequisite for condensin targeting.

1.1.3.4 Other biological functions of condensins

An elegant series of genetic and biochemical studies showed that condensin is required for maintaining proper centromere structure and kinetochore-microtubule interactions. In *S. cerevisiae* (Yong-Gonzalez et al., 2007), *C. elegans* (Hagstrom et al., 2002) *Xenopus* egg extracts (Wignall et al., 2003) and HeLa cells (Ono et al., 2004; Samoshkin et al., 2009) depletion of condensin caused severe defects in kinetochore-microtubule interactions, merotelic attachment of spindles and aberrant chromosome alignment and segregation. Moreover in several studies it was discovered that condensin subunits localize to centromeric chromatin and interact with centromeric proteins (Hagstrom et al., 2002; Jager et al., 2005; Nakaseko et al., 2001; Ono et al., 2004). Based on these observations, it was proposed that condensins might regulate the proper assembly of centromeric heterochromatin and help in the orientation of sister kinetochores. When this process is compromised, abnormal interactions between kinetochores and microtubules are observed.

The condensin complexes also play crucial roles in organization of meiotic chromosomes. In *S. cerevisiae*, condensin subunits localize to the axial core of pachytene chromosomes and contribute to their compaction and individualization (Yu and Koshland, 2003). These results are consistent with finding from *Arabidopsis* (Siddiqui et al., 2003), *C. elegans* (Chan et al., 2004) and *Drosophila* (Resnick et al., 2009). Recent studies also revealed that condensin is required for the resolution of the synaptonemal complex in meiosis I and perhaps as well for the segregation of sister chromatids in meiosis II (Resnick et al., 2009; Yu and Koshland, 2003).

Accumulating lines of evidence suggest that, apart from mitosis and meiosis, condensin complexes have important functions in gene regulation and chromosome stability. In *S. cerevisiae*, defects in condensin function interfere with silencing of certain genes. For example, yeast *ysc-4* (Cap-D2) mutants fail to repress the expression of the mating type loci, *HML α* (Bhalla et al., 2002). Another study in *S. cerevisiae* revealed that the SMC subunit *Smc2p* is involved in the locus-specific transcriptional

repression of the three silent domains rDNA, telomere-proximal regions, and mating-type loci. Condensin bound at rDNA is required for nucleolar organization and for localization of the silencing protein Sir2p at the telomere and rDNA. Partial loss in condensin function perturbs this organization and enhances spreading of silent chromatin within the rDNA; this in turn attracts Sir2p from telomeres to rDNA and consequently alters the strength of silencing in both loci (Machin et al., 2004).

Two independent studies in *Drosophila* revealed that the non SMC subunits of condensin I are involved in transcriptional repression. The first report indicated a role of Cap-G in transcriptional repression of the centromere-proximal heterochromatic region (Dej et al., 2004) and in a second study it was shown that Barren/Cap-H interacts with polycomb group protein (Lupo et al., 2001). Both proteins colocalize at polycomb response elements and cooperate to maintain the silenced state of homeotic genes (Lupo et al., 2001). Apart from gene regulation, the condensin I complex also plays an important role in DNA repair and the DNA damage checkpoint response in *S. pombe* (Aono et al., 2002) and in *S. cerevisiae* (Yu and Koshland, 2003). More recently, an interaction between human condensin I, DNA nick-sensor poly (ADP-ribose) polymerase I and the base excision repair (BER) factor XRCC1 complex was reported. It was also shown that condensin I is recruited at DNA damage sites, and depletion of condensin I *in vivo* compromises single stranded break repair (Heale et al., 2006).

1.1.4 Chromosome segregation

Proper segregation of chromosomes is essential for maintaining the integrity of the genome. Chromosome segregation is triggered by the dissolution of sister chromatid cohesion once the sister chromatids are individualized and condensed. After the dissolution of cohesion, they dissociate from each other and start to move to opposite poles of the cell.

1.1.4.1 Dissolution of the cohesin complex

In most of the eukaryotic cells, dissociation of cohesin complexes from chromosomes occurs in a two-step manner during mitosis. In the first step known as

the prophase pathway, the bulk of cohesin complex is removed from the chromosome arms during prophase (Losada et al., 1998; Sumara et al., 2000; Waizenegger et al., 2000). Several studies have shown that this process is facilitated by a mitotic kinase called polo-like kinase 1 (Plk1) (Hauf et al., 2005; Lenart et al., 2007; Losada et al., 2002; Sumara et al., 2000). Plk1 phosphorylates the C-terminal domain of the Scc3 homolog SA1/SA2 (Hauf et al., 2005). This phosphorylation is believed to be responsible for cohesion removal from chromosomes. However, the exact mechanism is still unknown. The two proteins Wapl (wings apart-like) and Pds5 have also been reported to play a direct role in unloading cohesin during prophase. Wapl is a cohesin-binding protein. It was reported in HeLa cells that Wapl facilitates cohesin's removal from chromosome arms during prophase (Gandhi et al., 2006). Wapl depleted cells arrest in prometaphase with chromosomes that display poorly resolved sister chromatids with a high level of cohesin still attached to chromatin (Gandhi et al., 2006; Kueng et al., 2006). Initial studies in yeast showed that Pds5 is required for the maintenance of sister chromatid cohesion during G2 phase (Hartman et al., 2000; Panizza et al., 2000). Recent studies showed that Wapl interacts with Pds5 (Gandhi et al., 2006) and this interaction regulates the release of cohesin from chromosomes in *Xenopus* egg extract (Shintomi and Hirano, 2009). Mechanistically, it was proposed that the Wapl-Pds5 complex modulates conformational changes in cohesin to make it competent for dissociation from chromatin during prophase (Shintomi and Hirano, 2009).

Although a major proportion of the cohesin complex is removed from chromosome arms by the prophase pathway, a small population of cohesin remains protected at centromeres until all chromosomes are correctly bioriented in metaphase. This protection is mainly accomplished by members of the “shugoshin” family. Shugoshins are centromere specific proteins. The first member of the shugoshin family MEI-S332, was found in *Drosophila* (Kerrebrock et al., 1995; Tang et al., 1998) and subsequently identified in yeast (Katis et al., 2004) and vertebrates (Kitajima et al., 2005; McGuinness et al., 2005). Subsequent studies showed that shugoshin associates with protein phosphatase 2A (PP2A) and colocalizes with it at centromeres (Kitajima et al., 2005; Tang et al., 2006). Based on these observations, it was proposed that shugoshin

recruits PP2A to the centromere, which keeps centromeric cohesin hypophosphorylated thereby preventing its dissociation in prophase during mitosis.

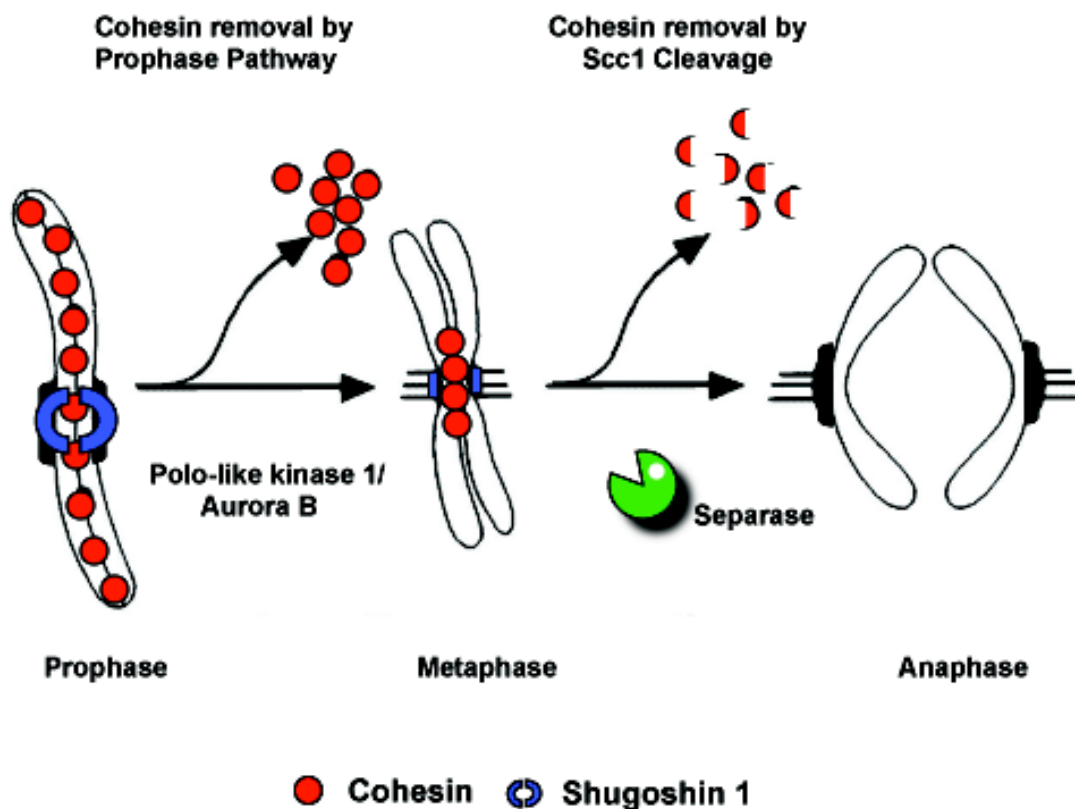


Figure 1.5 Dissolution of cohesin during mitosis. During mitosis cohesin is removed in two-steps. In the first step, the majority of cohesin is removed from chromosome arms in prophase via a pathway called prophase pathway. In this pathway the cohesin subunit Scc3 is phosphorylated by Polo-like kinase 1/ aurora B which leads to opening of the cohesin ring. At this stage the centromeric cohesion is protected by a protein called shugoshin 1. At the onset of anaphase, separase gets activated and cleaves the Scc1 subunit of the cohesin complex thereby removing residual cohesin complexes from centromeres.

The small fraction of cohesin which remains in the centromeric regions is released at the metaphase-to-anaphase transition (Sumara et al., 2000). Removal of centromeric cohesion is triggered by a protease called **separase** (Waizenegger et al., 2000), which specifically cleaves the α -kleisin subunit of the cohesin complex thereby separating the sister chromatids in anaphase (Buonomo et al., 2000; Ciosk et al., 1998; Hauf et al., 2001; Uhlmann et al., 1999). Separase is kept inactivated until the metaphase-to-

anaphase transition by an anaphase inhibitor called securin (Leismann et al., 2000; Yamamoto et al., 1996; Zou et al., 1999). Before the metaphase-to-anaphase transition securin forms a complex with separase and inhibits its activity (Ciosk et al., 1998; Leismann et al., 2000; Zou et al., 1999).

Once all the chromosomes are correctly bioriented and the mitotic check point (which monitors whether all the chromosomes are aligned at the metaphase plate and are under bipolar tension) is turned off at the onset of metaphase, securin is degraded by ubiquitin-dependent proteolysis mediated by the anaphase promoting complex (APC) (Cohen-Fix et al., 1996; King et al., 1996). After securin degradation, Separase cleaves the Scc1 subunit of the cohesin complex and triggers sister chromatid separation. However, several studies indicate that securin mediated inhibition is not the only mechanism for separase inhibition. Securin depleted yeast (Alexandru et al., 1999) and human cells (Jallepalli et al., 2001) undergo normal anaphase. Furthermore, securin knockout mice are viable (Mei et al., 2001). Subsequent studies suggested a second mechanism, which depends on inhibitory phosphorylation of separase by Cdk1-cyclin B1 and phosphorylation dependent binding of Cdk1-cyclin B1 to separase, which plays a crucial role in separase inhibition until anaphase (Gorr et al., 2005; Stemmann et al., 2001).

The removal of the cohesin complex during meiosis was reported to be separase dependent in most of the organisms studied (Buonomo et al., 2000; Gorr et al., 2006; Kudo et al., 2006; Salah and Nasmyth, 2000; Terret et al., 2003). During meiosis I, cohesin is removed from the chromosome arms at the metaphase I to anaphase I transition which allows terminalization of chiasmata and subsequent segregation of homologous chromosomes. The centromeric cohesin complex remains associated with paired sister chromatids until the onset of anaphase II (Moore and Orr-Weaver, 1998). Members of the shugoshin family protect the removal of this cohesin around centromeres during meiosis I by recruiting protein phosphatase 2A (PP2A) to centromeric regions (Katis et al., 2004; Kerrebrock et al., 1995; Kitajima et al., 2004; Kitajima et al., 2006; Riedel et al., 2006; Tang et al., 1998). This maintenance of cohesion between sister chromatids is required for a faithful reductional division during meiosis. Thereafter, this residual cohesin is cleaved by a second wave of separase activity during meiosis II.

1.1.4.2 Role of condensin I complex in sister chromatid segregation

In many organisms, condensin loss results in chromosome segregation defects during anaphase (Bhat et al., 1996; Coelho et al., 2003; Dej et al., 2004; Gerlich et al., 2006a; Jager et al., 2005; Oliveira et al., 2005; Ono et al., 2004; Savvidou et al., 2005; Steffensen et al., 2001). Later it was also shown that condensin I facilitates the removal of cohesin from chromosomes during mitosis (Hirota et al., 2004) and meiosis (Yu and Koshland, 2005). Furthermore, in yeast condensin regulates the dissolution of cohesin-independent chromosome linkages at repeated DNA in a Cdc14 dependent manner (D'Amours et al., 2004; Sullivan et al., 2004a). Recent studies have also revealed that the segregation defect occurring during anaphase is due to the premature loss of compact organization of chromosomes in early anaphase (Gerlich et al., 2006a; Vagnarelli et al., 2006). These pieces of evidence suggest that condensin complexes play a crucial role in chromosomes segregation.

Aims of the thesis

To gain a comprehensive insight into the localization and dynamic behavior of the condensin I complex subunits, the first part of this thesis was aimed to analyze the dynamic behavior of CapG using a fully functional EGFP-tagged CapG protein. To this end, several genomic and UAS transgenic lines were characterized and the intracellular localization pattern of CapG-EGFP was studied during early embryonic mitotic divisions. After determining the biological functionality of CapG-EGFP, a complete profile of CapG-EGFP loading was determined and the loading initiation sites were investigated. Furthermore, the dynamic properties of chromatin-associated CapG-EGFP were analyzed using Fluorescence Recovery after Photobleaching (FRAP) experiments. The results were compared with studies performed previously using a functional EGFP-tagged variant of the condensin I α -kleisin subunit CapH/Barren.

The second part of the thesis was aimed to elucidate a possible cohesive role for the mitotic cohesin subunit Rad21 during meiosis in *Drosophila* females. As C(2)M is discussed as another candidate cohesin subunit in *Drosophila*, a potential redundancy between Rad21 and C(2)M was analyzed during oogenesis. For this purpose, *Rad21^{ex8}* and *C(2)M^{EP};Rad21^{ex8}* mutant oocytes were generated by forced cleavage of a functional Rad21 variant containing engineered cleavage sites for the tobacco etch virus protease. To investigate the involvement of Rad21 in cohesion between sister chromatids during meiosis, homolog disjunction and premature sister chromatid segregation was scrutinized in *Rad21^{ex8}* and *C(2)M^{EP};Rad21^{ex8}* mutant oocytes during oogenesis and the meiotic divisions. Moreover, the question was addressed whether Rad21 plays a role in the maintenance of the synaptonemal complex during prophase I.

Chapter II Results

2.1 Localization and dynamic analysis of the condensin I subunit CapG

In order to analyze the localization of CapG and its association dynamics with chromatin, EGFP was fused to the C-terminus of *Drosophila* CapG and several UAS and genomic transgenic lines were created (S. Heidmann and K. Trunzer, unpublished).

2.1.1 Characterization of CapG-EGFP transgenic lines

The insertion positions of *UASPI-CapG-EGFP* transgenes were mapped to the second chromosome (lines II.1 and II.2) and third chromosome (III.1, III.2 and III.3). These three transgenes allow ectopic expression of CapG-EGFP using the binary *GAL4/UAS* system (Brand et al., 1993).

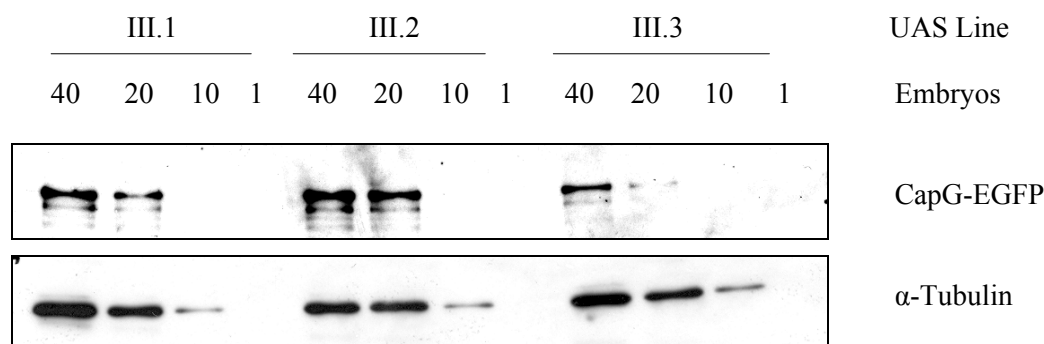


Figure 2.1 CapG-EGFP expression analysis. Individuals of different transgenic lines of *UASPI-CapG-EGFP* were crossed with *prd-GAL4* flies, 6-7 hrs old embryos were collected and extracts were prepared. Different amounts of extract (corresponding to 40, 20, 10 and 1 embryo equivalents) were loaded and the blot was probed with an antibody against EGFP to detect CapG-EGFP protein. Tubulin was used as loading control.

To determine the expression levels, individuals of all three third chromosomal lines were crossed with flies of the *paired-GAL4* driver line, which drives in early embryos the expression of Gal4-dependent transgenes unevenly in stripes in the second thoracic (T2), first, third, fifth and seventh abdominal segments (A1, A3, A5, A7) as well as throughout the gnathal segments (Brand et al., 1993). 6-7 hrs old embryos were collected, extracts were prepared and analyzed by western blotting

using an antibody against EGFP (Fig. 2.1). All the transgenic lines showed expression of CapG-EGFP.

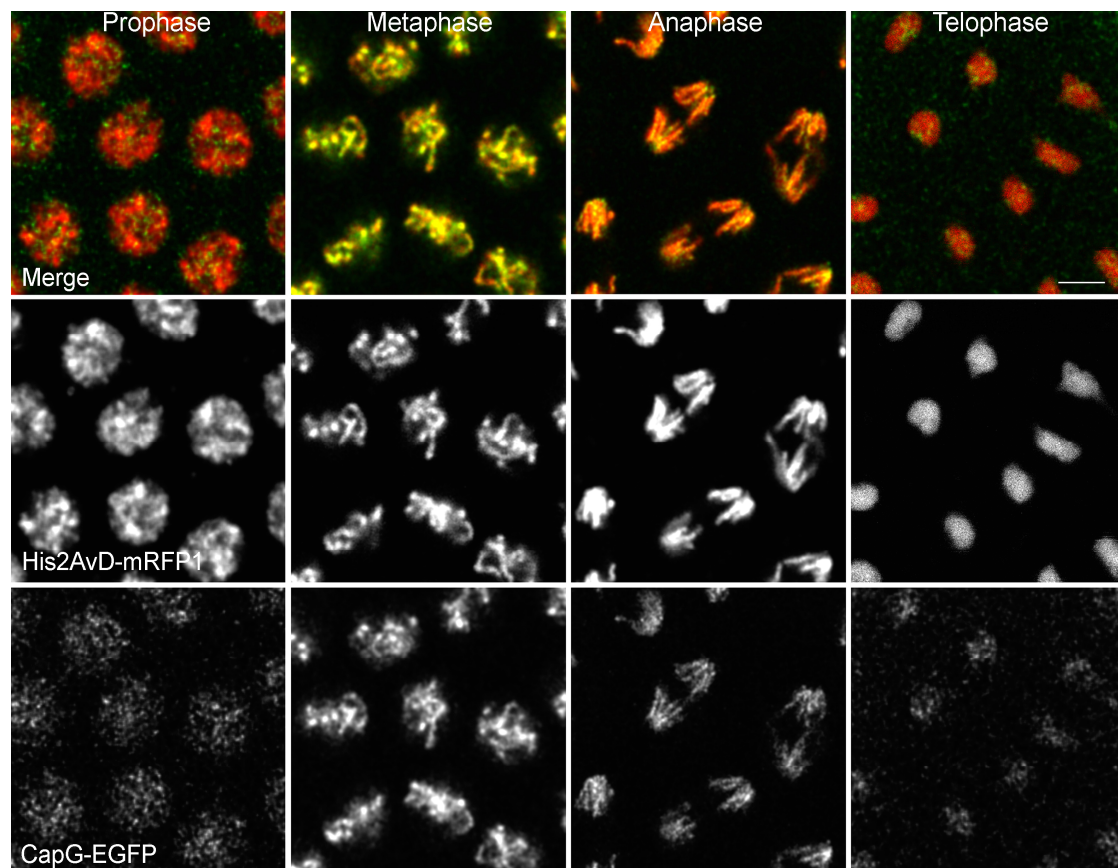


Figure 2.2 Intracellular localization of CapG. Time-lapse microscopy was performed on embryos co-expressing CapG-EGFP (green) and His2AvD-mRFP1 (red), progressing through mitotic cycle 13. (Scale bar 5 μ m). CapG was found to be nuclear enriched throughout the cell cycle.

To determine the intracellular localization of CapG-EGFP during the cell cycle, 1-2 hrs old embryos were collected from flies with the genotype *His2AvD-mRFP1 II.1/+; gCapG-EGFP1 III.1/+*, which express CapG-EGFP and the mRFP1 tagged *Drosophila* Histone 2A variant His2AvD to visualize chromatin. In the *gCapG-EGFP* transgenes, expression is directed by the genomic regulatory elements of the *CapG* locus. Mitosis 13 was analyzed using a confocal microscope. CapG-EGFP was found slightly enriched in the nucleus during interphase (Fig 2.2) unlike *Drosophila* Barren/CapH, a non SMC subunit of condensin I (Oliveira et al., 2007) and condensin I subunits in vertebrate cells (Hirota et al., 2004; Ono et al., 2004), which are mainly

cytoplasmic during interphase. During prophase, metaphase and anaphase, CapG-EGFP is localized along the condensed chromosome arms while it dissociates from chromatin in late mitosis and starting in late telophase it was again found to be slightly nuclear enriched (Fig. 2.2).

In order to check if the overexpression of CapG-EGFP leads to any phenotype, individuals of all UAS lines were crossed with flies from several eye specific *GAL4* drivers lines namely *eyeless-GAL4*, *GMR-Gal4* and *Sevenless-GAL4*. *eyeless-GAL4* directs expression throughout the eye imaginal discs during the early development of eye (Hazelett et al., 1998). *GMR-Gal4* causes high levels of transgene expression in the cells posterior to the morphogenetic furrow in eye imaginal discs (Freeman, 1996). *Sevenless-GAL4* drives expression in the photoreceptors and cone cells of the late developing eye disc (Bailey, 1999; Basler and Hafen, 1989). No obvious deleterious effects of CapG-EGFP overexpression on eye morphology were observed in any progeny of these crosses (data not shown).

2.1.2 CapG-EGFP is a biologically functional protein

To determine whether the fusion protein CapG-EGFP is biologically functional, rescue experiments were performed using three different mutants of *CapG* (*CapG¹*, *CapG³* and *CapG⁶*). *CapG¹* and *CapG⁶* contain nonsense mutations, which introduce premature stop codons instead of the triplets encoding amino acids 343 and 77, respectively, while *CapG³* has a missense mutation changing the arginine at position 558 to a tryptophan (Jager et al., 2005). When homozygous, all mutations cause embryonic lethality and mutant embryos display massive anaphase bridges during mitosis 15.

The transgenes *UAS-CapG-EGFP III.1*, *III.2* and *III.3* were expressed using a ubiquitously expressing driver, *daughterless-Gal4* (Wodarz et al., 1995) in different heterozygous *CapG* mutant backgrounds, by crossing virgins of the genotype either *CapG¹/CyO*; *da-GAL4/TM3,Sb* or *CapG³/CyO*; *da-GAL4/TM3,Sb* with males of the genotype either *CapG¹/CyO*; *UASPI-CapG-EGFP III.1* or *III.2* or *III.3/TM3,Sb* or *CapG³/CyO*; *UASPI-CapG-EGFP III.1* or *III.2* or *III.3/TM3,Sb* or *CapG⁶/CyO*; *UASPI-CapG-EGFP III.1* or *III.2* or *III.3/TM3,Sb*. For *gCapG-EGFP*, virgins of the

genotype of either *CapG¹ / CyO*; *gCapG-EGFP III.1/ TM3,Sb* or *CapG³ / CyO*; *gCapG-EGFP III.1/ TM3,Sb* were crossed with males of the genotype of either *CapG¹/ CyO* or *CapG³/ CyO* or *CapG⁶/ CyO*. The percentages of rescued flies were scored based on absence of the marker *Curly* (CyO).

The genomic transgene *gCapG-EGFP III.1 / TM3,Ser* rescues embryonic lethality of *CapG* mutants efficiently as rescued adult flies were obtained in all three heteroallelic mutant conditions (table 2.1). Among the UAS lines, only *UASPI-CapG-EGFP III.2* rescues the embryonic lethality in the *CapG³/CapG⁶* heteroallelic mutant condition, while *UASPI-CapG-EGFP III.1* and *UASPI-CapG-EGFP III.3* did not give rise to rescued adult flies. A possible reason for this could be that the amount of CapG-EGFP protein due to expression of the *UASPI-CapG-EGFP III.1* and *UASPI-CapG-EGFP III.3* transgenes is not sufficient to support development to the adult stage.

Table 2.1: Rescue of CapG mutants by CapG-EGFP transgenes

Genotype of rescued flies	Expected percentage of rescued flies among the progeny	Proportion of rescued flies
<i>CapG¹/CapG⁶;gCapG-EGFP III.1</i>	20%	16.75% of expected
<i>CapG¹/CapG³;gCapG-EGFP III.1</i>	20%	18.25% of expected
<i>CapG³/CapG⁶;gCapG-EGFP III.1</i>	20%	24.5% of expected
<i>CapG³/CapG⁶;UASPI-CapG-EGFP III.2 /da-GAL4</i>	14.2%	2.3% of expected

These results suggest that CapG-EGFP is a biologically functional protein and therefore its localization and dynamic behavior is very likely to reflect the dynamic properties of endogenous protein.

2.1.3 Chromatin association profile of CapG-EGFP during mitosis

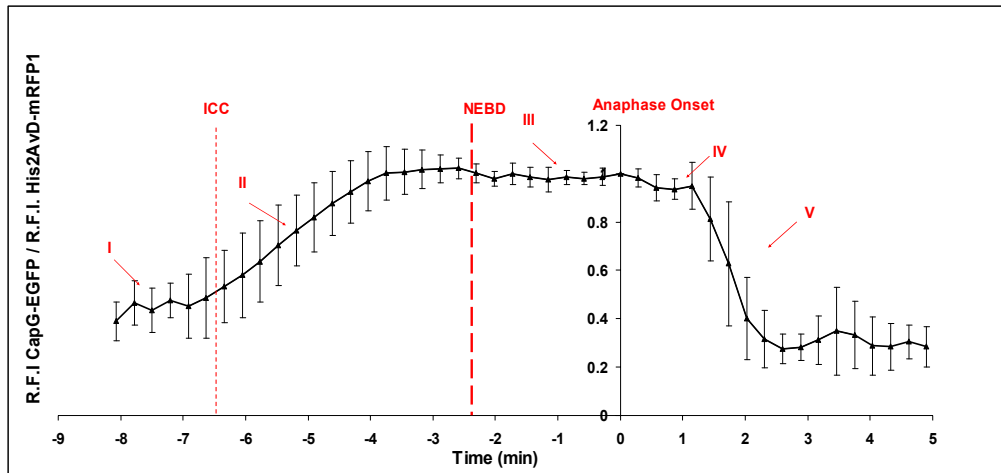
To determine the timing of CapG-EGFP association with chromatin during mitosis, I recombined *gCapG-EGFP III.1* with *His2AvD-mRFP1 III.1* (Schuh et al., 2007) and performed confocal microscopy on embryos co-expressing CapG-EGFP and His2AvD-mRFP1. Embryos progressing through mitosis 12 of early syncytial divisions were analyzed. It is advantageous to analyze mitosis during the syncytial nuclear divisions of the early *Drosophila* blastoderm embryo, because these divisions are extremely rapid (average time per division ≈ 10 mins) and occur meta-synchronously on the surface of the embryo, which allows simultaneous data acquisition from multiple nuclei arranged in the same optical plane. The diffuse and weak interphase nuclear signals of CapG-EGFP start to enrich in a dotlike pattern at the time of initiation of chromosome condensation (ICC) during early prophase, indicative of chromatin association.

ICC starts approximately 6.30 mins before anaphase onset ($t=0$), as adapted from Oliveira et al., (2007), where ICC was defined as the time point when the first condensed dots of His2AvD-mRFP1 were observed.

Further loading of CapG-EGFP occurred gradually and CapG-EGFP was maximally associated with chromosomes approximately 1.5 min before nuclear envelope break down (NEBD) (Fig. 2.3). NEBD in mitosis 12 occurs approximately 2.2 min before anaphase onset as described in Oliveira et al., 2007. These findings are at odds with previous studies in vertebrates, where condensin I was shown to gain access to chromatin only after NEBD (Hirota et al., 2004; Oliveira et al., 2007; Ono et al., 2004). Once loading was fully achieved, CapG-EGFP levels on the chromatin remained high until late anaphase when CapG-EGFP dissociated rapidly and chromosomes decondensed in the ensuing telophase (Fig. 2.3). These results indicate that CapG-EGFP might have an additional function independently of other condensin I subunits during interphase.

To analyze whether ectopically expressed CapG-EGFP behaves in a similar manner, flies with the genotype *UASPI-CapG-EGFP III.2, mat α - tub GAL4-VP16 / His2AvD-mRFP1 III.1* were generated and their progeny was analyzed by confocal microscopy while progressing through embryonic mitosis 12.

A



B

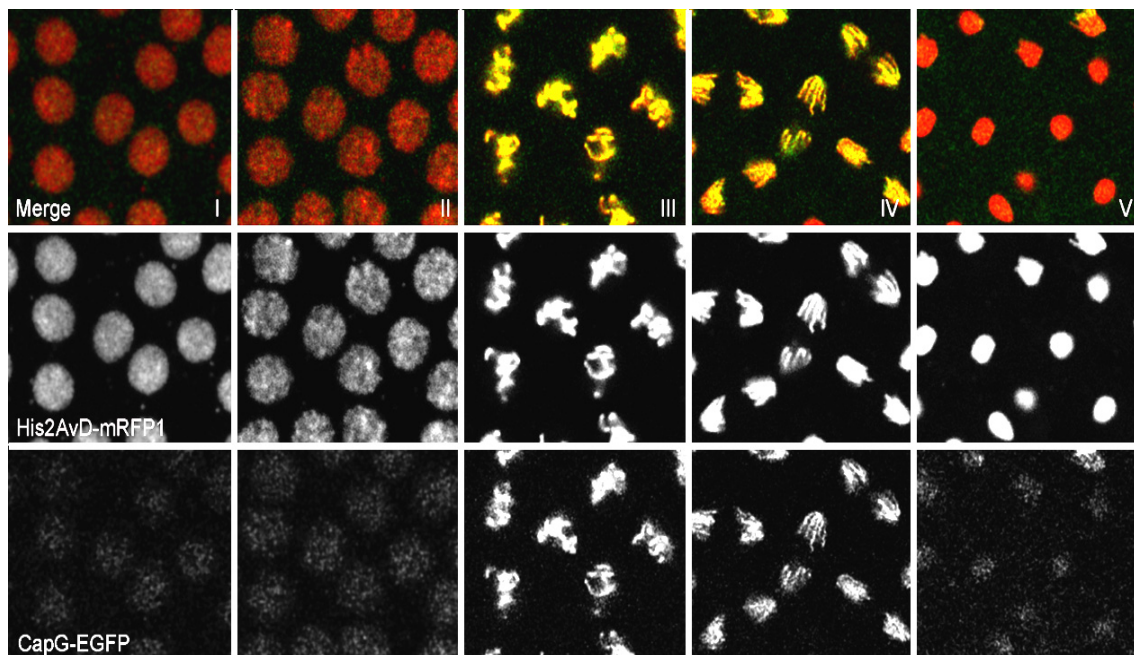


Figure 2.3 Chromatin association profile of CapG-EGFP during mitosis. A) Graphic representation of loading of CapG-EGFP onto chromosomes over time by quantifying fluorescence intensities in live embryos co-expressing CapG-EGFP and His2AvD-mRFP1 during mitosis 12. Data series were aligned accordingly to anaphase onset timing ($t=0$ =anaphase onset, 7 embryos, 15 nuclei) The times of Initiation of Chromosome Condensation (ICC) and Nuclear Envelope Breakdown (NEBD) are indicated by the continuous and dashed red lines, respectively. Error bars indicate standard deviation B) Representative images at different time points of the cycle (corresponding to the roman-numbered arrows in the graph in A). Cap-G is present in nuclei during interphase. Scale bar 5 μ m

The loading behavior shown by this ectopically expressed CapG-EGFP (*mat α - tub GAL4-VP16 > UASPI-CapG-EGFP1 III.2*) was the same as CapG-EGFP expressed under the control of the genomic *CapG* regulatory region (*gCapG-EGFP III.1*; data not shown).

In order to determine whether the rapid decrease of chromatin-associated CapG-EGFP fluorescence signal intensities during late mitosis might be caused by a decrease in total CapG-EGFP protein levels, those levels were carefully analyzed at different phases of mitosis 14. For this purpose, recombinant flies with the genotype *gCapG-EGFP III.1, string^{7B}, P[w⁺,Hs-string] / TM3, Ser* were generated. *string^{7B}* is a recessive embryonic lethal allele of *string* (Juergens et al., 1984), which is the *Drosophila* homologue of fission yeast *cdc25*. *cdc25/string* encodes a phosphatase which controls the G2/M transition by removing an inhibitory phosphorylation of the mitotic kinase Cdc2/Cdk1, thereby activating it (Edgar and O'Farrell, 1989). Embryos homozygous for *string^{7B}* arrest in G2 phase of mitosis 14. These arrested cells can be driven simultaneously in mitosis 14 by providing an ectopic pulse of *stg* expression after induction of the *hs-stg* transgene with a brief heat shock.

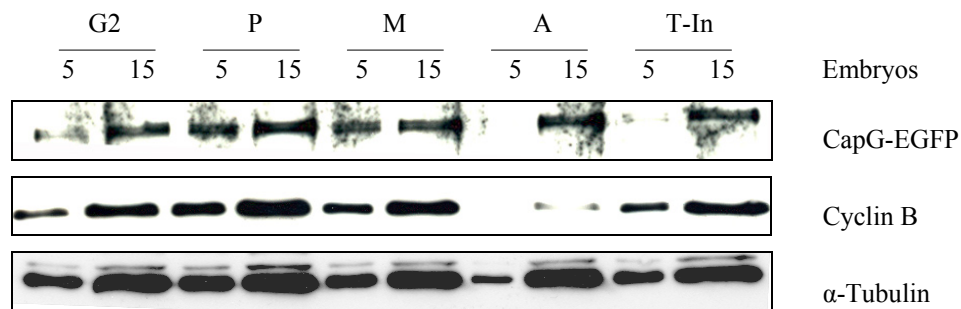


Figure 2.4 CapG-EGFP level during different phases of mitosis 14. Embryos from flies of the genotype *gCapG-EGFP III.1, string^{7B}, P[w⁺,Hs-string] / TM3, Ser*, were synchronized for mitosis 14 (see materials and methods). Embryos with all cells in G2 phase (before mitosis 14), prophase (P), metaphase (M), anaphase (A), and telophase (mitosis 14)/ interphase of mitosis 15(T-In) were sorted. Different amounts of protein extracts from synchronized embryos were loaded and probed with antibodies against EGFP, Cyclin B and tubulin. Cyclin B was used as sorting control and Tubulin was used as loading control. CapG-EGFP1 levels do not change appreciably throughout the cell cycle.

Embryos from *gCapG-EGFP III.1, string^{7B}, P[w⁺,Hs-string] / TM3, Ser* parents were collected, appropriately aged, treated with a heat shock, fixed, and stained for DNA. *stg* homozygous and mitotically synchronized embryos were identified microscopically and sorted for different phases of mitosis 14 (see materials and methods). Extracts from mitotically staged embryos were run on a SDS-PAGE, blotted and the blot was probed with an antibody against EGFP for determining the levels of CapG-EGFP (Fig 2.4).

CapG-EGFP levels do not change significantly during mitosis arguing against degradation of a significant proportion of the protein pool. Thus, the striking disappearance of CapG-EGFP from chromatin at late stages of mitosis most likely does not reflect degradation, but rather a delocalization of this condensin subunit.

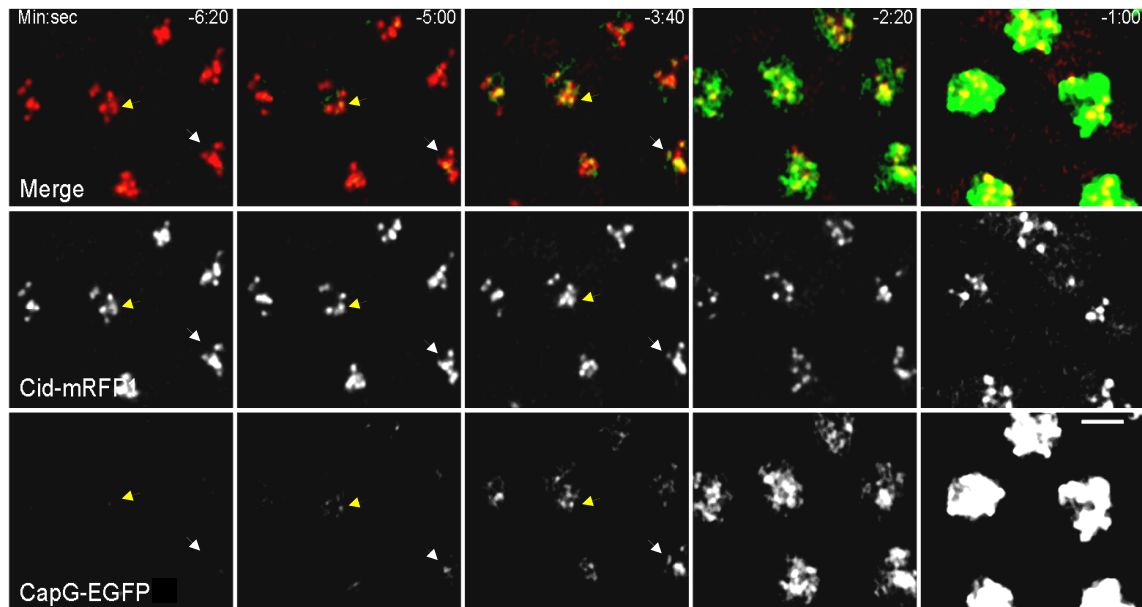
2.1.4 CapG-EGFP loading initiates at centromeres

The analysis of association of CapG-EGFP with chromatin revealed that CapG-EGFP1 loading initiates at focused loci on the chromosomes. As a physical association of CapG with the centromeric histone H3 variant Cid has been described (Jager et al., 2005), it was assessed whether mitotic CapG loading might initiate at the centromeric region. To this end, transgenic lines co-expressing CapG-EGFP and Cid-mRFP (Schuh et al., 2007) were generated. Cid is found exclusively at active centromeres throughout the cell cycle (Ahmad and Henikoff, 2002). Embryos progressing through the syncytial mitotic cycle 12 and post-blastodermal mitosis 14, were analyzed (Fig. 2.5).

For both mitotic divisions it was found that initial sites of CapG-EGFP accumulation were either at or very close to the centromeres. CapG-EGFP starts to colocalize with Cid-mRFP during late interphase, while in prophase the CapG-EGFP signals appeared to spread along the chromosome arms (Fig. 2.5). This observation was further confirmed by quantifying intensities of CapG-EGFP at centromeric proximal and distal regions (Fig 2.6 A) in embryos progressing through mitosis 12.

The quantification data revealed that CapG-EGFP starts to enrich at centromeric proximal regions during interphase approximately 2 min before ICC.

A



B

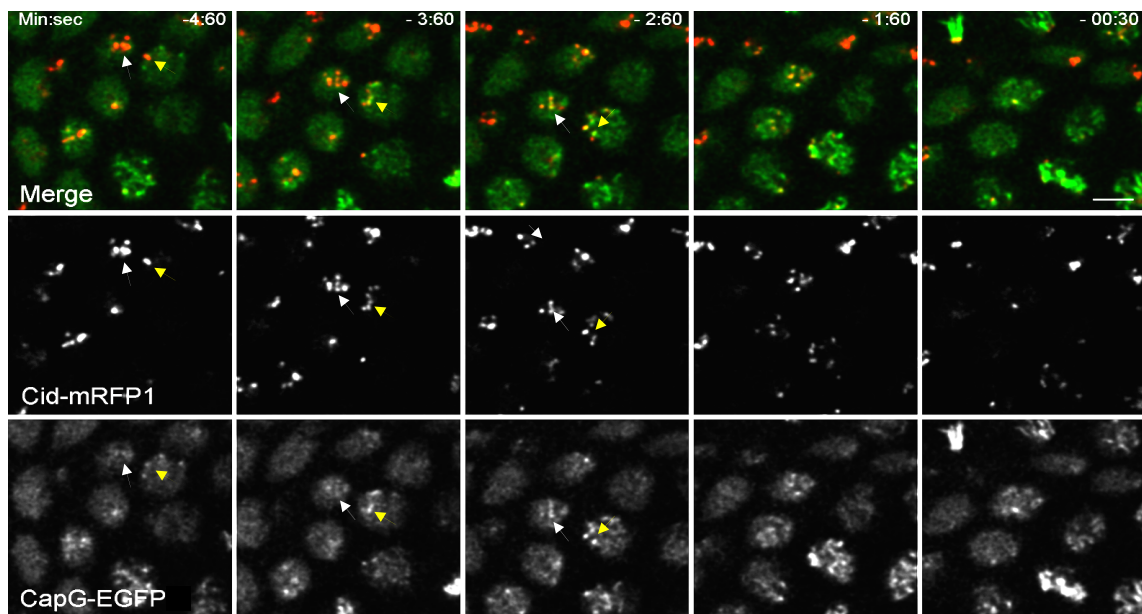
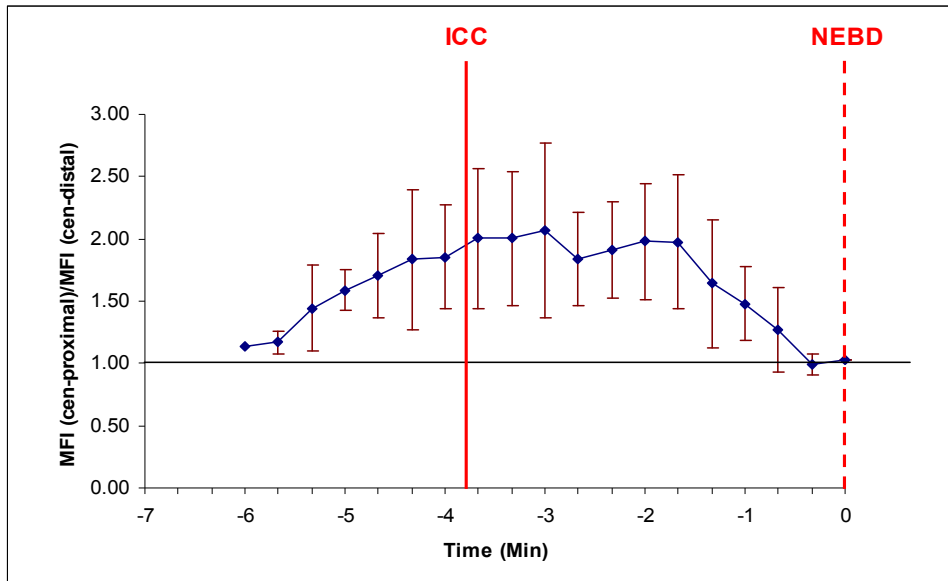


Figure 2.5 CapG-EGFP loading starts at centromeres. Embryos co-expressing CapG-EGFP and Cid-mRFP1 were analyzed to determine the initial sites of CapG-EGFP loading. Time-lapse microscopy was performed on embryos progressing through syncytial mitotic cycle 12 (A) and post-blastodermal mitosis 14 (B), individual frames for the indicated times are shown. ($t=0$, anaphase onset). In order to reduce nuclear fluorescence, color contrast was adjusted in (A) for better visualization of initial loading sites. Yellow and blue arrows indicate two individual CapG-EGFP loading initiation sites in two different nuclei. In the merged images, CapG-EGFP is shown in green and Cid-mRFP1 is in red. Scale bars 5 μm

A



B

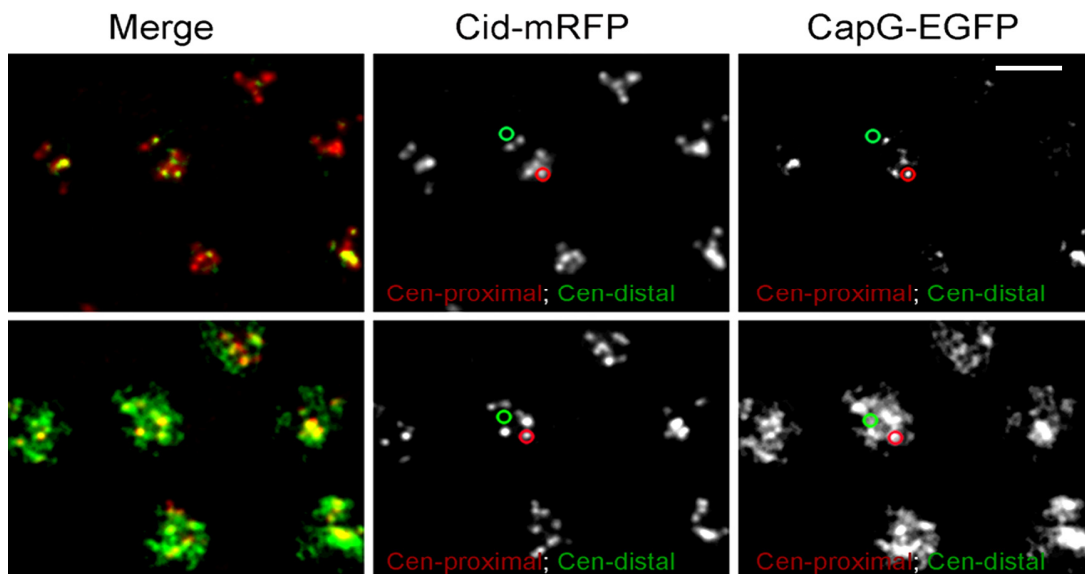


Figure 2.6 Quantification of initial accumulation of CapG-EGFP at centromeric regions. Embryos co-expressing CapG-EGFP1 (Green) and Cid-mRFP1 (red) were analyzed for initiation of CapG-EGFP1 loading at centromeric regions. (A) Graphic representation of the ratio between the mean fluorescence intensity of centromeric proximal region (MFI cen-proximal) and the mean fluorescence intensity of centromeric distal regions (MFI cen-distal), plotted over time for CapG-EGFP. Data series were aligned setting t_0 = Nuclear Envelope Break Down. The times of Initiation of Chromosome Condensation (ICC) and Nuclear Envelope Breakdown (NEBD) are indicated by the continuous and dashed red lines, respectively. The ICC time point is adapted from Oliveira et al., (2007). Error bars represent standard deviation. $n=62$, for each cen-proximal and cen-distal. (B) Example of centromeric proximal region (red circle) and centromeric distal region (green circle) used for the quantification of CapG-EGFP1 intensities represented in (A) Scale bar 5 μ m.

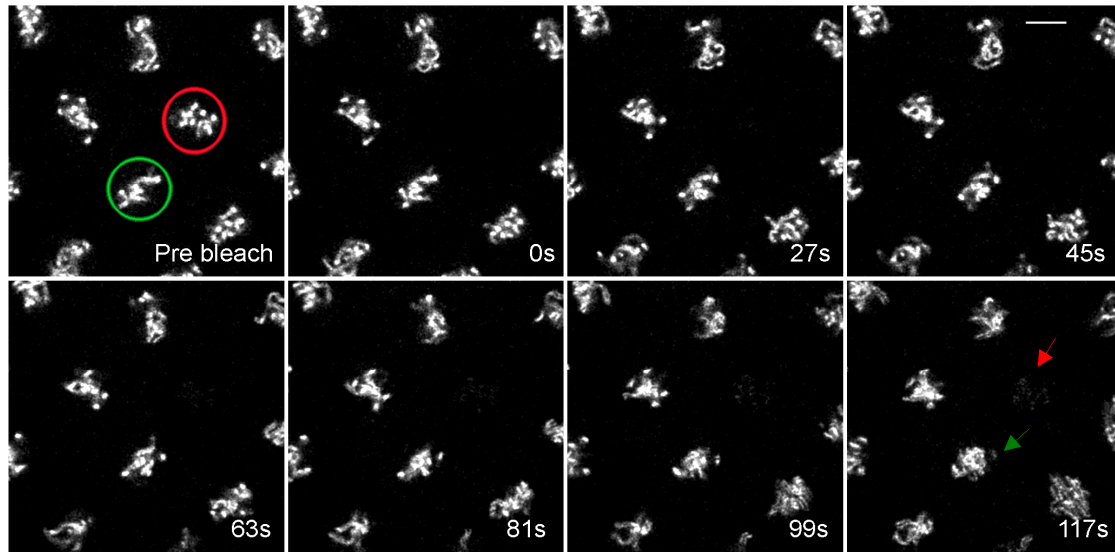
At later stages of prophase ($t = -3.00$ min), it spreads onto the chromosome arms as a decrease in the ratio between the mean fluorescence intensity of centromeric proximal region (MFI cen-proximal) and the mean fluorescence intensity of centromeric distal region (MFI cen-distal) was observed. Shortly before NEBD the ratio reaches 1, which indicates that CapG-EGFP is equally distributed between the centromeres and chromosome arm regions (Fig 2.6 B). These quantitative data confirm that CapG-EGFP indeed starts to accumulate initially at the centromeric region and then spreads along the chromosome arms.

2.1.5 CapG-EGFP shows stable association with chromatin

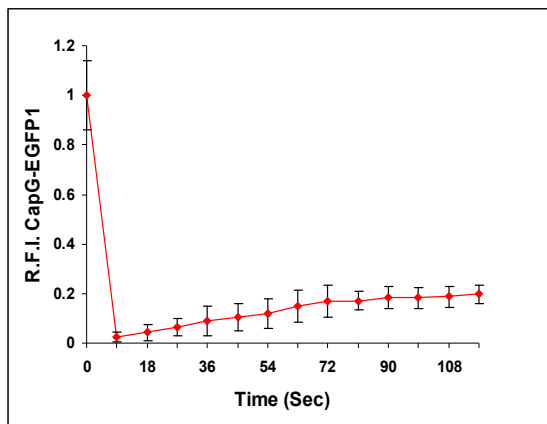
To analyze the kinetics and stability of CapG binding to chromatin, Fluorescent Recovery After Photobleaching (FRAP) experiments were performed on embryos co-expressing CapG-EGFP and His2AvD-mRFP1. FRAP analysis was done on embryos progressing through the syncytial mitotic cycle 12. There are several advantages of using syncytial embryos. First, all nuclei share the same cytoplasm and the proportion of bleached molecules is not a significant part of the total molecules which can rapidly diffuse away so photobleaching does only marginally affect the total fluorescence intensity of the embryo. Second, the syncytial mitotic divisions occur meta-synchronously, which allows using one of the neighboring nuclei going in same phase as a control (non-bleached metaphase). For quantification, photobleaching of an entire metaphase plate was done and the recovery of chromosome localized fluorescence was measured over time and analyzed by plotting the Relative Fluorescence Intensities (RFI). RFI was calculated as the ratio between the mean fluorescence intensities of bleached metaphase and non-bleached metaphase plates (see materials and methods). To determine the mobile fraction, data points were fit to a single exponential curve.

As a control, photobleaching of Barren-EGFP was performed. Barren-EGFP recovers significantly after photobleaching (Fig 2.7 C) and thus shows a highly dynamic association with chromatin as reported previously (Oliveira et al., 2007).

A



B



C

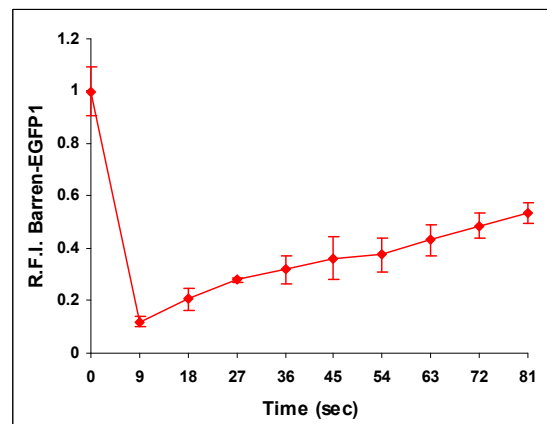


Figure 2.7 CapG-EGFP shows stable association with the chromatin. FRAP analysis was performed in syncytial embryos expressing CapG-EGFP or Barren-EGFP and His2AvD-mRFP1. An ROI was selected to bleach an entire metaphase plate, and subsequently images were collected every 9 s. Individual frames for the indicated times after photobleaching of CapG-EGFP are shown in (A). The red and green circles represent bleached and non bleached (control) metaphase plates respectively. Scale bar 5 μm . RFI of CapG-EGFP and Barren-EGFP are plotted over time and shown in (B) and (C) respectively. RFI was calculated as the ratio between the mean fluorescence intensity of the bleached metaphase and the mean fluorescence intensity of a nonbleached metaphase used as a control (for CapG-EGFP $n=10$ and Barren-EGFP $n=3$). CapG-EGFP binds rather stably to chromatin, while Barren-EGFP shows a significantly higher dynamic association with chromatin.

The quantitative analysis revealed that CapG-EGFP does not recover significantly after photobleaching. A major proportion of CapG-EGFP is stably bound to chromatin during metaphase and only 17.5% of CapG is mobile and turns over with a half time of 55.4 seconds (Fig 2.7 B).

2.2 Analysis of a potential cohesive role for Rad21 and redundancy between Rad21 and C(2)M during female meiosis.

In order to determine a potential cohesive role for Rad21 and C(2)M, a situation was generated in which Rad21 can be conditionally inactivated during oogenesis. Furthermore, to assess a potential redundancy between Rad21 and C(2)M, strains were constructed allowing Rad21 inactivation in a *c(2)M* mutant background. Females of these strains were analyzed for defects during oogenesis and meiotic divisions.

2.2.1 Generation of *Rad21^{ex8}* and *c(2)M^{EP};Rad21^{ex8}* mutant oocytes.

Pauli et al. (2008) have described a system to generate *Rad21* mutant tissues by conditional proteolysis of a Rad21 variant containing Tobacco Etch Virus (TEV) protease sites. This Rad21 variant is expressed in an otherwise *Rad21* mutant background. The mutation used in this context, *Rad21^{ex8}*, is an embryonic lethal allele, in which the first two exons are deleted. These exons encode the highly conserved N terminus of Rad21, which interacts with the ATPase head domain of Smc3 (Pauli et al., 2008). In the recombinant line *Rad21^{ex8}*, *Rad21-3TEV(271)-10myc* (Pauli et al., 2008) the Rad21 mutant phenotype is complemented by the expression of the *Rad21-3TEV(271)-10myc* transgene. This transgene directs expression of a C-terminally myc tagged Rad21 variant, which in addition contains three consecutive TEV protease cleavage sites (ENLYFQG) at position 271 (Pauli et al., 2008). TEV protease is highly specific, recognizing a linear epitope of the general form E-X-X-Y-X-Q-(G/S) and cleaves between Q and G or Q and S (Dougherty and Parks, 1989). TEV protease has no obvious targets in the Drosophila proteome and can be expressed in flies without detrimental effects (Harder et al., 2008; Pauli et al., 2008). To increase TEV activity, transgenic lines were established that allow expression of a TEV variant, which possesses a valine instead of a serine at position 219, which inhibits self cleavage of the protease and also results in about twofold higher activity levels (Kapust et al., 2001). This TEV variant will be called TEV^{SV} in the following. Furthermore, the TEV^{SV} coding region was cloned in the backbone of the pUASP1 vector, which enables GAL4-dependent expression in the female germline (Jager et al., 2005; Rorth, 1998). Finally, TEV^{SV} is fused to a V5 epitope tag allowing its convenient detection using commercially available anti-V5 antibodies.

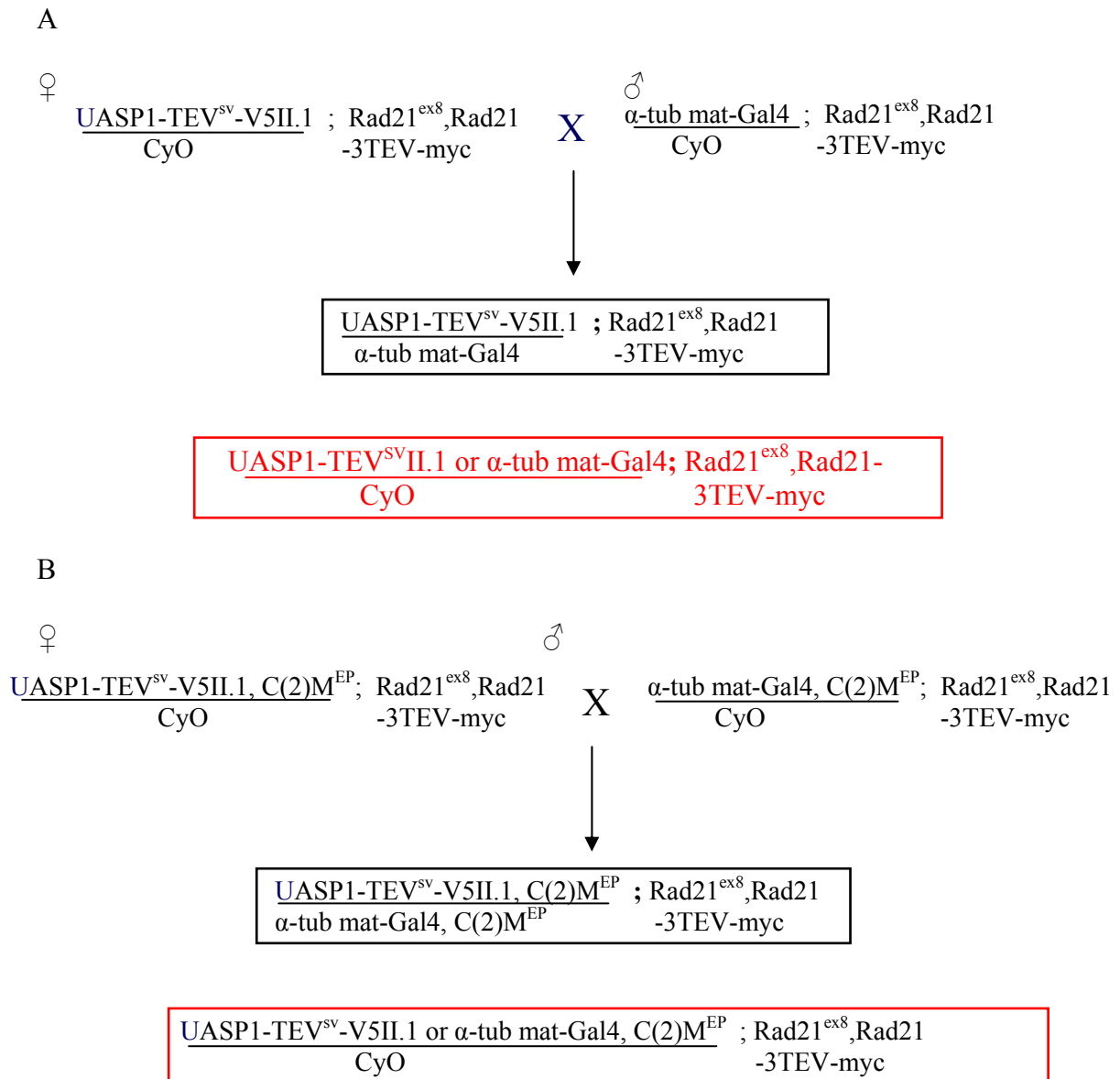


Figure 2.8 Crossing schemes for generating $Rad21^{ex8}$ and $c(2)M^{EP}; Rad21^{ex8}$ mutant oocytes. **A.** For generating $Rad21^{ex8}$ mutant oocytes, females of the genotype $UASP1-TEV^{SV} II.1/CyO; Rad21^{ex8}, Rad21-3TEV(271)-10myc$ were crossed with males of the genotype $\alpha-tub\ mat-GAL4/CyO; Rad21^{ex8}, Rad21-3TEV(271)-10myc$. From the progeny females of the genotype $UASP1-TEV-V5 II.1/ \alpha-tub\ mat-Gal4; Rad21^{ex8}, Rad21-3TEV(271)-10myc$ females (black box) were collected for isolating $Rad21^{ex8}$ mutant oocytes and females of the genotype $UASP1-TEV-V5 II.1/ CyO; Rad21^{ex8}; Rad21-3TEV(271)-10myc$ or $\alpha-tub\ mat-Gal4/ CyO; Rad21^{ex8}; Rad21-3TEV(271)-10myc$ (red box) for control. **B.** For generating $Rad21^{ex8}; c(2)M^{EP}$ double mutant oocytes, females of the genotype $UASP1-TEV^{SV} II.1, C(2)M^{EP} /CyO; Rad21^{ex8}, Rad21-3TEV(271)-10myc$ were crossed with males of the genotype $\alpha-tub\ mat-GAL4, C(2)M^{EP} /CyO; Rad21^{ex8}, Rad21-3TEV(271)-10myc$. From the progeny females of the genotype $UASP1-TEV-V5 II.1, C(2)M^{EP} / \alpha-tub\ mat-Gal4, C(2)M^{EP} ; Rad21^{ex8}, Rad21-3TEV(271)-10myc$ (black box) females were collected for isolating $Rad21^{ex8}; c(2)M$ double mutant oocytes and females of the genotype $UASP1-TEV-V5 II.1, C(2)M^{EP} / CyO; Rad21^{ex8}; Rad21-3TEV(271)-10myc$ or $\alpha-tub\ mat-Gal4, C(2)M^{EP} / CyO; Rad21^{ex8}; Rad21-3TEV(271)-10myc$ (red box) for control.

To allow expression of TEV^{SV}-V5 in oocytes in a *Rad21^{ex8}* mutant background, the lines *UASPI-TEV^{SV} II.1; Rad21^{ex8}*, *Rad21-3TEV(271)-10myc* and *α-tub mat-GAL4; Rad21^{ex8}, Rad21-3TEV(271)-10myc* were established. In these lines, the transgene *UASPI-TEV^{SV}-V5 II.1* is a conditional source for TEV^{SV}-V5 and *α-tub mat-Gal4* was used to drive expression of the *UAS-TEV^{SV}-V5* transgene. The *α-tub mat-GAL4* driver is a maternal driver, which starts the expression in stage 4 egg chambers during oogenesis (Micklem et al., 1997). To be able to assess *Rad21-3TEV-10myc* cleavage also in a *c(2)M* mutant background, the amorphic allele *c(2)M^{EP2115}* was in addition introduced. *c(2)M^{EP2115}* is a genetic null allele in which a P-element is inserted at the position encoding aa 185 in exon 3 (Manheim and McKim, 2003). For the sake of brevity, *c(2)M^{EP2115}* will be called *c(2)M^{EP}* in the following. For generating *c(2)M^{EP};Rad21^{ex8}* double mutant oocytes, the two recombinant lines *UASPI-TEV-V5 II.1, c(2)M^{EP}* and *α-tub mat-Gal4, c(2)M^{EP}* were first created. Then, the lines *UASPI-TEV-V5 II.1, c(2)M^{EP}; Rad21^{ex8}, Rad21-3TEV(271)-10myc* and *α-tub mat-Gal4, c(2)M^{EP}; Rad21^{ex8}, Rad21-3TEV(271)-10myc* lines were established.

To generate *Rad21* mutant oocytes, *UASPI-TEV-V5 II.1/ CyO; Rad21^{ex8},Rad21-3TEV(271)-10myc* females were crossed with *α-tub mat-Gal4/ CyO; Rad21^{ex8}, Rad21-3TEV(271)-10myc* males (Fig 3.8 A). From the progeny, *UASPI-TEV-V5 II.1/ α-tub mat-Gal4; Rad21^{ex8},Rad21-3TEV(271)-10myc* females were collected and used to obtain the mutant oocytes (black box in Fig 2.8 A).

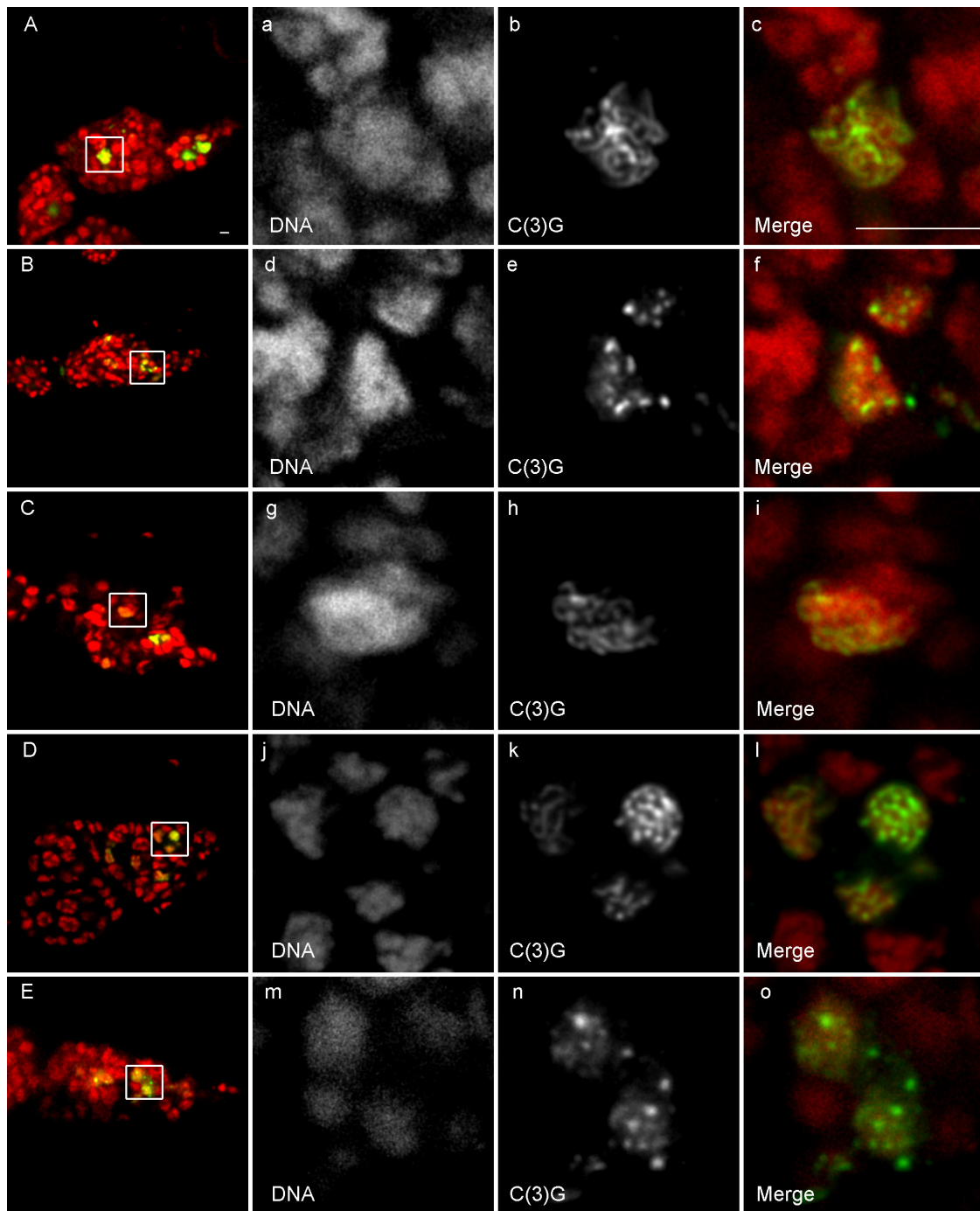


Figure 2.9 The localization of C(3)G in the pro-oocyte nucleus. A-D Germaria of individuals with the genotypes **A** w^1 , **B** $c(2)M^{EP}$, **C** $UASP1-TEV-V5 II.1, c(2)M^{EP}$ or $\alpha-tub mat-Gal4, c(2)M^{EP}/CyO;Rad21^{ex8}, Rad21-3TEV(271)-10myc$ **D** $UASP1-TEV-V5 II.1/ \alpha-tub mat-Gal4; Rad21^{ex8}, Rad21-3TEV(271)-10myc$, and **E** $UASP1-TEV-V5 II.1, c(2)M^{EP}/ \alpha-tub mat-Gal4, c(2)M^{EP}; Rad21^{ex8}, Rad21-3TEV(271)-10myc$ were stained with anti C(3)G (green) and propidium iodide to visualize DNA (red). Magnified views of boxed areas in **A, B, C, D** and **E** are shown in **a-c, d-f, g-i, j-l** and **m-o**, respectively. In the germarium of $UASP1-TEV-V5 II.1/ \alpha-tub mat-Gal4; Rad21^{ex8}, Rad21-3TEV(271)-10myc$, C(3)G localizes to the chromosomes in pro-oocyte nucleus (D and j-l), while in the $UASP1-TEV-V5 II.1, c(2)M^{EP}/ \alpha-tub mat-Gal4, c(2)M^{EP}; Rad21^{ex8}, Rad21-3TEV(271)-10myc$ pro-oocytes, localization of C(3)G was abrogated due to the presence of $c(2)M^{EP}$ (E and m-o). (Scale bars 5 μm)

The sibling females *UASPI-TEV-V5 II.1/ CyO; Rad21^{ex8}; Rad21-3TEV(271)-10myc* or *α-tub mat-Gal4/ CyO; Rad21^{ex8}; Rad21-3TEV(271)-10myc* were used as a control (red box in Fig 2.8 A).

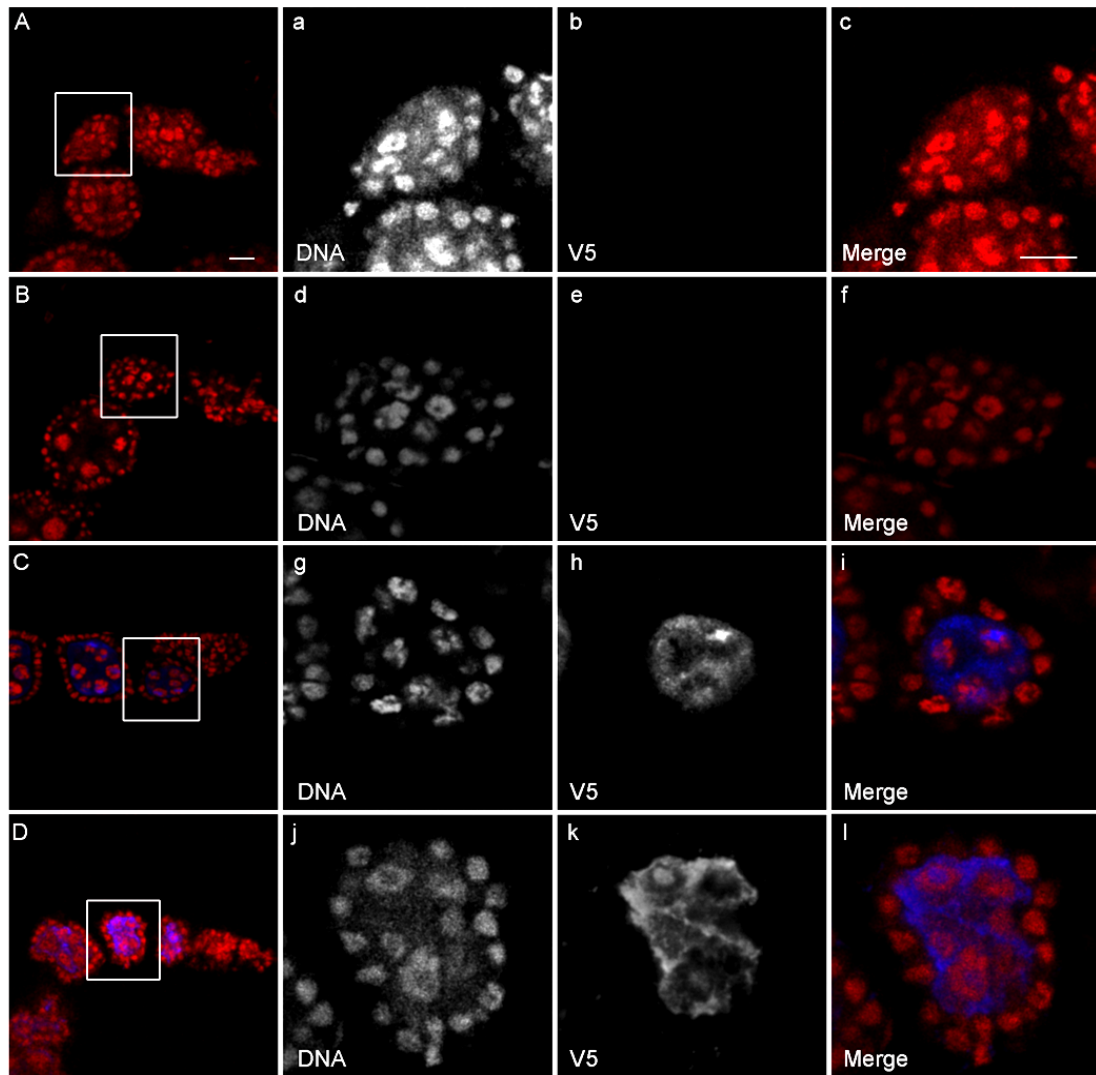


Figure 2.10 The expression of TEV^{SV}-V5 in Stage 4 egg chambers. A-D Ovarioles with early egg chambers of individuals with the genotypes **A** *w¹*, **B** *UASPI-TEV-V5 II.1, c(2)^{M^{EP}}* or *α-tub mat-Gal4, c(2)^{M^{EP}}/ CyO; Rad21^{ex8}, Rad21-3TEV(271)-10myc* **C** *UASPI-TEV-V5 II.1/ α-tub mat-Gal4; Rad21^{ex8}, Rad21-3TEV(271)-10myc*, and **D** *UASPI-TEV-V5 II.1, c(2)^{M^{EP}}/ α-tub mat-Gal4, c(2)^{M^{EP}}; Rad21^{ex8}, Rad21-3TEV(271)-10myc* were stained with anti V5 (blue) and propidium iodide to visualize DNA (red). Magnified view of insets in **A**, **B**, **C** and **D** are shown in **a-c**, **d-f**, **g-i**, and **j-l**, respectively. In the ovarioles from *UASPI-TEV-V5 II.1/ α-tub mat-Gal4; Rad21^{ex8}, Rad21-3TEV(271)-10myc* (**C**) and *UASPI-TEV-V5 II.1, c(2)^{M^{EP}}/ α-tub mat-Gal4, c(2)^{M^{EP}}; Rad21^{ex8}, Rad21-3TEV(271)-10myc* (**D**) females, the expression of TEV-V5 starts in stage 4 egg chambers. (Scale bars 10 μm)

To generate $c(2)M^{EP};Rad21^{ex8}$ double mutant oocytes, $UASPI-TEV-V5 II.1, c(2)M^{EP}/ CyO; Rad21^{ex8}, Rad21-3TEV(271)-10myc$ females were crossed with the $\alpha-tub mat-Gal4, c(2)M^{EP}/ CyO; Rad21^{ex8}, Rad21-3TEV(271)-10myc$ males (Fig 2.8 B). From the progeny, $UASPI-TEV-V5 II.1, c(2)M^{EP}/ \alpha-tub mat-Gal4, c(2)M^{EP}; Rad21^{ex8}, Rad21-3TEV(271)-10myc$ females (black box in Fig 2.8 B) were collected for the isolation of $c(2)M^{EP};Rad21^{ex8}$ double mutant oocytes. Siblings with the genotype $UASPI-TEV-V5 II.1, c(2)M^{EP}/ CyO;Rad21^{ex8}, Rad21-3TEV(271)-10myc$ or $\alpha-tub mat-Gal4, c(2)M^{EP}/ CyO;Rad21^{ex8}, Rad21-3TEV(271)-10myc$ (red box in Fig 2.8 B) were used as a control.

To confirm the presence of the $c(2)M^{EP}$ allele in the respective selected individuals, the localization behavior of C(3)G in pro-oocytes in germaria was observed by immunofluorescence microscopy (Fig 2.9). C(3)G is a transversal synaptonemal complex component, which localizes in a ribbon shaped thread-like pattern along the lengths of chromosomes in the nucleus of the pro-oocyte as well as of the pro-nurse cell in wild type flies (Fig 2.9 A and a-c) (Page and Hawley, 2001). In $c(2)M^{EP2115}$ homozygous mutants, the localization of C(3)G is abrogated; C(3)G fails to assemble into the long ribbon. Instead, it forms several short segments presumably incomplete synaptonemal complex structures, which are restricted to the pro-oocytes (Page and Hawley, 2001) (Fig 2.9 B and d-f). In the control ($UASPI-TEV-V5 II.1, c(2)M^{EP}$ or $\alpha-tub mat-Gal4, c(2)M^{EP}/ CyO;Rad21^{ex8}, Rad21-3TEV(271)-10myc$) germaria (Fig 2.9 C and g-h) and as well as in the $UASPI-TEV-V5 II.1/ \alpha-tub mat-Gal4; Rad21^{ex8},Rad21-3TEV(271)-10myc$ germaria (Fig 2.9 D and j-l), the localization of C(3)G in pro-oocyte nucleus was similar to that of wild type. C(3)G localizes to entire chromosomes in a ribbon shaped thread-like pattern. As expected, the localization pattern of C(3)G in the germaria of $UASPI-TEV-V5 II.1, c(2)M^{EP}/ \alpha-tub mat-Gal4, c(2)M^{EP}; Rad21^{ex8}, Rad21-3TEV(271)-10myc$ females was similarly disrupted than that of $c(2)M^{EP}$ females (Fig 2.9 E and m-o).

To determine the expression of TEV^{SV}-V5, ovarioles were stained for DNA and TEV-V5 using an antibody against theV5 tag. In ovarioles of $UASPI-TEV-V5 II.1/ \alpha-tub mat-Gal4; Rad21^{ex8},Rad21-3TEV(271)-10myc$ (Fig 2.10 C and i-l) and $UASPI-TEV-V5 II.1, c(2)M^{EP}/ \alpha-tub mat-Gal4, c(2)M^{EP}; Rad21^{ex8}, Rad21-3TEV(271)-10myc$ (Fig 2.10 D and m-p), the expression of TEV^{SV}-V5 was detected starting from stage 4

egg chambers. On the other hand, wild type germaria (Fig 2.10 A and a-c) and control germaria (*UASPI-TEV-V5 II.1, c(2)M^{EP}* or *α-tub mat-Gal4, c(2)M^{EP}/ CyO;Rad21^{ex8}, Rad21-3TEV(271)-10myc*) (Fig 2.10 B and d-f) did not stain positively with the anti V5 antibody, as expected.

In *UASPI-TEV-V5 II.1/ α-tub mat-Gal4; Rad21^{ex8}, Rad21-3TEV(271)-10myc* and *UASPI-TEV-V5 II.1, c(2)M^{EP}/ α-tub mat-Gal4, c(2)M^{EP}; Rad21^{ex8}, Rad21-3TEV(271)-10myc* females, the sole source of Rad21 is Rad21-3TEV-myc which is then cleaved by TEV-V5 protease during early oogenesis. As a result the oocytes produced by these females will be mutant for Rad21 (*Rad21^{ex8}*) and double mutant for Rad21 and C(2)M (*c(2)M^{EP};Rad21^{ex8}*), respectively.

2.2.2 The Rad21-3TEV(271)-myc protein is efficiently cleaved in oocytes

To determine whether Rad21-3TEV-myc was cleaved efficiently due to TEV^{SV}-V5 expression in developing egg chambers, stage 14 oocytes were isolated from *UASPI-TEV-V5 II.1/ α-tub mat-Gal4; Rad21^{ex8}, Rad21-3TEV(271)-10myc* and *UASPI-TEV-V5 II.1, c(2)M^{EP}/ α-tub mat-Gal4, C(2)M^{EP}; Rad21^{ex8}, Rad21-3TEV(271)-10myc* females. Protein extracts were prepared from these oocytes. Stage 14 oocytes from sibling females (*UASPI-TEV-V5 II.1* or *α-tub mat-Gal4/ CyO; Rad21^{ex8}; Rad21-3TEV(271)-10myc* and *UASPI-TEV-V5 II.1, c(2)M^{EP}* and *α-tub mat-Gal4, c(2)M^{EP}/ CyO;Rad21^{ex8}, Rad21-3TEV(271)-10myc*) were used as controls. Western blotting was performed using different amounts of extracts and the blot was probed with antibodies against myc, V5, and tubulin (Fig 2.11).

The anti myc antibody was used to visualize the full length protein and C-terminal cleavage products, anti V5 to determine the TEV-V5 expression and tubulin was used as a loading control. The result showed that the full length protein disappeared and a C-terminal cleavage product of the expected size (90 kDa) became visible (Fig 2.11). Moreover, based on the dilution series of extracts from oocytes not expressing TEV protease it can be concluded that more than 95% of Rad21TEV-myc protein was cleaved in TEV-V5 expressing oocytes.

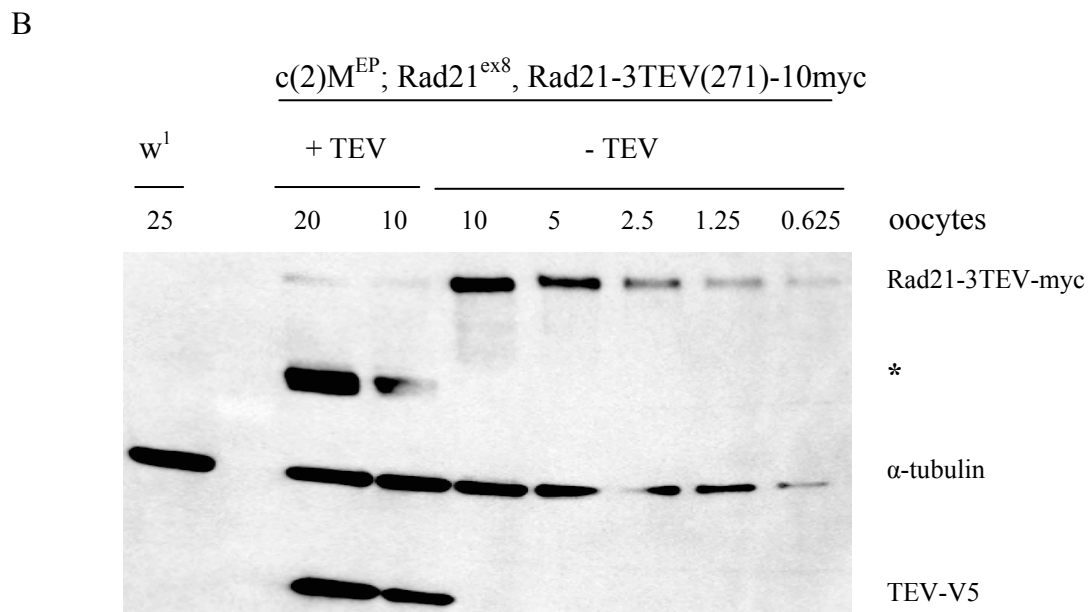
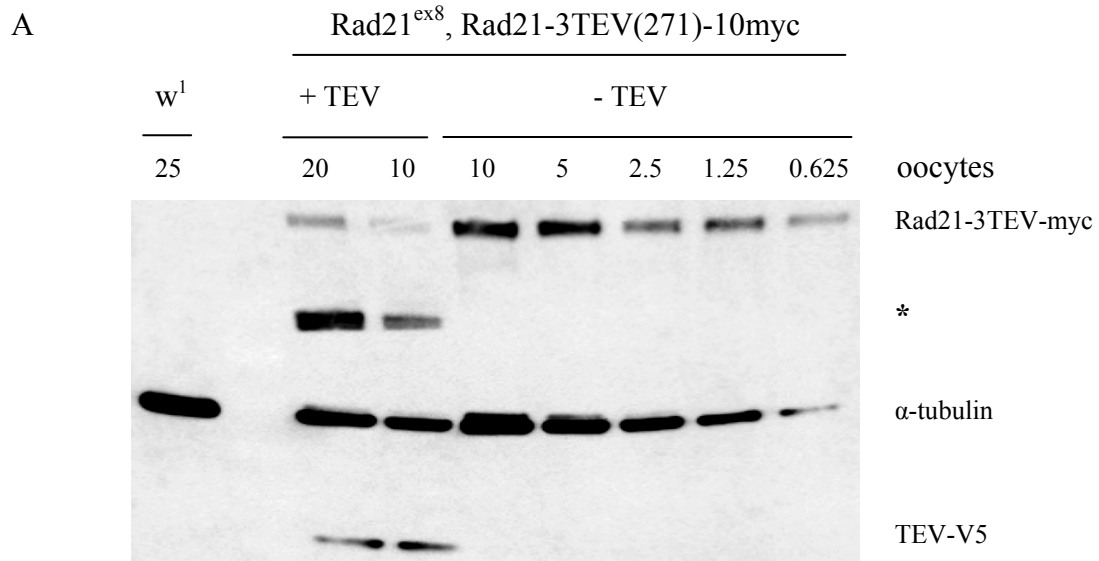


Figure 2.11 Rad21-3TEV-myc is efficiently cleaved in oocytes. Western blot analysis of in-vivo cleavage of Rad21-3TEV-myc. Different amounts of extracts from TEV expressing oocytes from the females with the genotype *UASPI-TEV-V5 II.1/ α -tub mat-Gal4; Rad21^{ex8}, Rad21-3TEV(271)-10myc* (+TEV in A) or *UASPI-TEV-V5 II.1, c(2)M^{EP}/ α -tub mat-Gal4, c(2)M^{EP}; Rad21^{ex8}, Rad21-3TEV(271)-10myc* (+TEV in B) were loaded. For comparison extracts from control oocytes (*UASPI-TEV-V5 II.1* or *α -tub mat-Gal4/ CyO; Rad21^{ex8}; Rad21-3TEV(271)-10myc* (-TEV in A) or *UASPI-TEV-V5 II.1, c(2)M^{EP} or α -tub mat-Gal4, c(2)M^{EP}/ CyO; Rad21^{ex8}, Rad21-3TEV(271)-10myc* (-TEV in B) were loaded. Blots were probed with antibodies against myc (to detect the full length protein and the cleavage product) and V5 (for checking TEV-V5 expression), and tubulin as a loading control. In both blots a prominent cleavage product (asterisks) is visible.

2.2.3 Rad21 cleavage causes disassembly of the synaptonemal complex

To assess the phenotypic consequences of Rad21 inactivation in the female germline, the integrity of the synaptonemal complex was scrutinized. To this end, C(3)G localization was observed in growing oocytes. Immunostaining using anti-C(3)G and anti-V5 antibodies was performed, and analysis of localization of C(3)G was done by confocal microscopy (Fig. 2.12).

The assembly of the SC starts in pro-oocytes at stage 2A while they are still in the germarium. The SC forms a ribbon-like structure (Page and Hawley, 2001). The disassembly of the SC occurs gradually, starting in stage 4 egg chambers. By the end of stage 9 while the oocyte is still in prophase I, the SC disassembles completely. The pattern of C(3)G localization during these stages is specific. In wild type females, when the SC is fully assembled C(3)G is localized solely on the chromosome axis of pro-oocytes (Fig 2.12 A and a-c). In the initial phases of SC disassembly, C(3)G starts to disperse from the chromosome axis and accumulate in the oocyte nucleus. At the time when the SC is completely disassembled, C(3)G is no longer detectable on the chromosomes and the protein is present throughout the oocyte nucleus (Page and Hawley, 2001). In *c(2)M^{EP2115}* mutants, the SC completely disassembles in stage 4 egg chambers and C(3)G is present in the oocyte nucleus (Page and Hawley, 2001) (Fig 2.12 B and d-f).

In control ovarioles heterozygous for *c(2)M^{EP}* and not expressing TEV protease (genotype: *UASPI-TEV-V5 II.1, c(2)M^{EP}* or *α-tub mat-Gal4, c(2)M^{EP}/CyO;Rad21^{ex8}, Rad21-3TEV(271)-10myc*), the C(3)G localization pattern was similar to that of wild type oocytes. In pro-oocytes in the germarium (Fig 2.9 C and g-h) and stage 4 oocytes (Fig 3.12 C and g-i), C(3)G localizes in the typical thread-like pattern on chromosomes. In *UASPI-TEV-V5 II.1/α-tub mat-Gal4; Rad21^{ex8}, Rad21-3TEV(271)-10myc* ovarioles, the SC localization in the germarium was similar to that of wild type (Fig 2.9 C and g-i). But surprisingly, the SC was completely disassembled after the cleavage of Rad21-3TEV-myc by TEV protease in stage 4 oocytes. C(3)G was no longer detectable on the chromosomes and was mainly distributed in the oocyte nucleus (Fig 2.12 D and j-l).

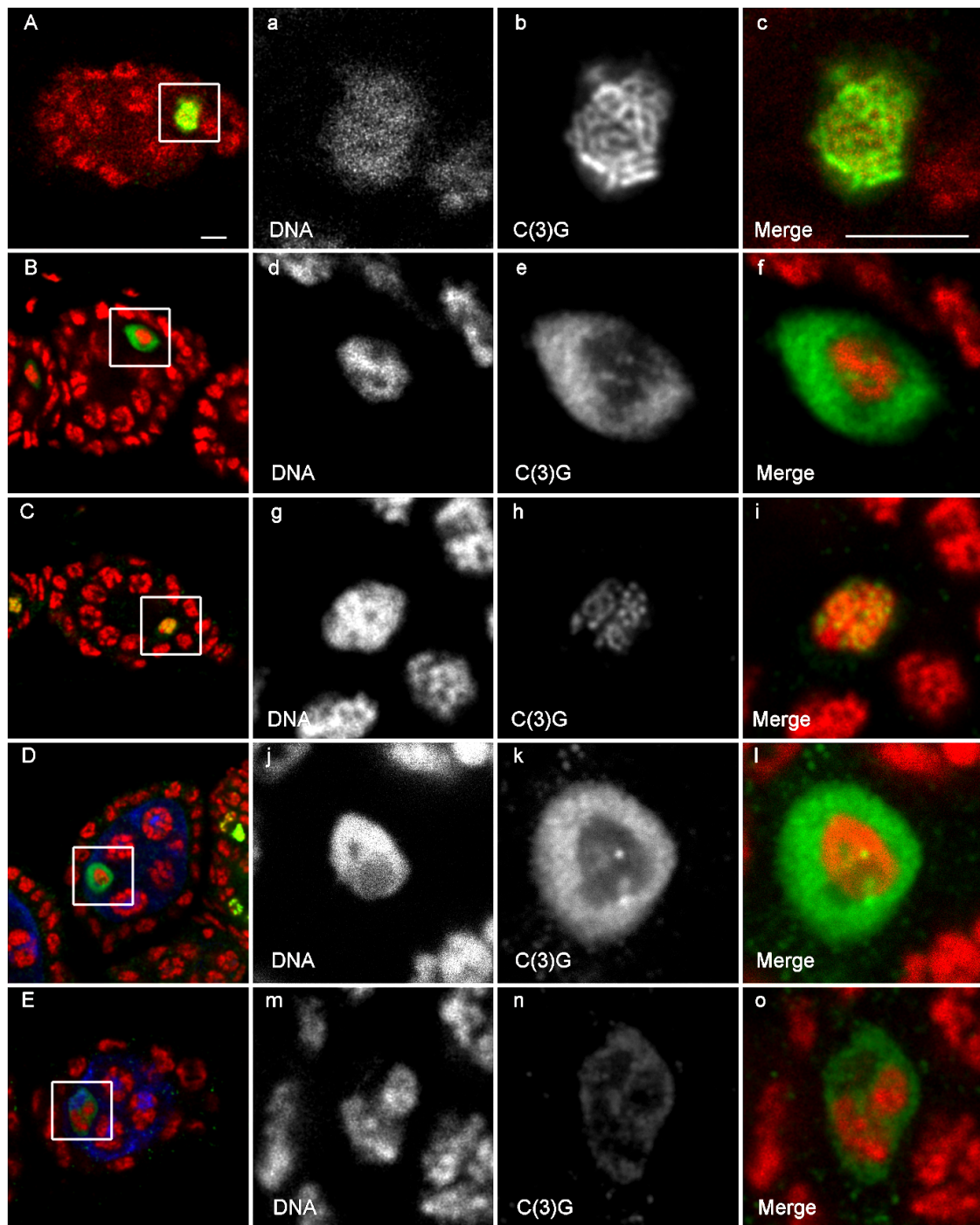


Figure 2.12 TEV induced cleavage of Rad21 causes disassembly of the synaptonemal complex. A- E Stage 4 egg chambers of individuals with the genotype **A** w^l , **B** $c(2)M^{EP}$, **C** $UASPI-TEV-V5 II.1$, $c(2)M^{EP}$ or $\alpha-tub mat-Gal4$, $c(2)M^{EP}/CyO;Rad21^{ex8}$, $Rad21-3TEV(271)-10myc$ **D** $UASPI-TEV-V5 II.1/\alpha-tub mat-Gal4$; $Rad21^{ex8},Rad21-3TEV(271)-10myc$, and **E** $UASPI-TEV-V5 II.1$, $c(2)M^{EP}/\alpha-tub mat-Gal4$, $c(2)M^{EP}$; $Rad21^{ex8}$, $Rad21-3TEV(271)-10myc$ were stained with anti V5 (blue), anti C(3)G (green) and propidium iodide to visualize DNA (red). Magnified view of boxed area in **A**, **B**, **C**, **D** and **E** are shown in **a-c**, **d-f**, **g-i**, **j-l** and **m-o**, respectively. In the merged images on the right DNA is shown in red and C(3)G signal is depicted in green. The synaptonemal complex is disassembled in stage 4 oocytes after TEV mediated cleavage of Rad21-3TEV-myc in $UASPI-TEV-V5 II.1/\alpha-tub mat-Gal4$; $Rad21^{ex8},Rad21-3TEV(271)-10myc$ oocytes (D and j-l) (Scale bars 5 μm).

In *UASPI-TEV-V5 II.1, c(2)^{MEP}/ α -tub mat-Gal4, c(2)^{MEP}; Rad21^{ex8}, Rad21-3TEV(271)-10myc* ovarioles, the localization pattern of C(3)G was similar to that in *c(2)^{MEP}* homozygous mutants. The pro-oocytes showed punctuate staining of C(3)G (Fig 2.9 E and m-o), which represents the incomplete synaptonemal complex formation and which was then completely resolved in stage 4 oocytes (Fig. 2.12 E and m-o). Thus, these results strongly suggest a role of Rad21 for the maintenance of the SC.

2.2.4 Chromosomal localization of Smc1 in oocyte nuclei is abolished after Rad21 cleavage

If Rad21 cleavage in the female germline results in inactivation of a *bona fide* cohesion complex, one would expect dissociation of the other cohesion complex components from the chromatin, as has been shown for mitotic cohesion complexes in other systems. In order to examine the effects of Rad21 cleavage on the localization of the cohesin complex, I stained ovarioles with an anti-Smc1 antibody and analyzed stage 6 oocytes by confocal microscopy.

The localization behaviour of Smc1 during *Drosophila* oogenesis is well characterised. In wild type oocytes, Smc1 localizes in a thread-like pattern along the entire length of the chromosomes from stage 1 until stage 6 (Khetani and Bickel, 2007), similar to C(3)G. In *c(2)^{MEP}* homozygous mutant oocytes, this thread-like staining is completely absent and Smc1 localises to DNA in patches which colocalize with the centromeres (Khetani and Bickel, 2007).

Analysis of Smc1 localization, in oocytes in Rad21 mutant oocytes, in which Rad21-3TEV-myc has been cleaved, revealed that the chromosomal localization of Smc1 in *Rad21^{ex8}* stage 5 oocytes was abolished. Smc1 was no longer associated with chromosomes and was mainly dispersed in the oocyte nucleus (Fig. 2.13 D, j-l). Smc1 localization in *c(2)^{MEP};Rad21^{ex8}* mutant oocytes was similar to that in *Rad21^{ex8}* oocytes (data not shown). In control oocytes (*UASPI-TEV-V5 II.1* or *α -tub mat-Gal4/ CyO; Rad21^{ex8}, Rad21-3TEV(271)-10myc*), Smc1 was localized to chromosomes as in *w¹* and *c(2)^{MEP}* homozygous mutants, which is consistent with a previous report

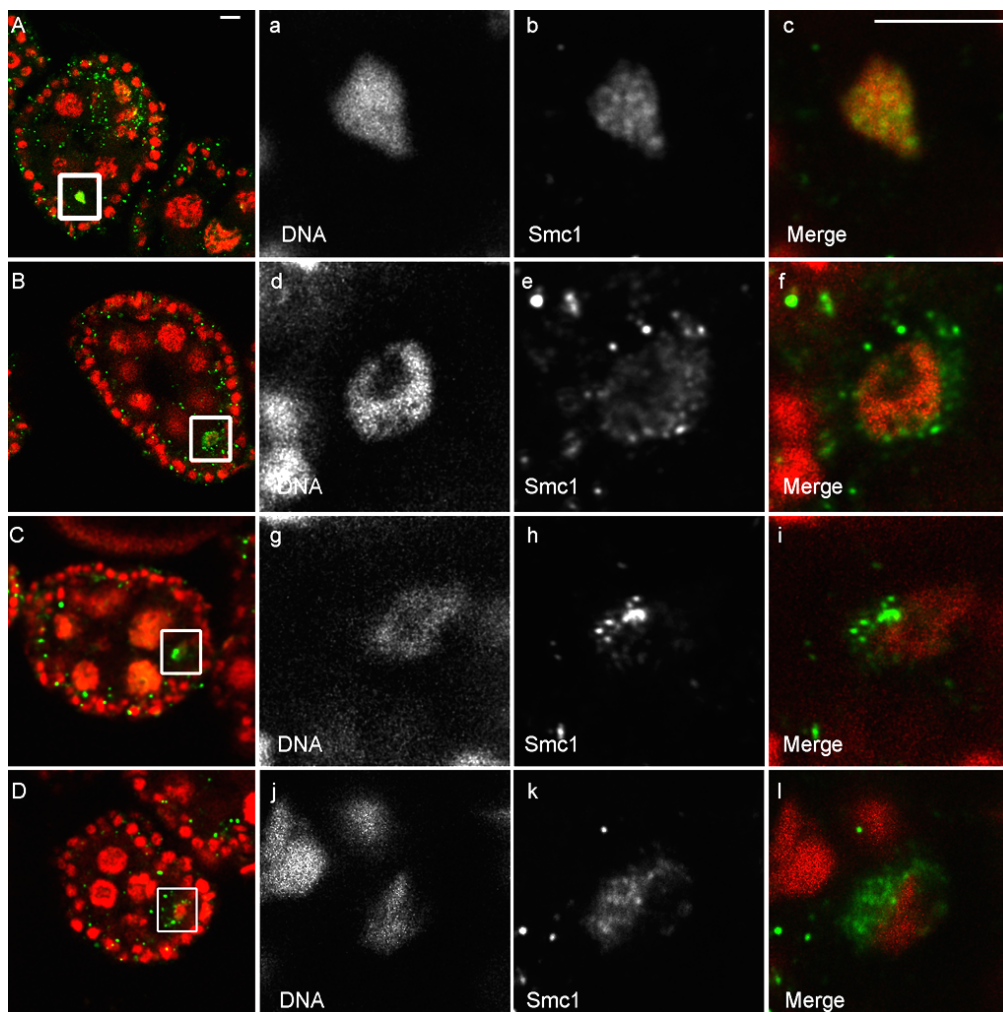


Figure 2.13 Chromatin localization of Smc1 is abolished after Rad21 cleavage. **A-D** Stage 5 egg chambers of individuals with the genotype **A** w^1 , **B** *UASP1-TEV-V5 II.1* or *α -tub mat-Gal4/CyO; Rad21^{ex8}, Rad21-3TEV(271)-10myc*, **C** *c(2)M^{EP}* and **D** *UASP1-TEV-V5 II.1/ α -tub mat-Gal4; Rad21^{ex8}, Rad21-3TEV(271)-10myc*, were stained with anti Smc1 (green) and propidium iodide to visualize DNA (red). Magnified view of the boxed areas in **A**, **B**, **C** and **D** are shown in **a-c**, **d-f**, **g-i**, and **j-l**, respectively. In w^1 (**A** and **a-c**) and *UASP1-TEV-V5 II.1* or *α -tub mat-Gal4/CyO; Rad21^{ex8}, Rad21-3TEV(271)-10myc* oocytes (**B** and **e-f**) Smc1 localizes to DNA of oocytes, while in *Rad21^{ex8}* oocytes Smc1 localization to oocyte DNA is abolished. (Scale bars 5 μ m).

(Khetani and Bickel, 2007). These results indicate that Rad21 is required for chromosomal localization of Smc1 to chromosomes in oocyte nuclei consistent with the notion that Rad21 assembles in cohesin complexes in the female germline of *Drosophila*.

2.2.5 Rad21 cleavage causes loss of cohesion between homologue chromosomes during prophase I

In order to check if the cohesion between homologs was affected in *Rad21^{ex8}* and *c(2)M^{EP};Rad21^{ex8}* mutant oocytes, ovarioles were stained with antibodies against Cenp-C, a constitutive component of the inner kinetochore (Heeger et al., 2005). Premature dissociation of homologous chromosomes and/or sister chromatids is expected to result in an increase of centromeric signals. Stage 6-10 oocytes progressing through meiotic prophase I were analyzed by confocal microscopy. In 95% of wild type oocytes (n=21), the numbers of anti Cenp-C foci were 2 to 4 (Fig 2.14 A and a-c). Similarly, in control oocytes not expressing TEV protease (genotype: *UASPI-TEV-V5 II.1, c(2)M^{EP}* or *α-tub mat-Gal4, c(2)M^{EP}/CyO;Rad21^{ex8}, Rad21-3TEV(271)-10myc*) (n=15) the numbers of Cenp-C foci were 2 to 4 (Fig 2.14 C and g-i).

The number of Cenp-C foci exhibited by 95% of *c(2)M^{EP}* oocytes (n=19) were also 4 or less than 4 (Fig 2.14 B and d-f). In contrast 86% of *Rad21^{ex8}* oocytes (Fig 2.14 D and j-l; n=21) and 90% of *c(2)M^{EP};Rad21^{ex8}* oocytes (Fig 2.14 E and m-o; n=10) exhibited more than 4 Cenp-C foci during prophase I indicating that in these oocytes homologs and/or sister chromatids separate prematurely.

2.2.6 Rad21 cleavage causes homologue nondisjunction and premature sister chromatid segregation during meiosis I

To examine the effects of Rad21 cleavage on meiotic chromosome segregation, mature oocytes were activated *in vitro* for 20 min and Fluorescent in situ hybridization (FISH) was performed using an X-chromosomal specific probe (359 bp). DNA was counterstained and oocytes were observed for abnormal meiotic figures. The observed phenotypes were placed in three different categories, namely homologue nondisjunction (Fig 2.15 G and I), premature sister chromatid separation (Fig 2.15 B,D,F and H) and spread chromosomes (Fig 2.15 J).

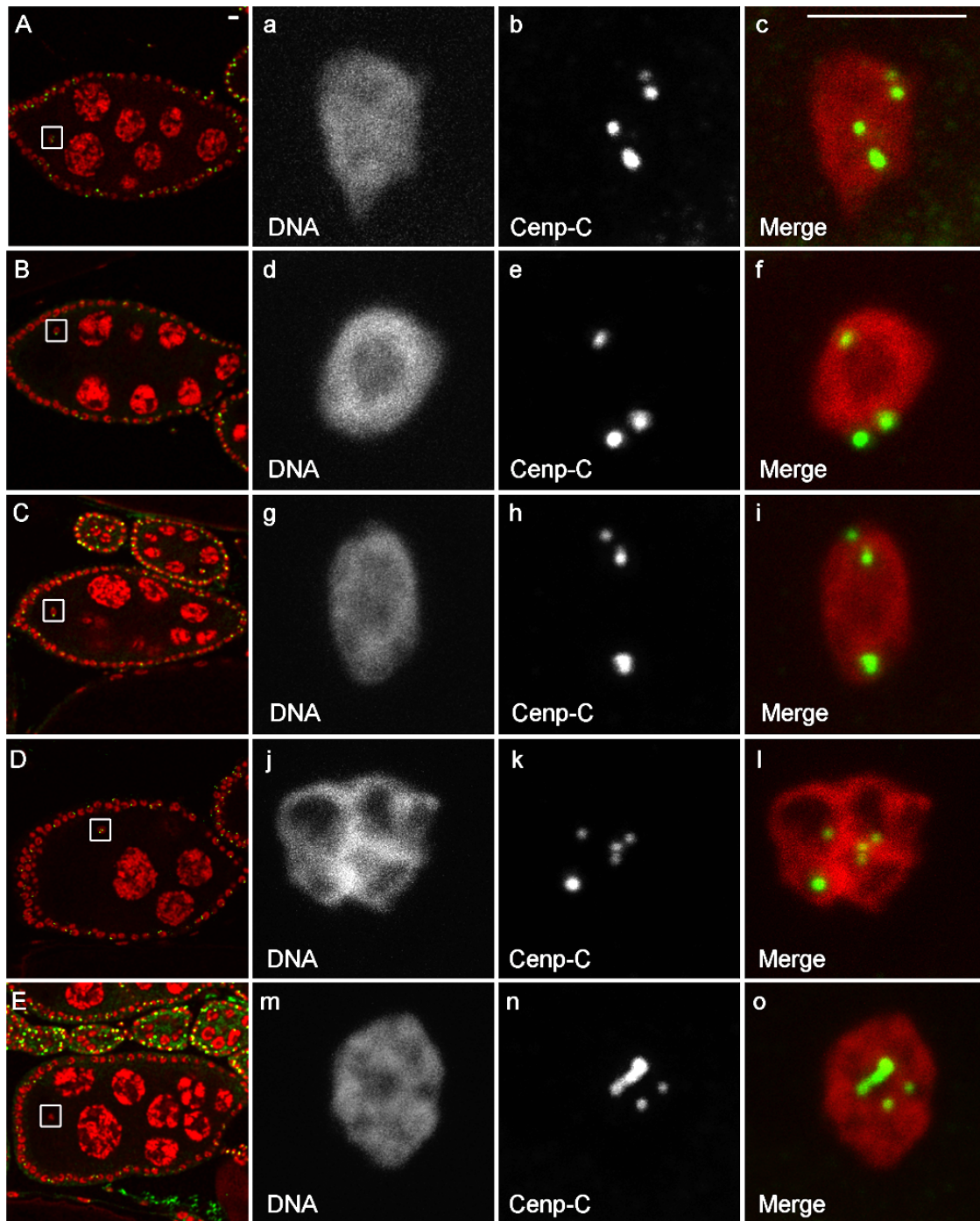


Figure 2.14 Cohesion is lost in prophase I after Rad21 cleavage. A-E Stage 6 egg chambers of individuals with the genotype **A** w^1 , **B** $c(2)^{M^{EP}}$, **C** $UASPI-TEV-V5 II.1, c(2)^{M^{EP}}$ or $\alpha-tub mat-Gal4, c(2)^{M^{EP}}/ CyO; Rad21^{ex8}$, $Rad21-3TEV(271)-10myc$ **D** $UASPI-TEV-V5 II.1/ \alpha-tub mat-Gal4; Rad21^{ex8}, Rad21-3TEV(271)-10myc$, and **E** $UASPI-TEV-V5 II.1, c(2)^{M^{EP}}/ \alpha-tub mat-Gal4, c(2)^{M^{EP}}; Rad21^{ex8}, Rad21-3TEV(271)-10myc$ oocytes were stained with anti Cnp-C (green) and propidium iodide to visualize DNA (red). Maximum projections of z series stacks were performed to obtain Cnp-C signals from the complete nuclear volume. Magnified view of boxed area in **A, B, C, D** and **E** are shown in **a-c, d-f, g-i, j-l** and **m-o**, respectively. (Scale bars 5 μm). w^1 , $c(2)^{M^{EP}}$ and $UASPI-TEV-V5 II.1, c(2)^{M^{EP}}$ or $\alpha-tub mat-Gal4, c(2)^{M^{EP}}/ CyO; Rad21^{ex8}, Rad21-3TEV(271)-10myc$ oocytes exhibited 2-4 Cnp-C foci, whereas $Rad21^{ex8}$ and $c(2)^{M^{EP}}; Rad21^{ex8}$ oocytes exhibited more than 4 foci.

Three phenotypes were assigned in the homologue nondisjunction category (1) X-chromosomes are not segregated equally in meiosis I, but the DNA masses appear equal (Fig 2.15 I). (2) Segregation of X-chromosomes is equal but the sizes of DNA masses are unequal after anaphase I (Fig 2.15 G), and (3) segregation of X-Chromosomes and other chromosomes (DNA mass) is unequal. The second category of abnormal phenotypes “premature sister chromatid separation” is based on the appearance of more than 2 X-chromosome FISH spots before metaphase II. Oocytes with more than 4 DNA masses were put in the third category “Spread chromosome”.

Genotype of oocytes	Normal meiotic figures	Abnormal meiotic figures		
		Homologue nondisjunction	Premature sister chromatid separation	Spread chromosome
w^1 (n=21)	18	1	-	2
$c(2)M^{EP}$ (n=57)	39	9	-	9
Control (n=89)	60	7	-	22
$c(2)M^{EP}; Rad21^{ex8}/ TM3, Ser$ (n=61)	38	17	-	6
$Rad21^{ex8}$ (n=46)	19	12	8	7
$c(2)M^{EP}; Rad21^{ex8}$ (n=59)	10	25	13	11

Table 2.2 Abnormal meiotic figures shown by $Rad21^{ex8}$ and $c(2)M^{EP}; Rad21^{ex8}$ mutant oocytes. Abnormal figures shown by activated oocytes were categorized in three classes (1) homologue nondisjunction (2) premature sister chromatid separation and (3) spread chromosomes. $Rad21^{ex8}$ and $c(2)M^{EP}; Rad21^{ex8}$ show higher number of homologue nondisjunction and premature sister chromatid separation than w^1 , $c(2)M^{EP}$ and Control (control: $UASPI-TEV-V5 II.1$, $c(2)M^{EP}$ or $\alpha-tub mat-Gal4$, $c(2)M^{EP}/CyO$; $Rad21^{ex8}$, $Rad21-3TEV(271)- 10myc$; n total number of oocytes observed).

In wild type, 86% of the oocytes showed normal meiotic figures (Fig 2.15 A,C and E), 4.7% showed homologue nondisjunction with unequal DNA masses and 9.5% showed a chromosome spread phenotype (n=21). In the $c(2)M^{EP}$ mutant oocytes, 68% showed normal meiotic figures (n=57) and 21% had homologue nondisjunction and 11% showed the chromosome spread phenotype.

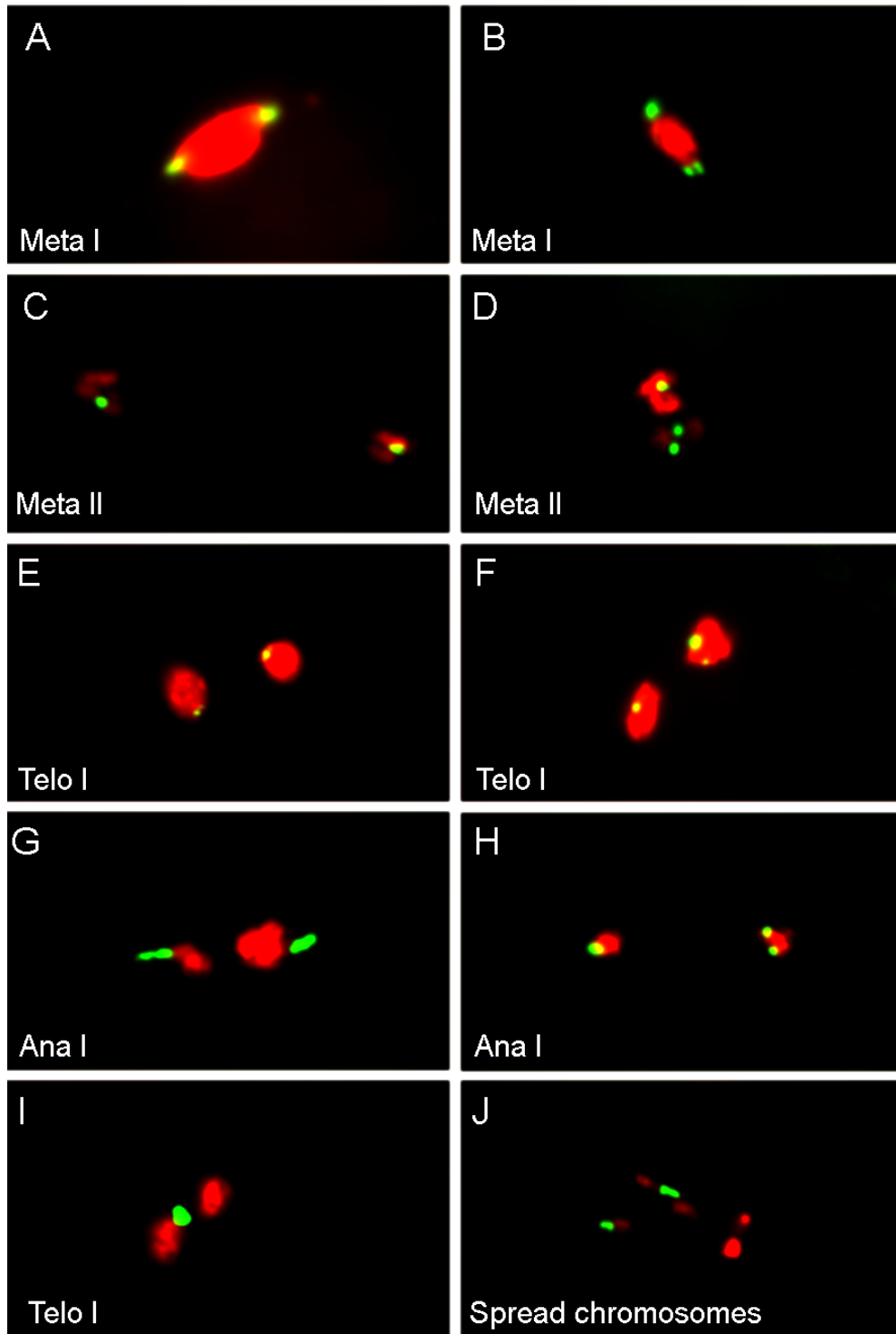


Figure 2.15 Abnormal meiotic figures shown by mutants after *in-vitro* activation: Mature oocytes were activated *in vitro*, stained for DNA (red) and Fluorescent in situ hybridization (FISH) was performed on them using an X-chromosomal specific probe (359 bp; green). A, C and E represent normal meiotic figures. G (X-chromosome segregation is equal while sizes of DNA masses are unequal) and I (X-chromosomes segregate unequally) exhibit homologue nondisjunction. B, D, F and H show premature sister chromatid separation and J represents spread chromosomes phenotype.

Among the control oocytes (*UASPI-TEV-V5 II.1*, *c(2)M^{EP}* or *α-tub mat-Gal4*, *c(2)M^{EP}/ CyO;Rad21^{ex8}*, *Rad21-3TEV(271)-10myc*) 67% showed normal meiotic figures, 7.8% exhibited homologue nondisjunction and 24.7% oocytes displayed the chromosome spread phenotype (n=89). In *Rad21^{ex8}* mutant oocytes, the number of abnormal mitotic figures was increased to 59% and 41% showed normal meiotic figures (n=46). Out of these 59% abnormal oocytes, 26% displayed homologue nondisjunction, 17% showed premature sister chromatid separation and 16% were put in the ‘spread chromosome’ category.

In order to check if there is a redundancy between Rad21 and C(2)M, meiotic divisions were observed in *c(2)M^{EP};Rad21^{ex8}* double mutant oocytes. As control oocytes were isolated from females, which were homozygous for *c(2)M^{EP}* and heterozygous for *Rad21^{ex8}* (*c(2)M^{EP};Rad21^{ex8}/TM3,Ser*). In the control *c(2)M^{EP};Rad21^{ex8}/TM3,Ser* oocytes, 62.3% displayed normal meiotic figures, 27.8% showed nondisjunction and 9.9% had a ‘spread chromosomes’ phenotype. In the double mutant *c(2)M^{EP};Rad21^{ex8}*, the number of abnormal meiotic figure was even higher ; only 17% of the oocytes exhibited normal meiotic figures while 42% showed nondisjunction, 22% showed premature sister chromatid separation and 19% showed the ‘spread chromosome’ phenotype (n=59).

Clearly, *Rad21^{ex8}* mutant oocytes show a high proportion of homolog nondisjunction and the premature sister chromatid separation phenotype is only observed when Rad21 was cleaved. Together, these results clearly suggest that Rad21 is indeed involved in sister chromatid cohesion during female meiosis in *Drosophila*.

2.3 Analysis of a cohesive role of C(2)M during female meiosis

For analyzing the consequences of forced proteolysis of C(2)M during oogenesis and female meiosis in *Drosophila*, several transgenic lines expressing C-terminal HA-tagged TEV protease cleavable C(2)M-variants under the control of the *c(2)M* regulatory region were created and analyzed for protein expression and biological functionality.

2.3.1 Generation of TEV cleavable genomic C(2)M transgenic lines

In order to create transgenic lines expressing TEV cleavable C(2)M-variants, the 3xTEV protease cleavage site-encoding sequences were inserted at three different positions in the coding regions of the *c(2)M* gene: position I (after Asn191), position II (after Thr250) and position III (after Arg339). These positions lie within the motif D/EXXR, which has been reported as a separase cleavage site consensus motif (Sullivan et al., 2004b). These potential separase cleavage sites were also found to be conserved in several members of the Drosophilidae family. Moreover, these sites are localized in the linker region between the N and C-terminal α -kleisin domains of C(2)M, which are predicted to bind to the ATPase heads of Smc1 and Smc3 (Heidmann et al., 2004). The insertion of TEV cleavage sequences at these sites is advantageous, as these are the potential separase cleavage sites and therefore are expected to be exposed to the solvent and thus to be easily accessible for the protease.

Furthermore a new PhiC31-integrase mediated transgenesis systems was used to create the transgenic lines. In this system, site-specific bacteriophage PhiC31 integrase mediates an irreversible and sequence-directed integration between a bacterial attachment site (attB) present in the plasmid construct and a phage attachment site (attP) present in the genome of donor fly line (Bischof et al., 2007). This method is advantageous because the predetermined integration position saves the time and effort required to map transgene insertions. The second advantage are the purported identical expression levels when comparing different transgenes, as position effects are ruled out due to the same insertion position. Two second-chromosomal donor lines, *ZH-attp-58A* and *ZH-attp-51D* (Bischof et al., 2007), were used to create transgenic lines and Several genomic *c(2)M* transgenic lines for each position of the TEV cleavage

sequence (191/250/339) and HA tagged C(2)M without TEV cleavage sites (*gc(2)M-HA*) were established.

2.3.2 Transgene expression and *in-vitro* cleavage of C(2)M-3TEV (191/250/339)-HA

After the establishment of transgenic lines, they were analyzed for protein expression by immunoblotting. Females were dissected and protein extracts were prepared from egg chambers up to stage 10, and the blot was probed with an anti HA antibody.

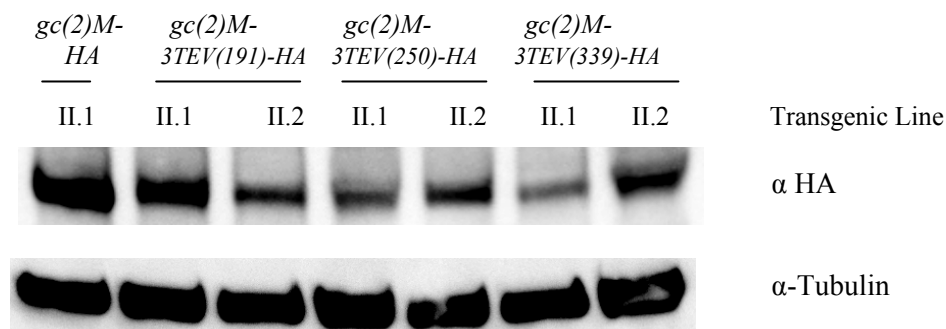


Figure 2.16 Analysis of expression of C(2)M-HA and TEV cleavable C(2)M-HA in *ZH-attp-51D* transgenic lines. Extracts were prepared from ovarioles up to stage 10 egg chambers from 10 females of each transgenic line. The blot was probed with antibodies against the HA tag to detect expression of HA-tagged C(2)M and anti-alpha tubulin was used as a loading control. All transgenic lines show C(2)M-HA protein expression.

One transgene for C(2)M-HA (II.1) and two independent transgenes (II.1 and II.2) for each TEV cleavable C(2)M-HA construct inserted in the *ZH-attp-51D* line were analyzed for protein expression. All those lines showed expression of the respective protein (fig. 2.16), while none of the *ZH-attp-58A* lines showed protein expression (data not shown). Furthermore, despite the same insertion position in all transgenes in *ZH-attp-51D*, differences in levels of protein expression were observed. The expression of TEV cleavable C(2)M-HA was higher in *gc(2)M-3TEV(191)-HA II.1*, *gc(2)M-3TEV(250)-HA II.2* and *gc(2)M-3TEV(339)-HA II.2* than in *gc(2)M-3TEV(191)-HA II.2*, *gc(2)M-3TEV(250)-HA II.1* and *gc(2)M-3TEV(339)-HA II.1*. Moreover, the expression of C(2)M without engineered TEV sites (C(2)M-HA)

appeared to be higher than in all the TEV cleavable C(2)M-HA expressing lines (fig. 2.16).

To analyze if the TEV cleavage sites present in C(2)M-HA are accessible to TEV protease, an *in-vitro* cleavage assay was performed. Protein extracts were prepared from egg chambers up to stage 10 and incubated with recombinant His-TEV protease. The blot was probed with an antibody against HA.

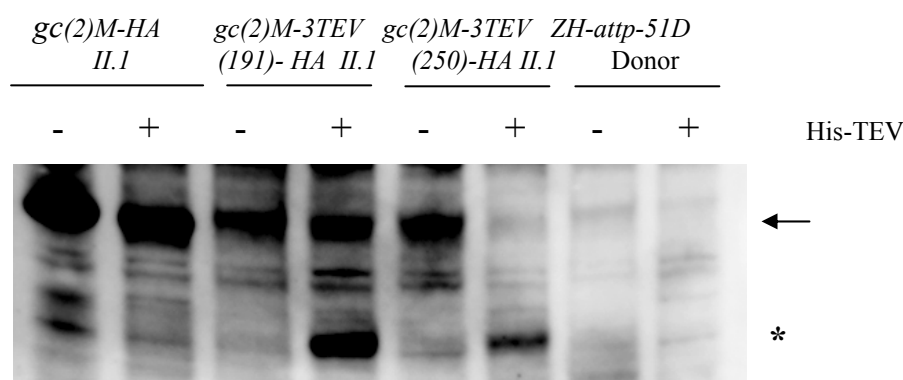


Figure 2.17 In-vitro cleavage of TEV cleavable C(2)M-HA protein. Extracts were prepared from ovarioles up to stage 10 egg chambers from 20 females and incubated at 30°C with (+) or without (-) recombinant His-TEV protease. Western blot analysis using an antibody against HA shows full length protein (arrow) and C-terminal TEV cleavage products (asterisk).

Western blot analysis showed that both C(2)M-3TEV(191)-HA and C(2)M-3TEV(250)-HA were cleaved. As expected, a 57 kDa C-terminal fragment for position 191 aa and a 50 kDa fragment for position 250 aa were visible after cleavage with His-TEV protease (Fig 2.17).

2.3.3 Localization of C(2)M-HA and C(2)M-3TEV(191/250/339)-HA

To determine the subcellular localization of the C(2)M-3TEV(191/250/339)-HA variants, immunofluorescence microscopy was performed on ovarioles using co-staining of C(3)G. Consistent with previous reports (Manheim and McKim, 2003) (Heidmann et al., 2004) C(2)M-HA, C(2)M-3TEV(191)-HA and C(2)M-3TEV(250)-HA were found to localize to the pro-nurse cell and the pro-oocyte in a thread-like pattern along the lengths of chromosomes (Fig 2.18 i,1,o). However C(2)M-

3TEV(191)-HA and C(2)M-3TEV(250)-HA were more diffusely localized in the nucleus. In contrast, the third variant C(2)M-3TEV(339)-HA did not localize to the pro-nurse cell and the pro-oocyte (fig. 2.18 r). The *gC(2)M-myc III.3* transgenic line was used as positive control; C(2)M-myc had previously been shown to localize to the pro-nurse cell and the pro-oocyte (Fig 2.18 f) (Heidmann et al., 2004).

2.3.4 The TEV cleavable C(2)M-HA variants are not biologically functional

To determine whether the TEV cleavable C(2)M proteins are biologically functional, rescue experiments were performed using the *c(2)M^{EP2115}* mutant. As reported previously, the localization and organization of the transversal SC component C(3)G is abrogated in *c(2)M^{EP2115}* mutants (Manheim and McKim, 2003). To check biological functionality, C(2)M-HA and C(2)M-3TEV(191 or 250)-HA were expressed in a *c(2)M^{EP2115}* mutant background and the C(3)G localization pattern was observed.

For this purpose, recombinant flies of the genotypes *gc(2)M-HA II.1, c(2)M^{EP2115}/CyO* and *gc(2)M-3TEV(191 or 250)-HA II.1/II.2, c(2)M^{EP2115}/CyO* were created. These recombinants were then crossed with *c(2)M^{EP2115}* mutants to obtain *gC(2)M-HA II.1, c(2)M^{EP2115} / c(2)M^{EP2115}* and *gC(2)M-3TEV(191 or 250)-HA II.1/II.2, c(2)M^{EP2115}/c(2)M^{EP2115}* females. The transgene *gC(2)M-myc III.1*, which had previously been reported to rescue the *c(2)M^{EP2115}* mutant phenotype (Heidmann et al., 2004), was used as a positive control. Ovaries were dissected and stained for DNA and C(3)G. Confocal microscopy was performed to analyze C(3)G localization.

As expected, the localization of C(3)G is abrogated in the *c(2)M^{EP2115}* mutant: C(3)G fails to assemble into the long ribbons like wild-type and instead several short segments of C(3)G staining were visible (Fig 2.19 A, a-c), which were restricted to the pro-oocytes as previously reported (Manheim and McKim, 2003). As shown previously, this phenotype of *c(2)M^{EP2115}* was completely rescued by the *gc(2)M-myc III.3* transgene (Fig 2.19). Similarly, the localization of C(3)G in the germaria of the *gc(2)M-HA II.1, c(2)M^{EP2115} / c(2)M^{EP2115}* females was comparable to that of wild type (Fig 2.19 E, m-o) suggesting that C(2)M-HA is a biologically functional protein.

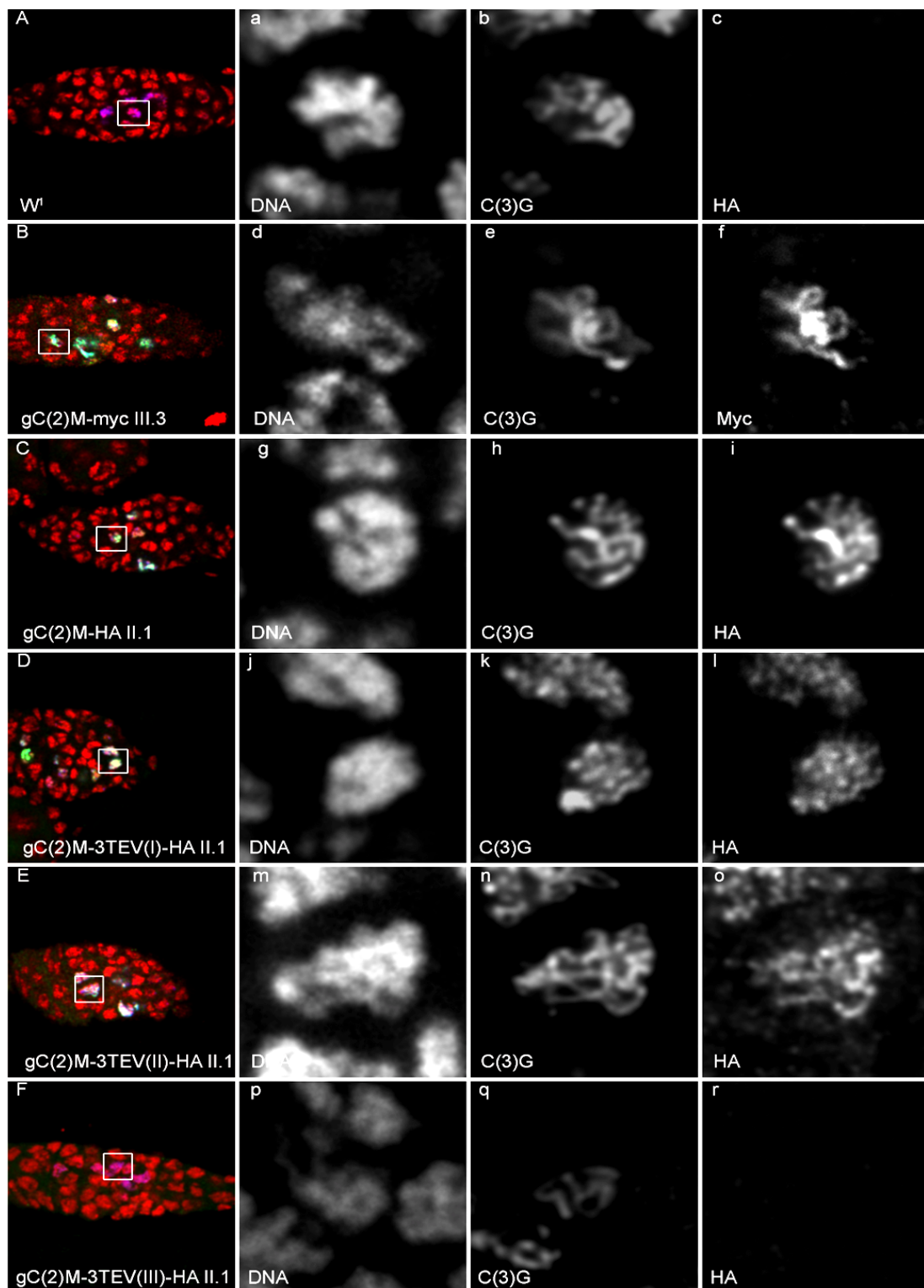


Figure 2.18 C(2)M-HA, C(2)M-3TEV(I)-HA and C(2)M-3TEV(II)-HA colocalize with C(3)G in a thread like pattern associated with nuclear DNA of pro-oocyte. A-F Germaria of individuals with genotype **A** *w¹*, **B** *gC(2)M-myc III.3*, **C** *gC(2)M-HA II.1*, **D** *gC(2)M-3TEV(191)-HA II.1*, **E** *gC(2)M-3TEV(250)-HA II.1* and **F** *gC(2)M-3TEV(339)-HA II.1* were stained with anti-HA or anti-myc in B, d-f (blue in the left panels) to detect transgenic C(2)M, anti-C(3)G (green in the left panels) to visualize the nuclei of the pro-oocytes, and DNA (red in the left panels). **a-c**, **d-f**, **g-i**, **j-l**, **m-o** and **p-r** are the enlargements of insets shown in **A**, **B**, **C**, **D**, **E** and **F** respectively, with the focus on pro-oocyte nuclei.

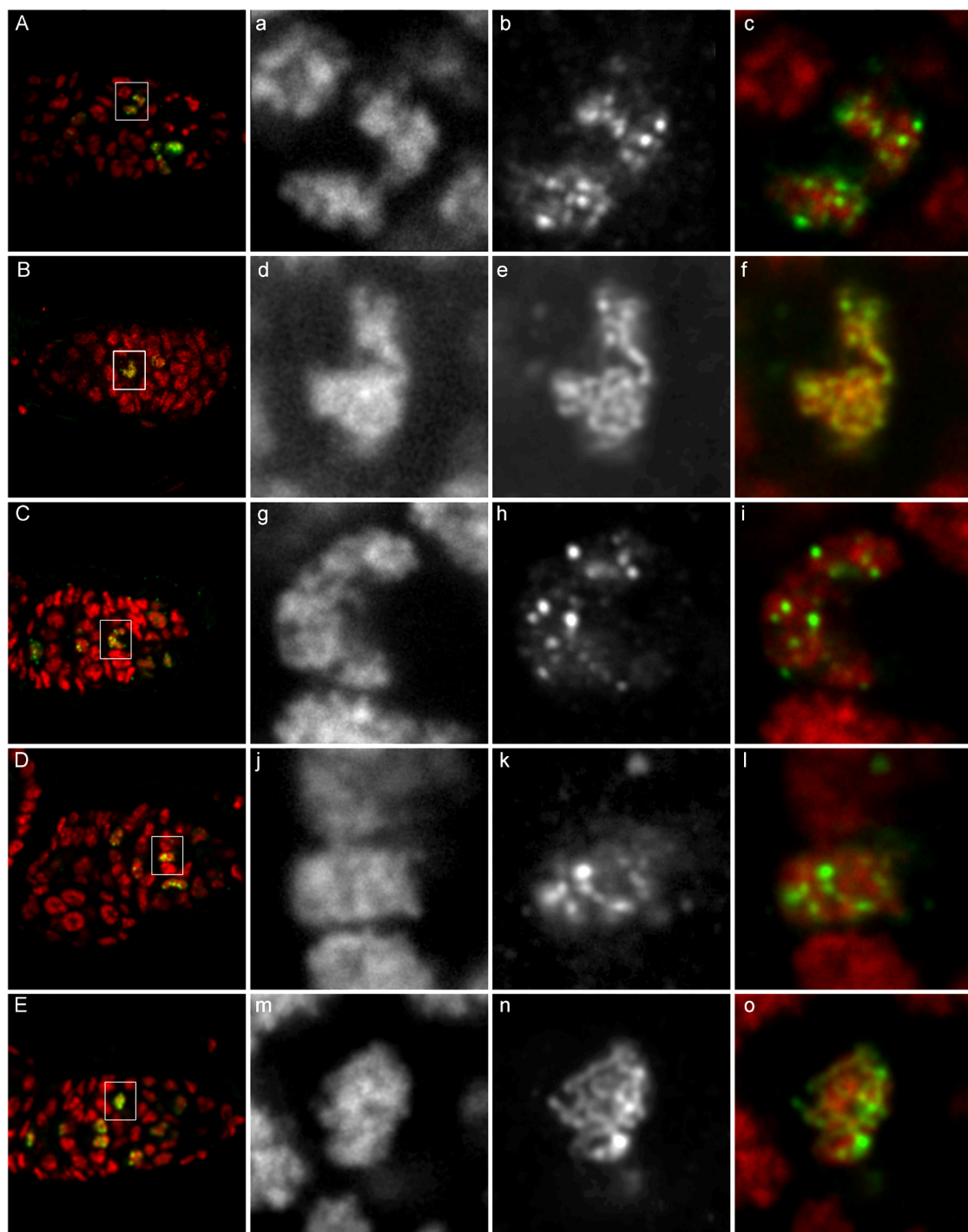


Figure 2.19 Rescue of C(3)G localization in $c(2)M^{EP2115}$ mutant by C(2)M transgenes. A-E Germlaria of individuals with the genotypes **A** $c(2)M^{EP2115}$, **B** $c(2)M^{EP2115}$, $gc(2)M-myc\ III.3$, **C** $c(2)M^{EP2115}$, $gc(2)M-3TEV(191)-HA\ II.1/c(2)M^{EP2115}$, **D** $c(2)M^{EP2115}$, $gc(2)M-3TEV(250)-HA\ II.2/c(2)M^{EP2115}$ and **E** $c(2)M^{EP2115}$, $gC(2)M-HA\ II.1/c(2)M^{EP2115}$ were stained with anti-C(3)G (green) and DNA (red). A magnified view of insets in **A**, **B**, **C**, **D** and **E** are shown in **a-c**, **d-f**, **g-i**, **j-l** and **m-o** respectively. **a**, **d**, **g**, **j**, **m** Stained for DNA. **b** **e**, **h**, **k**, **n** Stained for C(3)G. **c**, **f**, **i**, **l**, **o** are merged images of **a-b**, **d-e**, **g-h**, **i-k** and **m-n** respectively. Localization of C(3)G is rescued by $gC(2)M-HA\ II.1$ but not by $gc(2)M-3TEV(191)-HA\ II.1$ or $gc(2)M-3TEV(250)-HA\ II.2$.

In contrast, in the case of the TEV cleavable C(2)M-HA variants C(2)M-3TEV(191)-HA and C(2)M-3TEV(250)-HA, the localization pattern of C(3)G was similar to that of *c(2)M^{EP2115}* mutants (Fig 2.12), indicating that these proteins are not biologically functional.

Chapter III Discussion

Faithful duplication and segregation of genetic information to daughter cells is a fundamental attribute of life. There are two essential prerequisites for accurate segregation of chromosomes: First, the compaction and individualization of chromosomes into a transportable form, which must be completed prior to metaphase. Second, the cohesion between the replicated sister chromatids, which is established during replication, should be maintained until the onset of anaphase and timely resolved at the metaphase-to-anaphase transition.

Accumulating lines of evidence suggest that in higher eukaryotes, the establishment of a correct mitotic chromosome structure is regulated by two related heteropentameric protein complexes, condensin I and condensin II (Hirano et al., 1997; Ono et al., 2003). However, it is still unknown how these complexes compact interphase chromatin into a well-organized mitotic chromosome. While the contributions of the two condensin complexes in early mitosis has been clearly demonstrated in vertebrates (Gerlich et al., 2006a; Hirota et al., 2004; Ono et al., 2004; Ono et al., 2003) and plants (Fujimoto et al., 2005), the situation is less clear in *Drosophila*. Among the condensin II-specific non-SMC subunits, homologues for CapH2 and CapD3 have been identified (Hartl et al., 2008; Savvidou et al., 2005). However, a homolog for CapG2 still awaits its identification leading to the supposition that CapG might be a common component of both condensin I and condensin II (Resnick et al., 2009). Consistent with this notion, the localization studies using CapG-EGFP demonstrate nuclear enrichment in interphase, which has also been found for vertebrate condensin II subunits, while the vertebrate condensin I-specific subunits are mainly cytoplasmic (Hirota et al., 2004; Ono et al., 2004). However, several lines of evidence indicate that in *Drosophila* CapG is not part of a condensin II-like complex and a bona fide condensin II complex might not be involved in mitotic chromosome condensation at all. First, genetic and biochemical assays fail to support an interaction between CapG with CapH2 and/or CapD3 (S. Herzog, unpublished). Second, CapD3 (Savvidou et al., 2005) and CapH2 (S. Herzog, unpublished) do not localize to mitotic chromatin. Third, CapH2 and CapD3 loss-of-function mutants are viable, but male sterile (Hartl et al., 2008; Savvidou et al., 2005). Thus, specific roles for these two proteins during male meiosis have been suggested (Hartl et al., 2008; Savvidou et al.,

2005). CapH2 mutants also show defects during dispersal of polytene chromosomes in nurse cells and an enhancement of transvection phenomena, which are based on influences in gene expression patterns across paired homologous chromosomes in somatic cells. Thus, it has been proposed that condensin II in *Drosophila* might inhibit homology-dependent chromosomal interactions in diploid somatic cells (Hartl et al., 2008). Taken together, the available data suggest that in *Drosophila* CapD3 and CapH2 have evolved to fulfill roles other than establishing/maintaining a mitotic chromosome structure. They probably do so without participation of CapG and may act either without a CapG2 homolog or a CapG2-related protein that has considerably evolved thus escaping detection using sophisticated bioinformatic queries.

If CapG does not function within a condensin II complex, what is the significance of its nuclear localization in interphase, which is clearly distinct from the localization pattern of both CapH/Barren and CapD2 as well as Smc4 (Oliveira et al., 2007; Savvidou et al., 2005; Steffensen et al., 2001) CapG might be involved in gene regulation as has been suggested earlier by demonstrating a dominant suppression of position effect variegation (PEV) at the *white^{m4h}* locus by one copy of embryonic lethal CapG alleles (Dej et al., 2004). PEV is the effect on gene expression mediated by the chromatin structure associated with heterochromatic regions (Reuter and Spierer, 1992). A subsequent study investigating a different *CapG*-allele also demonstrated an effect on PEV, albeit in the opposite direction (enhancement), a result which might be due to the nature of this allele (missense vs. nonsense)(Cobbe et al., 2006). However, how CapG might perform the enhancement/suppression of PEV is still unknown.

Additional experiments are required to assess whether the nuclear localized CapG is associated with chromatin or whether it is distributed in the nucleoplasm. Furthermore, it needs to be established whether CapG fulfills any interphase function independent of the other condensin I subunits or whether it functions outside the condensin complex. Even though the localization studies of CapH/Barren, Smc4 and CapD2 demonstrate a preferential cytoplasmic localization of these proteins, they do not rule out that a fraction of these proteins is present in the nuclei and associated with CapG.

The dynamic analyses have revealed further differences between the condensin subunits. The results obtained for CapG are best comparable with those published for

CapH/Barren, as in both cases the same technology for analyzing the behavior of biologically functional, EGFP-tagged variants was employed. CapH/Barren starts to associate with chromatin before nuclear envelope breakdown (NEBD) unlike vertebrates where condensin I gains access to the chromosomes only after NEBD (Oliveira et al., 2007). Based on this observation it was suggested that in *Drosophila* condensin I is the major complex required for the organization of mitotic chromosomes (Oliveira et al., 2007). CapG also starts to load well before NEBD but loading is complete at the time of NEBD while in the case of CapH/Barren loading is about 50% complete and reaches maximal levels about 1 min after NEBD. This difference suggests that CapG can associate with chromatin independent of CapH/Barren. Whether this difference in timing of chromatin association is of functional significance needs to be addressed in future experiments. Moreover, dynamic analysis of CapG-EGFP showed that the majority of CapG-EGFP ($\approx 82.5\%$) was stably bound to chromatin during metaphase and only 17.5% was mobile while for CapH/Barren it was reported that the majority of chromatin bound protein ($\approx 84\%$) exchanged dynamically with the cytoplasmic pool (Oliveira et al., 2007). Finally, localization analyses of CapG fragments have shown that the C-terminal third of CapG preferentially associates with chromatin in late anaphase, at a time point when chromatin is vigorously depleted of CapH/Barren (S. Herzog, personal communication). These observations also suggest that CapG can interact with chromatin independent of CapH/Barren, which implies that the textbook model of the condensin complex topology (see Fig. 1.4) which has been corroborated experimentally (Onn et al., 2007) may not apply throughout the cell cycle or at every occasion. These findings also suggest that the condensin complex does not associate with the chromatin as a pre-assembled complex as reported previously (Hirano et al., 1997), rather it appears that the condensin I complex is assembled sequentially. CapG and CapD2 (Savvidou et al., 2005) associate with chromatin during late interphase and then in early mitosis CapH/Barren and presumably SMC subunits join, forming the holocomplex. However, to further confirm this hypothesis it would be necessary to compare data from different subunits using the same methodology.

The simultaneous in-vivo analysis of CapG-EGFP and Cid-mRFP1 revealed that CapG loading initiates at the centromere/centromeric proximal regions. Afterwards

CapG spreads along the chromosomes arms. This finding is consistent with a previous report where a similar pattern of loading was reported for the condensin I subunit CapH/Barren (Oliveira et al., 2007). This observation, together with a previous report where it was shown that *Drosophila* CapG genetically and physically interacts with Cid (Jager et al., 2005), support the notion that condensin I might use the kinetochore as an entry point for chromatin association. Interestingly, the physical interaction between Cid and CapG could be demonstrated only for an N-terminal CapG-fragment (Jager et al., 2005) and none of the N-terminal truncated CapG fragments associates with chromatin in early to mid mitosis. This could mean that either the N-terminal truncated fragments do not bind mitotic chromatin because they can't access the entry point, or, alternatively, the truncations destroy the interface of interaction with other condensin subunits. Further experiments are required to resolve this issue.

In the second part of my thesis, a cohesive role for Rad21 and C(2)M during female meiotic divisions was analyzed. In most organisms, meiotic cohesion is mediated by a specialized cohesin complex, in which the α -kleisin subunit Rad21/Scc1 has been replaced by the meiosis-specific α -kleisin Rec8 (Eijpe et al., 2003; Kitajima et al., 2003; Klein et al., 1999; Pasierbek et al., 2001). In budding yeast, the other three cohesin subunits correspond to the complement found in the mitotic complex, while in humans also meiotic variants of SCC3 (STAG3) and of SMC1 (SMC1 β) are incorporated into the complex. Surprisingly, in *Drosophila* no clear homologue of Rec8 has been identified yet. An α -kleisin family protein, C(2)M, has been reported to be expressed during meiosis (Manheim and McKim, 2003; Heidmann et al., 2004). C(2)M is a SC protein which was shown to interact with the Smc3 subunit of the cohesin complex (Heidmann et al., 2004). Due to its α -kleisin nature and interaction with Smc1 protein, it was speculated that C(2)M is a divergent homologue of Rec8 in *Drosophila*, and that it is involved in meiotic sister chromatid cohesion. However, C(2)M accumulates predominantly after the pre-meiotic S-phase and it disappears too early from oocyte chromatin to be involved in mediating cohesion during meiosis I. Furthermore, separase dependent cleavage products cannot be detected and a putative non-cleavable variant has no effect on the fidelity of meiotic chromosome segregation. Thus, these results suggested that C(2)M has either no role in meiotic sister chromatid

cohesion or that it functions redundantly with the mitotic α -kleisin Rad21, which is also expressed during meiosis (Heidmann et al., 2004).

To assess the role of Rad21 during female meiosis in *Drosophila*, cohesion between homologues and sister chromatids was analyzed in *Rad21^{ex8}* and *c(2)M^{EP};Rad21^{ex8}* mutant oocytes. For generating *Rad21^{ex8}* mutant oocytes, TEV protease was expressed in growing oocytes of females which contain Rad21-3TEV-myc as the sole source of Rad21. Similarly, for generating *C(2)M^{EP};Rad21^{ex8}* oocytes, TEV protease was expressed in oocytes of females homozygous for the *c(2)M* mutant allele *c(2)M^{EP}*, and Rad21-3TEV-myc as the sole source of Rad21. Western blot analysis for Rad21-3TEV-myc cleavage showed that the expression of TEV protease causes up to 95% cleavage of full length Rad21-3TEV-myc in stage 14 oocytes.

There are several studies which suggest that cohesin in general and Rec8 in particular are required for the formation of axial elements of the SC in various systems (Eijpe et al., 2000; Eijpe et al., 2003; Klein et al., 1999; Lee et al., 2003; Pelttari et al., 2001; Pezzi et al., 2000; Revenkova et al., 2004). I checked whether the mitotic α -kleisin Rad21 is required for SC assembly. The analysis of C(3)G localization in *Rad21^{ex8}* oocytes showed that after Rad21 cleavage, C(3)G delocalizes from the chromosomes and the SC disassembles. Thus, this result clearly indicates that Rad21 has a role in the maintenance of SC. It is impossible from the presented experiments to deduce whether Rad21 is also required for the formation of the SC, because TEV expression initiates at a time point when the SC has been formed already. The SC phenotype shown by *Rad21^{ex8}* oocytes was similar to that of *c(2)M^{EP}* mutant oocytes, and *c(2)M^{EP};Rad21^{ex8}* double mutant oocytes did not show a more severe phenotype. This indicates that both proteins work in the same pathway. To assess epistatic relationships, experiments should be performed in which the localization of Rad21-myc is analyzed in *c(2)M^{EP}* mutant oocytes and of epitope tagged C(2)M in *Rad21^{ex8}* oocytes. Furthermore, it should be analyzed how Rad21 contributes to SC formation/maintenance and whether it provides the basis for SC and recruits SC components by interacting with them like Rec8 does (Eijpe et al., 2003; Hartsuiker et al., 2001; Lee et al., 2003; van Heemst and Heyting, 2000).

Smc1 localization analysis in oocytes revealed that Smc1 appeared to be lost from chromosomes after Rad21 cleavage. This result clearly indicates that Rad21 is required

for Smc1 localization to chromosomes during meiosis, just like the integrity of Rad21 is required for chromosomal association of Smc1/Smc3 during mitotic divisions. In analogy to cohesion dissolution during mitotic divisions, this disappearance most likely is due to opening the tripartite ring formed by Smc1, Smc3 and Rad21/Sccl which entraps replicated sister chromatids (Gruber et al., 2003). The cohesin ring opens after Rad21 cleavage which then falls off from chromosomes and Smc1 can no longer localize to chromosomes. Loss of cohesion after forced Rad21 cleavage was further confirmed by observing Cenp-C foci during prophase I. The number of Cenp-C foci observed in *Rad21^{ex8}* and *C(2)M^{EP};Rad21^{ex8}* mutant oocytes were more than four. However, 16 foci expected for fully separated homologs and sister chromatids were never observed. Most likely, in the absence of pulling forces the majority of chromosomes and chromatids remain closely associated despite the destruction of cohesin. The number of Cenp-C foci in *c(2)M^{EP}* mutant oocytes were 4 four or less than 4 four. Importantly, an increase in the number of Cenp-C foci in mutants was *Rad21^{ex8}* observed despite the presence of wild type C(2)M protein. This strongly suggests that C(2)M does not play a redundant role with Rad21 in meiotic cohesion.

The *in-vitro* activation data revealed that almost 60% of *Rad21^{ex8}* mutant oocytes showed abnormal meiotic figures. During meiosis I, homolog nondisjunction was observed due to the loss of cohesion between them. Moreover, *Rad21^{ex8}* mutant oocytes also exhibited complete separation of sister chromatids in both meiotic divisions. In contrast, although 30% of *c(2)M^{EP}* mutant oocytes also exhibited homolog non- disjunction, no premature sister chromatid separation was observed. In *c(2)M^{EP};Rad21^{ex8}* double mutant oocytes, 83% exhibited abnormal meiotic figures. Both phenotypes, homolog non- disjunction and premature sister chromatid separation, were observed during meiosis I and II. The increase in the number of abnormal meiotic figures in the *c(2)M^{EP};Rad21^{ex8}* double mutant oocytes most likely is due to the additive effect of Rad21 cleavage and presence of the *c(2)M^{EP}* homozygous mutant situation.

Altogether these preliminary results suggest that Rad21 is the α -kleisin subunit incorporated in the cohesin complex during *Drosophila* female meiosis, and in that way involved in maintenance of the SC as well as in keeping sister chromatids in association until the onset of the meiotic divisions at the time of fertilization. Thus,

this work identifies the first example of a eukaryotic system in which the mitotic α -kleisin functions also in meiosis.

Recently, a novel protein called Sisters on the Loose (SOLO) has been identified to be required for sister chromatid cohesion in male meiosis in *Drosophila* (Yan et al., 2010). SOLO colocalizes with Smc1 on meiotic chromatin, disappears at anaphase II and mutants show high rates of chromosome missegregation associated with an unusual high number of centromeric foci in developing sperm (Yan et al., 2010). Thus, SOLO displays characteristics of a meiotic cohesin, with the exception that the primary sequence of the protein does not show any homology to one of the known cohesin components. At present, the exact function of SOLO with respect to cohesin formation and establishment is unclear, however, it will be interesting to investigate a possible interaction between SOLO and Rad21, e.g. whether they coexist in the same complex in males and maybe also females.

Chapter IV Materials and methods

All the solutions used in this section are listed in table 4.17, and antibodies and their dilutions are listed in table 4.18.1 through 4.18.3.

4.1 *Drosophila* lines

All the *Drosophila* lines used in this thesis work are listed below, where the nature of the *w** allele is not certain.

Table 4.1.1 List of mutant strains

Genotype	Chromosome	Reference
<i>w^l</i>	X	Lindsley and Zimm, 1992
<i>w*</i> ; <i>CapG^l/ CyO, P[ry⁺, ftz lacZ]</i>	II	Jager et al., 2005
<i>w*</i> ; <i>CapG³/ CyO, P[ry⁺, ftz lacZ]</i>	II	Jager et al., 2005
<i>w*</i> ; <i>CapG⁶/ CyO, P[ry⁺, ftz lacZ]</i>	II	Jager et al., 2005
<i>w*</i> ; <i>CapG⁶⁴/ CyO, P[ry⁺, ftz lacZ]</i>	II	Cobbe et al., 2006
<i>w*</i> ; <i>CapG^{EP(2)2346}/ CyO, P[ry⁺, ftz lacZ]</i>	II	Jager et al., 2005
<i>w*</i> ; <i>string^{7B}, P[w⁺, Hs-string] /TM3, Ser</i>	III	Sauer et al., 1995
<i>w*</i> ; <i>Rad21^{ex3} / TM3, Ser</i>	III	Pauli et al., 2008
<i>w*</i> ; <i>c(2)M^{EP2115}</i>	II	Manheim and McKim, 2003

Table 4.1.2 List of GAL4 strains

Genotype	Chromosome	Source	Reference
<i>mat α- tub-GAL4- VP16</i>	II	Bloomington	Micklem et al., 1997
<i>mat α- tub-GAL4-VP16</i>	III	Bloomington	Micklem et al., 1997
<i>w*</i> ; <i>P[w⁺, ey-GAL4]</i>	II	Bloomington	Hazelett et al., 1998
<i>w*</i> ; <i>P[w⁺, GMR-GAL4]</i>	II	Bloomington	Freeman, 1996
<i>w*</i> ; <i>P[w⁺, -da-GAL4] G.32</i>	III	Bloomington	Wodarz et al., 1995
<i>w*</i> ; <i>P[w⁺, prd-GAL4]</i>	III	Bloomington	Brand and Perrimon, 1993

Table 4.1.3 List of Balancer stocks

Strain	Chromosome	Reference
<i>w*</i> ; <i>Sco / CyO, P[ry⁺, ftz lacZ]</i>	II	Lindsley and Zimm, 1992
<i>w*</i> ; <i>Sb / TM3, Ser</i>	III	Lindsley and Zimm, 1992
<i>w*</i> ; <i>Sco / CyO, ftz-lacZ ; D/TM3, Sb, P[w⁺, Ubx-lacZ]</i>	II & III	Lindsley and Zimm, 1992

Table 4.1.4 List of transgenic strains

Genotype	Chromosome	Reference
<i>w*</i> ; <i>P[w⁺, UASPI-CapG-EGFP]</i> <i>III.1/TM3,Ser</i>	III	S. Heidmann, K. Trunzer Unpublished
<i>w*</i> ; <i>P[w⁺, UASPI-CapG-EGFP]</i> <i>III.2/TM3,Ser</i>	III	S. Heidmann, (K. Trunzer) Unpublished
<i>w*</i> ; <i>P[w⁺, UASPI-CapG-EGFP]</i> <i>III.3/TM3,Ser</i>	III	S. Heidmann, K. Trunzer Unpublished
<i>w*</i> ; <i>P[w⁺, UASPI-CapG-</i> <i>mRFP1]</i> <i>III.1/TM3,Ser</i>	III	S. Heidmann, K. Trunzer Unpublished
<i>w*</i> ; <i>P[w⁺, UASPI-CapG-</i> <i>mRFP1]</i> <i>III.2/TM3,Ser</i>	III	S. Heidmann, K. Trunzer Unpublished
<i>w^l</i> ; <i>pBAC[3xP3-EGFP,gCapG-</i> <i>EGFP III.1] /TM3,Ser</i>	III	S. Heidmann, K. Trunzer Unpublished
<i>w*</i> ; <i>pBAC[3xP3-EGFP gCapG-</i> <i>mRFP1]</i> <i>III.1/TM3,Ser</i>	III	S. Heidmann, K. Trunzer Unpublished
<i>w*</i> ; <i>pBAC[3xP3-EGFP gCapG-</i> <i>mRFP1]</i> <i>/TM3,Ser</i>	III	S. Heidmann, K. Trunzer Unpublished
<i>w*</i> ; <i>P[w⁺, His2AvD-mRFP1]</i> <i>III.1] /TM3,Ser</i>	III	Schuh et al., 2007
<i>Cid-mRFP-Cid II.1,II.2/ CyO,</i> <i>P[ry⁺, ftz lacZ]</i>	II	Schuh et al., 2007
<i>w*</i> ; <i>P[w⁺, UASPI-Barren-</i> <i>EGFP III.1]/ MKRS</i>	III	Oliveira et al., 2007
<i>Rad21^{ex3}, tubpr<Rad21 (3TEV-</i> <i>271) myc10 (AP405)</i>	III	Pauli et al., 2008
<i>Rad21^{ex8}, tubpr<Rad21 (3TEV-</i> <i>271) myc10 (AP360)</i>	III	Pauli et al., 2008

Table 4.1.5 List of UAS and genomic transgenic strains created in this work

Genotype	Chromosome	position
<i>w*</i> ; <i>P[w⁺, UASPI-TEV] II.1</i>	II	-
<i>w*</i> ; <i>P[w⁺, UASPI-TEV^{S219V}] II.1</i>	II	-
<i>w*</i> ; <i>pattB[w⁺, gC(2)M-HA] II.1</i>	II	58A
<i>w*</i> ; <i>pattB[w⁺, gC(2)M-3TEV(I)-HA]II.1</i>	II	58A
<i>w*</i> ; <i>pattB[w⁺, gC(2)M-3TEV(II)-HA]II.1</i>	II	58A
<i>w*</i> ; <i>pattB[w⁺, gC(2)M-HA] II.1</i>	II	51D
<i>w*</i> ; <i>pattB[w⁺, gC(2)M-3TEV(I)-HA]II.1</i>	II	51D
<i>w*</i> ; <i>pattB[w⁺, gC(2)M-3TEV(I)-HA]II.2</i>	II	51D
<i>w*</i> ; <i>pattB[w⁺, gC(2)M-3TEV(II)-HA]II.1</i>	II	51D
<i>w*</i> ; <i>pattB[w⁺, gC(2)M-3TEV(II)-HA]II.2</i>	II	51D
<i>w*</i> ; <i>pattB[w⁺, gC(2)M-3TEV(III)-HA]II.1</i>	II	51D
<i>w*</i> ; <i>pattB[w⁺, gC(2)M-3TEV(III)-HA]II.2</i>	II	51D

Genotype	Chromosome	position
<i>w*</i> ; <i>pBAC[3xP3-EGFP,gC(2)M-3TEV(I)-HA] III.1</i>	III	-
<i>w*</i> ; <i>pBAC[3xP3-EGFP,gC(2)M-3TEV(II)-HA] III.1</i>	III	-

Table 4.1.6 List of stocks generated in this work

All stocks carry an uncharacterized allele in the *white* gene (*w**) . For clarity, the allele and the nature of the transposons (P-element, piggy Bac) have been omitted from the genotypes in the list. The exact genotype of the various transgenes insertions can be found in tables 4.1.1 to 4.1.5.

Genotype	Chromosomes
<i>CapG¹/ CyO; da-GAL4/ TM3,Sb</i>	II & III
<i>CapG³/ CyO; da-GAL4/ TM3,Sb</i>	II & III
<i>CapG⁶/ CyO; da-GAL4/ TM3,Sb</i>	II & III
<i>CapG^{1/3/6}/ CyO; UASPI-CapG-EGFP III.1/ TM3,Sb</i>	II & III
<i>CapG^{1/3/6}/ CyO; UASPI-CapG-EGFP III.2/ TM3,Sb</i>	II & III
<i>CapG^{1/3/6}/ CyO; UASPI-CapG-EGFP III.3/ TM3,Sb</i>	II & III
<i>CapG^{1/3/6}/ CyO; UASPI-CapG-mRFP1 III.1/ TM3,Sb</i>	II & III
<i>CapG^{1/3/6}/ CyO; UASPI-CapG-mRFP1 III.2/ TM3,Sb</i>	II & III
<i>CapG^{1/3/6}/ CyO; gCapG-EGFP III.1/ TM3,Sb</i>	II & III
<i>CapG^{1/3/6}/ CyO; gCapG- mRFP1 III.1/ TM3,Sb</i>	II & III
<i>CapG^{1/3/6}/ CyO; gCapG- mRFP1 III.2/ TM3,Sb</i>	II & III
<i>UASPI-TEV II.1/CyO ; D/TM3,Sb</i>	II & III
<i>mat α- tub-GAL/CyO ; D/TM3,Sb</i>	II & III
<i>Sco/CyO ; Rad21^{ex3}, tubpr<Rad21 (3TEV-271) 10myc /TM3,Sb</i>	II & III
<i>Sco/CyO ; Rad21^{ex8}, tubpr<Rad21 (3TEV-271) 10myc /TM3,Sb</i>	II & III
<i>UASPI-TEV II.1/CyO ; Rad21^{ex8}, tubpr<Rad21 (3TEV-271) 10myc /TM3,Sb</i>	II & III
<i>mat α- tub-GAL4/CyO ; Rad21^{ex8}, tubpr<Rad21 (3TEV-271) 10myc /TM3,Sb</i>	II & III
<i>UASPI-TEV II.1, C(2)M^{EP}/CyO ; Rad21^{ex8}, tubpr<Rad21 (3TEV-271)10 myc /TM3,Sb</i>	II & III
<i>mat α- tub-GAL4, C(2)M^{EP}/CyO ; Rad21^{ex8}, tubpr<Rad21 (3TEV-271) 10myc /TM3,Sb</i>	II & III
<i>UASPI-TEV^{SV} II.2, C(2)M^{EP} /CyO ; Rad21^{ex8}, tubpr<Rad21 (3TEV-271)10 myc /TM3,Sb</i>	II & III
<i>C(2)M^{EP}/CyO ; Rad21^{ex8} /TM3,Sb</i>	II & III
<i>gCapG-EGFP III.1, His2AvD III.1/ TM3, Ser</i>	III
<i>UASPI-CapG-EGFP III.2, mat α- tub-GAL4-VP16 / TM3,Ser</i>	III
<i>gCapG-EGFP III.1, string^{7B}, P[w⁺,Hs-string] / TM3, Ser</i>	III
<i>gC(2)M-HA II.1 (51D), C(2)M^{EP} / CyO</i>	II

Genotype	Chromosomes
<i>gC(2)M-3TEV-HA II.1(51D), C(2)M^{EP} / CyO</i>	II
<i>gC(2)M-3TEV-HA II.1 (51D), C(2)M^{EP} / CyO</i>	II
<i>UASPI-TEV II.1, C(2)M^{EP}</i>	II
<i>mat α- tub-GAL4, C(2)M^{EP}</i>	II
<i>UASPI-TEV^{S219V} II.2, C(2)M^{EP}</i>	II

4.2 Quantitative analysis of loading of CapG-EGFP onto the chromatin

For analyzing loading of CapG-EGFP during early mitotic divisions, 60-90 min old embryos from *gCapG-EGFP III.1* with *His2AvD-mRFP1 III.1/ TM3, Ser* females were collected, dechorionated in 50% Bleach for 3 min, mounted on a coverslip and covered with halocarbon oil (VoLTALEF 10S, Lehmann & Voss & co.). Two dimensional stacks of embryos going through mitosis 12 were acquired every 18s with a Zeiss LSM 510 confocal microscope equipped with 63x/ 1.40 oil immersion objective, a 488 nm Ar laser line and a 543 nm He/Ne laser line were used to excite EGFP and mRFP1 respectively. The intensities of the laser lines were adjusted to minimize photo damage while allowing recording significant, but not saturating fluorescent signals (typically 3% intensity for the 488 nm laser line and 7% for the 543 nm laser line). All movies were aligned by setting the last metaphase plate as time point $t = 0$. In order to select for the chromosomal area, images from both channels were split, based on a 85% threshold in the His2AvD-mRFP1 channel. The CapG-EGFP mean intensities within the chromosomal area were normalized (by setting the last metaphase plate intensity = 1) and corrected for chromatin compaction changes (by dividing by the normalized mean intensity of HisH2Av-mRFP1 at the same time point), using the formula: $\text{Relative Fluorescent Intensity (R.F.I.)} = [I_{\text{CapG}}^t / I_{\text{CapG}}^{t_0}] / [I_{\text{Hist}}^t / I_{\text{Hist}}^{t_0}]$, where $I_{\text{CapG}/\text{Hist}}$ equals the mean fluorescence intensity of CapG-EGFP / HisH2Av-mRFP1 at each time point. Quantitative analysis was performed using Image J 1.3v (<http://rsb.info.nih.gov/ij/>). All calculations were done using Microsoft Excel.

4.3 Quantitative analysis of dynamic association of fluorescently labeled condensin subunits with chromatin

Embryos expressing either CapG-EGFP or Barren-EGFP (Oliveira et al., 2007) in combination with His2AvD-mRFP1 were collected for 1 hr and aged for 30 min, dechorionated, aligned on a glass cover slip and covered with halocarbon oil (VoLTALEF 10S, Lehmann & Voss & co.). Fluorescent Recovery After Photobleaching (FRAP) analysis was performed using the FRAP WIZARD of a Leica SP5 confocal microscope (Leica Microsystems, Germany) equipped with 63x/ 1.40 oil immersion objective. A metaphase plate was selected as region of interest (R.O.I.), after acquiring a pre-bleach image; the entire metaphase plate was photobleached by 2 pulses of 20% 488 nm Ar laser and post-bleach images were recorded every 9s by using 10% of the 488 nm Ar laser and 7% of a 561 nm DPSS561 laser. R.F.I. was calculated after background correction (B_C), as the ratio between the mean fluorescence intensity of bleached metaphase (I_B) and the mean fluorescence intensity of a non bleached metaphase plate (I_{NB}) of the same time point, using the formula : $R.F.I. = (I_B - B_C) / (I_{NB} - B_C)$. Data points were fit to a single exponential curve using the Origin version 8.0 software (Origin lab) by regression to: $y = A * (1 - e^{-b.x}) + y_0$. Half times of recovery were determined based on the formula: $t_{1/2} = \ln(0.5) / -b$. The mobile fraction (Fm) was calculated using the formula: $Fm = (RFI_{\infty} - RFI_0) / (1 - RFI_0)$, where RFI_{∞} is the maximal recovery and RFI_0 is the RFI at time zero (last metaphase plate). Both were calculated based on the regression curve equation).

4.4 Protein extraction and western blotting

4.4.1 Protein preparation from embryos

Embryos were collected for 3 hrs on apple juice agar plates, dechorionated in 50% bleach (Klorix) for 3 min, washed with NaCl-Tx (0.7% NaCl, 0.07% Triton-X 100) and homogenized using an eppendorf homogenizer in an appropriate volume of 3x laemmli buffer (see section 7.17) with protease inhibitors (2 mM Pefabloc, 0.35 mM Benzamidin, 10 µg/ml Aprotinin, 2 µg/ml Pepstatin and 10 mg/ml Leupeptin).

4.4.2 Protein preparation from embryos of different phases of mitosis 14

Synchronization of cell cycle and extract preparation from embryos of different phases of mitosis 14 was done as described in Sauer et al. (1995) with some modifications. Embryos were collected from *gCapG-EGFP III.1, string^{7B}, P[w⁺,Hs-string] / TM3, Ser* flies on apple juice agar plates for 30 min and aged for 160 min. At this time point all cells of homozygous mutant embryos are arrested in the G2 phase of mitosis 14. To obtain embryos in different mitotic phases, the collection plates were floated for 20 min in a water bath set at 37°C for 20 min to give a heat shock for inducing expression of Hs-String followed by recovery at 25°C for different time periods (5', 8', 12' and 15'). For preparing extracts from arrested G2 embryos, the collections were kept at 25°C for 20 min without the heat shock. All embryos were dechorionated, washed with EB buffer, fixed in heptane/methanol for 5 min on a wheel, treated with Hoechst 33258 (1 µg/ ml in EB) for 5 min on a wheel to stain the DNA and stored at -20 °C in EB buffer with 60% glycerol. Embryos were sorted according to their DNA morphology for different phases of mitosis 14 under an inverted Axiovert 25 microscope (Carl Zeiss, Germany), pooled and homogenized in KEB sample buffer.

4.4.3 Protein preparation from stage 6 to stage 10 egg chambers /ovaries

Stage 6 to stage 10 egg chambers or ovaries were dissected in 1xPBS and homogenized in an appropriate volume of 3 x laemmli buffer with protease inhibitors.

4.4.4 Sample preparation and western blotting

After homogenization samples were heated at 95°C for 5 min and centrifuged at maximum speed for 5 min in an eppendorf table-top centrifuge to sediment cellular debris. Samples of the supernatants were run on SDS Polyacrylamide gels at 100 volts in a BIO RAD MINI PROTEIN NTM system followed by blotting onto a nitrocellulose membrane (AmershamTM HybondTM ECL) for 1 hr at 100 volts in a wet transfer system (BIO RAD MINI PROTEIN NTM). The membrane was blocked with blocking buffer for 1 hr at room temperature and then probed with primary antibody diluted in

0.02% NaN₃ containing blocking buffer overnight at 4°C. After washing, the membrane was incubated with secondary antibody diluted in blocking buffer for 2 hrs at room temperature and further developed either by Amersham™ ECL plus or Amersham™ ECL advance kits from Amersham- GE Healthcare. Chemiluminescence signals were impressed on X-ray films (Amersham Hyperfilm™ ECL, Amersham- GE Healthcare) followed by development in a semi automatic machine (X-ray processor SRX-100, Konica) or directly recorded and digitized by an LAS 4000 (FUJIFILM Corporation, Europe). Images were processed by using Adobe Photoshop (Adobe Systems Inc., San Jose, CA, USA) and quantification of chemiluminescence signal was done by image analysis software MultiGauge (FUJIFILM Corporation, Europe).

4.5 In vitro cleavage assay using purified TEV protease

Ovaries were isolated in PBS, transferred to TEV protease reaction buffer, homogenized and incubated with 2 µl of TEV protease (5000 U/ µl, Prof. Olaf Stemman) at 30°C for 1 hr. Reactions were stopped by adding 3x Laemmli buffer. Samples were prepared and analyzed by western blotting as described above.

4.6 Mass isolation of S14 oocytes

Isolation of stage 14 (S14) oocytes was done by the mass isolation procedure of Theurkauf and Hawley, (1992). 1 day old females were fed on yeast for 4-5 days. Females were anesthetized and ground in 25 ml of Isolation buffer (prewarmed to room temperature (RT) by pulsing 5-6 times in a blender. The homogenate was filtered through a mesh, the debris was collected and again blended for 3 rounds in another 25 ml of Isolation buffer. Homogenates were pooled and filtered through a small mesh. Oocytes were allowed to settle by gravity and supernatants were removed with a vacuum pump. Fresh isolation buffer was added.

4.7 In vitro activation of S14 oocytes

In *Drosophila*, Mature oocytes (stage 14) arrest at metaphase I (Mahowald et al., 1983). Usually, these arrested oocytes are activated when they pass through the

oviduct. Ovulation triggers the resumption of meiosis and the two meiotic divisions are completed by the time the egg is fertilized and laid (Page and Orr-Weaver, 1997). However, meiosis can also be resumed by *in vitro* activation (Mahowald et al., 1983; Page and Orr-Weaver, 1997). For *in vitro* activation two Ca⁺ containing buffers are used in sequence; Activation buffer (AB) and Zalokar's buffer (ZAB). AB is a hypotonic solution in which oocytes get activated and ZAB is an isotonic buffer which allows recovery of oocytes (Mahowald et al., 1983; Page and Orr-Weaver, 1997). The osmotic and hydrostatic pressure applied by AB triggers the *in vitro* activation of oocytes. For activation of S14 oocytes protocol was adapted from (Page and Orr-Weaver, 1997). All the buffers were pre-warmed to room temperature. Mass isolated oocytes were incubated in activation buffer (prewarmed to RT) for 5 min with constant shaking. Activation buffer was replaced by Zalokar's buffer (prewarmed to RT) and oocytes were incubated for different time lengths with constant shaking at RT. For 5 min activation, oocytes were washed and fixed immediately after incubation in activation buffer. For 10 min and 20 min activation, oocytes were incubated in Zalokar's buffer for 5 min and 15 min, respectively. After activation, oocytes were washed with PBS, dechorionized, and fixed in two ways. Oocytes which were activated for 20 min were dechorionated in 50% bleach (klorix) for 3 min and fixed by shaking in a heptane /methanol in 1:1 mixture, while oocytes activated for 5 min and 10 min were transferred to the frosted surface of a glass slide, most of the PBS was removed and another glass slide with a frosted surface was placed on top. The oocytes were gently rolled between the frosted areas of the two glass slides to remove chorion and the vitelline membrane. Activated oocytes were stained for DNA with Hoechst 33258 (1 µg/ml in PBS) and mounted in mounting medium.

4.8 Cytological analysis and immunofluorescence

4.8.1 Immunostaining of embryos

Embryos were collected on apple juice agar plates, dechorionated in 50% bleach (klorix) for 3 min and washed with NaCl-Tx. Fixation was done in a heptane / methanol (1:1) mixture for 5 min at RT on a wheel. After fixation, embryos were rinsed thrice with methanol and rinsed thrice with PBTx. Embryos were blocked in PBTx-10% Normal Goat Serum (NGS)/ Fetal Bovine Serum (FBS) for 1 hr. After

blocking, embryos were incubated in primary antibody (diluted in PBTx/ 10% NGS/ 0.02% NaN₃) for 4 hrs at room temp or overnight at 4°C. Embryos were rinsed twice with PBTx, washed twice with PBTx for 30 min each and incubated with secondary antibody (diluted in PBTx/ 10% NGS) for 2 hrs at room temp followed by rinsing twice and washing twice with PBTx, 30 min each. Embryos were incubated with Hoechst 33258 (1 µg/ml in PBS) for 5 min on a rotor, rinsed once with PBS, washed once for 5 min with PBS and mounted in mounting medium.

4.8.2 Immunostaining of ovarioles

Ovaries were dissected in 1xPBS, fixed in oocyte/ovariole fixation buffer for 10 min at room temp on a wheel followed by rinsing thrice and washing twice for 5 min with PBS-Tw. Ovaries were blocked with PBS-Tw-10% NGS/FBS and incubated with the primary antibodies (diluted in PBS-Tw-10% NGS/FBS) supplemented with RNaseA (final conc 10 mg/ml) for 2 hr at room temperature or overnight at 4°C. These ovaries were rinsed once, washed thrice for 5 min with PBS-Tw and incubated with the secondary antibodies for 2 hrs at room temp followed by washing twice with PBS-Tw, 20 min each. Ovaries were incubated in Propidium iodide (1 µg/ml in PBS-Tw, Molecular Probes, P-3566) for 20 min at room temp, rinsed once, washed once in PBS-Tw for 10 min and mounted in Antifade prolong gold mounting medium (Molecular Probes).

4.8.3 Immunostaining of S14 oocytes

Immunostaining of S14 oocytes was performed as described in Theurkauf et al., (1992). Mass isolated oocytes were fixed in oocyte fixation buffer for 10 min at room temp on a wheel, rinsed thrice with PBS and extracted with PBS- 1% Tx for 2 hrs at room temp. After rinsing twice with PBS-0.5% Tx, extracted oocytes were transferred to the frosted surface of a glass slide, most of the PBS was removed and another glass slide with a frosted surface was placed on top. The oocytes were gently rolled between the frosted areas of the two glass slides to remove chorion and the vitelline membrane. Rolled oocytes were rinsed with PBS-0.5% Tx, extracted with PBS- 1% Tx for 2 hrs at room temp, and rinsed again twice with PBS-0.5% Tx. After blocking in PBTx-10%

NGS/FBS for 1 hr the oocytes were incubated in primary antibody (diluted in PBTx-10% NGS-0.02% NaN₃) for 4 hrs at room temp or overnight at 4°C. Oocytes were rinsed twice with PBTx, washed twice with PBTx for 30 min each and incubated with secondary antibody (diluted in PBTx-10% NGS) for 2 hrs at room temp followed by rinsing twice and washing twice with PBTx, 30 min each. Oocytes were incubated with Hoechst 33258 (1 µg/ml in PBS) for 5 min on a wheel, rinsed once with PBS, washed once for 5 min with PBS and mounted in mounting medium.

4.9 Fluorescent in situ hybridization on S14 oocytes

Fluorescent in situ hybridization (FISH) analysis was done on S14 oocytes as described in Dernburg et al., (1996) with some modifications. Chromosomal specific probes were prepared/obtained; as X chromosomal probe, the 359-bp repeat was amplified from genomic DNA by PCR, using SH230 and SH231 primers. For preparing an II chromosomal probe and an III chromosomal probe the BAC clones RP98-13M11 and RP98-48K07 from Berkeley Drosophila Genome Project were used, respectively. For detecting the IV chromosome, single-stranded oligonucleotides consisting of AATAT repeats of 20 b length were obtained from Metabion international AG, Germany. BACs-DNA and the amplified 359- bp repeats were digested overnight at 37°C with a mixture of the restriction enzymes AluI, HaeIII, TruII, MspI, RsaI and Sau3AI. Digested DNA was precipitated by adding 1/10 volume of 3 M NaOAc (pH 5.2), 2.5 volumes cold Ethanol and 20 µg glycogen. Precipitated DNA was resuspended in 35 µl of water, denatured in a PCR thermocycler at 100°C for 1 min and chilled on ice immediately. Tailing of all the probes was done by using Terminal deoxynucleotidyl Transferase (Roche 03333574001) at 37°C for 2 hrs in a reaction mixture containing 200 mM Na Cacodylate (pH 7.2), 100 µM DTT, 1 mM CoCl₂, 50 µM Aminoallyl dUTP (ARESTM DNA AlexaTM Fluor 555 labeling kit, Molecular probes, Inc, USA), 5 µM unlabeled dTTP. Reactions were stopped by adding 5 mM EDTA. Tailed probes were precipitated, resuspended in water and labeled with Alexa Fluor 555 or 647 (ARESTM DNA AlexaTM Fluor 555/647 labeling kit, Molecular probes, Inc, USA) in labeling buffer for 2 hrs in the dark followed by quenching of the reactions with 150 µM hydroxylamine. Labeled probes were purified

using the Qiagen PCR purification kit (Qiagen, Germany), precipitated, resuspended in elution buffer and stored at -20°C.

For FISH, oocytes were fixed in oocyte fixation buffer, rinsed thrice in 2X SSCT, sequentially washed with 2X SCCT-20% formamide, 2X SCCT-40% formamide, 2X SCCT-50% formamide for 10 min each followed by incubation in fresh 2X SCCT-50% formamide for 1-2 hrs at 37°C. Oocytes were transferred to a thin walled PCR tube containing 36 µl of hybridization buffer, 25-400 ng probe (diluted in 4 µl water) was added and mixed. Probe and chromosomal DNA were denatured at 91°C in a PCR thermocycler for 2 min, and the hybridization reaction was carried out overnight at 37°C for the X, II and III chromosomal probes and at 30°C for IV chromosomal probe. The next day 500 µl of prewarmed (37°C or 30°C) 2X SCCT-50% formamide was added to the sample mix and oocytes were allowed to settle. Oocytes were washed thrice with prewarmed (37°C or 30°C) 2X SCCT-50% formamide, once with 2X SCCT-40% formamide and 2X SCCT-20% formamide for 10 min/wash. Then, the oocytes were washed thrice with 2X SCCT for 10 min each, rinsed thrice with PBST and stained with Hoechst 33258 (1 µg/ml in PBS) for 5 min at room temp on a wheel, rinsed once with PBS, washed once with PBS for 5 min and mounted in mounting medium.

4.10 Genomic DNA preparation from single flies

A single fly was squashed in 50 µl of freshly prepared squashing buffer. The extract was incubated at 37°C for 30 min, heated at 95°C for 5 min and centrifuged at max speed for 5 min. 5 µl of the supernatant was used as genomic DNA template in 25 µl PCR reaction.

4.11 Cloning

Standard molecular biology techniques were followed according to Sambrook et al (1989). PCR reactions were performed using Pfu DNA polymerase (Fermentas), or self made Taq DNA polymerase in a 25 µl reaction mixture containing 50 ng of plasmid DNA template or 5 µl of single fly prep genomic DNA, 1x PCR buffer, 1.5 mM MgCl₂ (for Taq DNA polymerase), deoxyribonucleotide mix (2.5 mM of each

dNTP) and 0.4 μ M of each primer, in a RoboCycler Gradient 96 Hot Top Combo (Stratagene). Amplified PCR products were purified by using the Qiagen PCR purification kit (Qiagen, Germany) and analyzed on a 1% agarose gel in 1x TBE buffer). Isolation of plasmid DNA from *E. coli* grown in LB medium with appropriate antibiotics was done by using the QIAGEN Plasmid Mini Kit or the QIAGEN Plasmid Midi Kit (Qiagen, Germany). Digestion of plasmid DNA or PCR products was performed with appropriate restriction enzymes following manufacturer's instructions. For sub-cloning DNA fragments were cut out from plasmids, run on a 0.7% agarose gel and extracted from the gel using the QIAquick gel extraction kit (Qiagen, Germany). Linearized vector DNA was dephosphorylated by adding 1U of shrimp alkaline phosphatase and the mixture was incubated at 37°C for 30 min followed by heat inactivation of the enzyme at 65°C for 15 min. Ligation reactions were performed using 4 U T4 DNA Ligase (Promega) in 10 μ l reaction mixtures containing 1x ligation buffer and a 3:1 ratio of insert to vector, for 2 hrs at room temp. Ligation mixtures were purified and 1 μ l of ligation mix was transformed into electro-competent DH10B cells. Several colonies were checked by colony PCR or restriction digestion for the presence and orientation of the insert. Positive clones were sent for sequencing to Sequencing Laboratories, Goettingen, Germany. Sequence alignment and analysis was done using Gene Runner (Hastings Software) and web based program Multalin: (<http://multalin.toulouse.inra.fr/multalin/multalin.html>), (Corpet, 1988)

4.12 Construction of HA tagged TEV protease cleavable *c(2)M* transgenes

Transgenic lines expressing HA tagged TEV protease cleavable C(2)M were generated by germline transformation of pattB-gC(2)M-3TEV (I/II/III)-HA into *ZH-attp-58A* and *ZH-attp-51D* embryos (Bischof et al., 2007) and pBac- gC(2)M-3TEV (I/II/III)-HA into *w¹* embryos. The construct pCaSpeR-gC(2)M-myc (Heidmann et al., 2004) was used as a source for the *c(2)M* genomic region. The *c(2)M* gene contains an internal BamHI site at 1.7 kb downstream of start of 5' UTR. This site was used in combination with XhoI and XbaI enzymes to obtain the complete C(2)M genomic region in two fragments and the resulting fragments XhoI-C(2)M-BamHI and BamHI-C(2)M-XbaI were gel extracted. The Fragment XhoI-C(2)M-BamHI was subcloned into pLitmus28 (New England Biolabs) in which the SpeI site of the polylinker has

been destroyed by digesting with SpeI followed by filling in and relegation. The second fragment BamHI-C(2)M-XbaI was subcloned into pBSSK⁺ (Stratagene). Positive clones were checked by restriction analysis. For inserting the 6xHA tag in the construct pBSSK⁺ - BamHI-C(2)M-XbaI, an AgeI site was introduced before the stop codon by inverse PCR using the C(2)M7/C(2)M8 primer pair. Confirmation of the presence of the AgeI site in pBSSK⁺ - BamHI-C(2)M-(AgeI)-XbaI and the integrity of the PCR amplified coding sequence was done by restriction digestion with AgeI (New England Biolabs) and DNA sequencing.

For creating pattB-gC(2)M-3TEV-HA, the XhoI-C(2)M-BamHI fragment was first cloned into pBSSK⁺ - BamHI-C(2)M-(AgeI)-XbaI to get pBSSK⁺ - gC(2)M-(AgeI). Then the 6xHA tag was cloned into the unique AgeI site, From the resulting construct pBSSK⁺ - gC(2)M-HA , gC(2)M-HA was inserted into the pattB vector (Bischof et al., 2007) as a 4.2 kb NotI-gC(2)M-HA-Asp718 fragment.

For creating pattB-gC(2)M-3TEV (I/II)-HA, in the construct pLitmus28- XhoI-C(2)M-BamHI, a SpeI site was introduced individually at two different positions Asn 191 (I) and Thr 250 (II) by inverse PCR by using the C(2)M1/ C(2)M2 and C(2)M4 /C(2)M9 primer pairs respectively. The resultant constructs pLitmus28- XhoI-C(2)M-SpeI (I)-BamHI and pLitmus28- XhoI-C(2)M-SpeI (II)-BamHI were confirmed for the presence of the SpeI site by restriction digestion with SpeI and DNA sequencing. The coding region for the 3xTEV protease cleavage sequence [3x(GAGAATTTGTATTTTCAGGGT)] was obtained from the pBS-Rad21-[SpeI(3TEV)AvrII] construct (Pauli et al., 2008) (see chapter 7.16) as a SpeI(3TEV)AvrII fragment, gel eluted using DEAE membrane and cloned into the SpeI site in pLitmus28- XhoI-C(2)M-SpeI (I or II)-BamHI. Positive clones for pLitmus28- XhoI-C(2)M-3TEV (I/II)-BamHI were checked for orientation of the 3TEV sequence by several restriction digestions and DNA sequencing. In pLitmus28- XhoI-C(2)M-3TEV (I or II)-BamHI, the fragment BamHI-C(2)M-(AgeI)-XbaI was cloned to get pLitmus28-g C(2)M-(AgeI), followed by HA tag cloning in the AgeI site. To create final the constructs pattB-gC(2)M-3TEV (I/II)-HA , the gC(2)M-3TEV (I/II)-HA fragment from pLitmus28-g C(2)M-3TEV(I or II)-HA was cloned as a NotI/Asp718 fragment into pattB. For creating pattB-gC(2)M-3TEV(III)-HA, a SpeI site was introduced in pBSSK⁺ - BamHI-C(2)M-(AgeI)-XbaI vector at position Arg

339 (III) in C(2)M using the C(2)M /C(2)M8 primer pair to get pBSSK⁺ - BamHI-C(2)M-SpeI(III)-(AgeI)-XbaI, the 3TEV sequence was cloned into this SpeI site, positive clones for pBSSK⁺ -BamHI-C(2)M-3TEV (III)-(AgeI)-XbaI were checked for orientation, and subsequently the XhoI-C(2)M-BamHI (obtained from pCasper-gC(2)M-myc) was cloned into pBSSK⁺ -BamHI-C(2)M-3TEV (III)-(AgeI)-XbaI to get pBSSK⁺ -gC(2)M-3TEV (III)-(AgeI). The coding sequence for 6xHA tag was cloned into AgeI site and for making the final construct, the fragment gC(2)M-3TEV(III)-HA was cloned into pattB vector between the NotI and Asp718 sites.

pBac-gC(2)M-3TEV (I/II/III)-HA construct were made in two steps. The fragment gC(2)M-3TEV(I/II/III)-HA obtained from pattB-gC(2)M-3TEV (I/II/III)-HA were first cloned between NotI/Asp718 into pSLfa1180fa and then cleaved out as FseI-gC(2)M-3TEV(I/II/III)-HA-AscI fragments and cloned into the pBac-3X3p vector (Ernst Wimmer).

4.13 Construction of UASP1-TEV-V5 strains

For generating the UASP1-TEV-V5 lines, the pUAST-NLS-V5-TEV construct (Pauli et al., 2008) was digested with EcoRI /XbaI, the NLS-V5-TEV-NLS fragment was gel extracted and cloned into pUASP1(Jager et al., 2005). The pUASP1-NLS-V5-TEV-NLS construct was co-injected with the helper plasmid turbo Δ 2-3 for mediating germ line transformation into *w¹* embryos. Several independent transgenic lines were established, insertions were mapped on 2nd or 3rd chromosomes and the exact genomic location was determined by inverse PCR.

4.14 Inverse PCR

To determine the exact location of P-Elements in the genome, inverse PCR was performed according to the protocol published by the Berkeley Drosophila Genome project with some modifications (<http://www.fruitfly.org/about/methods/inverse.pcr.html>). For isolating genomic DNA, approximately 30 flies were anesthetized, homogenized in 400 µl of buffer A and incubated at 65°C for 30 min. 900 µl of LiCl/ KAc (1 part of 5 M KAc: 2.5 part of 6 M LiCl) was added to the homogenate, the mixture was incubated on ice for 10 min and centrifuged for 15 min

at room temp. The supernatant was transferred to a fresh eppendorf tube, 540 μ l of isopropanol was added, mixed and centrifuged for 15 min at room temp. The supernatant was discarded and the pellet was washed with 70% Ethanol, dried in air and resuspended in 120 μ l of TE buffer. The isolated genomic DNA (10 μ l) was digested for 2.5 hrs at 37°C with MspI or Sau3AI in a 25 μ l reaction mixture containing an appropriate buffer and 100 μ g/ml RNase A and heat inactivated for 20 min at 65°C. 5 μ l of digested genomic DNA was ligated in 200 μ l volume overnight at 4°C. 20 μ l of LiCl/ KAc and 500 μ l of ethanol were added to the ligation product, mixed and precipitated at -20°C for 10 min. The DNA was precipitated by centrifugation for 15min at 4°C and the pellet was washed with 70% ethanol and resuspended in 75 μ l of TE. PCR reactions were carried out using Taq DNA polymerase and two different primer sets Pwht1/ Plac1 and Pry4/Pry1 for MpsI and Sau3AI digested genomic DNA. Amplified products were analyzed on a 1% agarose gel, purified and sent for sequencing. Primers SP1 and Spel1 were used to sequence Pwht1/ Plac1 and Pry4/Pry1 amplified products, respectively.

4.15 DNA isolation from agarose gel with DEAE membrane

DNA was separated on a 1% agarose gel, and a small incision, closely ahead of the desired band, was made in the gel. A piece of DEAE membrane was soaked in water, and then inserted into the incision within the gel, and the gel was run for additional 10 min at 100 volts. The membrane was removed, checked under UV light for the presence of DNA and washed with water. The membrane was then transferred to a fresh eppendorf tube and submerged in 50 μ l of DEAE elution buffer, incubated at 65°C for 45 min, centrifuged for 1 min at room temp and the supernatant was transferred to a new eppendorf tube. 50 μ l of butanol (saturated with 1 M NaCl) was added to the supernatant, mixed and centrifuged for 5 min at room temp. The lower phase was transferred to a fresh eppendorf tube, 5 μ l of DNA loading dye was added and the sample incubated at 65°C for 10 min with the lid open. DNA was desalted by spin dialysis.

4.16 Microscopy and image processing

Fluorescence images were acquired by a Leica SP2 confocal microscope (Leica Microsystems, Germany), a Leica SP5 confocal microscope (Leica Microsystems, Germany), or a Zeiss Axioplan 2 widefield microscope equipped with an AxioCam MRm and software AxioVision 3.1 (Carl Zeiss, Germany). All images were processed by using Adobe Photoshop (Adobe Systems Inc., San Jose, CA, USA).

4.17 Solutions

All chemicals and reagents were purchased from AppliChem (Darmstadt), Biomol (Hamburg), Biorad (München), Fermentas (St.Leon-Rot), Fisher Scientific (Schwerte), GE Healthcare (Munich), Invitrogen (via Fisher Scientific, Schwerte), Merck (Darmstadt), Millipore (Schwalbach), New England Biolabs (NEB, Frankfurt), Promega (Mannheim), Roche Diagnostics (Mannheim), Roth (Karlsruhe), Serva (Heidelberg) and Sigma-Aldrich (Steinheim).

3x Laemmli buffer

6% w/v SDS
0.3 M β -Mercaptoethanol
30% glycerol
0.3% (w/v) Bromophenol blue
0.15 M Tris.Cl (pH 6.8)

Running buffer for protein electrophoresis

2.5 mM Tris (pH 8.3)
19.1 mM Glycine
0.1% (w/v) SDS

Transfer buffer

200 mM Glycine
25mM Tris
20% (v/v) Methanol

1xPBS

137 mM NaCl
2.7 mM KCl
10 mM KH_2PO_4

PBS-Tx

PBS, 0.1%
Triton-X 100

PBS-Tw

PBS

0.2% Tween 20

Blocking buffer

PBS

0.1% Tween

5% milk powder (Sucofin, Zeven)

EB buffer

10 mM Tris.Cl (pH 8.0)

80 mM Na- β -glycerophosphate

20 mM EGTA

15 mM MgCl₂2 mM Na₃VO₄1mM Na₂S₂O₅

1 mM Bezamidin

0.2 mM PMSF

KEB sample buffer

10 mM Glycerol

2.7 mM β -mercaptoethanol

3% SDS

185 mM Tris.Cl, pH 8.8

0.01% Bromophenol blue

50 mM NaF

20 mM EGTA, pH 8.0

2 mM Na₃VO₄1mM Na₂S₂O₅**Isolation buffer (pH 7.2)**

55 mM NaOAc

40 mM KOAc

110 mM Sucrose

1.2 mM MgCl₂1 mM CaCl₂

100 mM Hepes

Activation buffer (pH 6.8)3.3 mM NaH₂PO₄16.6 mM KH₂PO₄

10 mM NaCl

5% PEG 8000

2 mM CaCl₂

50 mM KCl

Zalokar's buffer (pH 6.8)

9 mM MgCl₂
10 mM MgSO₄
2.9 mM NaH₂PO₄
0.22 mM NaOAc
5 mM Glucose
27 mM Glutamic acid
33 mM Glycin
2 mM Malic acid
7 mM CaCl₂

Mounting medium

70% Glycerol
50 mM Tris.Cl (pH 9.5)
10 mg/ml Propylgallat
0.5 mg/ml p-Phenylendiamin
1xPBS

10x TBE buffer (1lit)

216 g Tris
110 g Borat
10 μM EDTA, pH 8.0

TE

10 mM Tris.Cl, pH 8.0
1 mM EDTA , pH 8.0

DNA loading dye

50% Glycerol
0.1 M EDTA
0.02% Xylencyanol
0.02% Bromophenol blue
0.02% (w/v) SDS

TEV protease reaction buffer

50 mM Tris.Cl pH 7.5
1 mM EDTA
5 mM DTT
0.1% Triton-X 100
50% glycerol

Hybridization buffer

1 g Dextran sulfate
1.5 ml 20X SCCT
5 ml formamide water up to 9 ml

Oocyte/ Ovariole fixation buffer

100 mM Na cacodylate, pH 7.2
 100 mM Sucrose
 40 mM Potassium acetate
 10 mM Sodium acetate
 10 mM EGTA
 8% EM grade formaldehyde

2X SSCT

3.0 M NaCl
 0.3 M Sodium citrate
 0.1 Tween 20

Squashing buffer

10 mM Tris.Cl, pH 8.2
 1 mM EDTA
 25 mM NaCl
 200 µg/ml Proteinase K

LB medium (pH 7.2)

1% (w/v) Bacto trypton
 0.5% (w/v) Yeast extract,
 1% NaCl

Buffer A (for genomic DNA isolation)

100 mM Tris-Cl (pH 7.5)
 100 mM EDTA
 100 mM NaCl
 0.5% (w/v), SDS)

DEAE elution buffer

20mM Tris.Cl pH 7.6
 1.5 M NaCl
 1 mM EDTA

4.18 Antibodies

Primary and secondary antibodies used in this study are listed in tables below.

Table 4.18.1 List of primary antibodies

Antibody	Dilution for Immunofluorescence	Dilution for Western Blot	Reference
Anti EGFP IS28	1:3000	1:4000	Duerr (2004)
Anti mRFP1	1:3000	1:4000	Herzog (2006)
Anti C(3)G	1:3000	-	Gift from M. Lily

Antibody	Dilution for Immunofluorescence	Dilution for Western Blot	Reference
Anti myc (9E10 hybridoma supernatant)	1: 10	1:30	Evan et al., 1985
Anti α -tub	1: 8000	1: 18000	Sigma-Aldrich
Anti V5	1:500	1: 5000	Invitrogen
Anti HA (12CA5 hybridoma supernatant)	1: 100	1:100	Niman et al., 1983
Sperm tail	1:20	-	Karr, 1991
Anti Cenp-C	1:3000	-	Heeger et al., 2005
Anti Smc1	1:500	-	Gift from C. Sunkel

Table 4.18.2 List of secondary antibodies for immunofluorescence

Antibodies	Dilution	Source
Alexa 488 anti mouse	1: 600	Molecular probes
Alexa 488 anti Rabbit	1: 600	Molecular probes
Alexa 488 anti guinea pig	1: 600	Molecular probes
Cy3 anti mouse	1: 600	Jackson Immunochemicals
Cy3 anti Rabbit	1: 600	Jackson Immunochemicals
Cy3 anti guinea pig	1: 600	Jackson Immunochemicals
Cy5 anti mouse	1: 600	Jackson Immunochemicals
Cy5 anti Rabbit	1: 600	Jackson Immunochemicals
Cy5 anti guinea pig	1: 600	Jackson Immunochemicals

Table 4.18.3 List of secondary antibodies for western blotting

Antibodies	Dilution	Source
POD goat anti mouse	1:3000	Jackson Immunochemicals
POD goat anti rabbit	1:3000	Jackson Immunochemicals

4.19 Primers

All the primers used for cloning and DNA sequencing are listed below.

Primer	Sequence	Details
C(2)M1	TCTATCACTAGTCCCCGG AGTTGCACTCAGTC	Forward primer for introducing a SpeI site into <i>C(2)M</i> at Asn 191 (I)
C(2)M2	CAGGAGACTAGTAATAGA CTTTTTGCGAAAAATG	Reverse primer for introducing a SpeI site into <i>C(2)M</i> at Asn 191 (I)
C(2)M4	TGAGTTACTAGTGCCATC TTTGGGGTAAAGC	Reverse primer for introducing a SpeI site into <i>C(2)M</i> at Thr 250 (II)

Primer	Sequence	Details
C(2)M5	GAATAGACTAGTGAGCAG CTGGTGAAGCAT	Forward primer for introducing a SpeI site into <i>C(2)M</i> at Arg 339 (III)
C(2)M6	CTGCTGACTAGTGTATTC AATTCGTTTGTCTACT	Reverse primer for introducing a SpeI site into <i>C(2)M</i> at Arg 339 (III)
C(2)M7	GGTGAGACCGGTTGAATA TTTTAGATAATTTTTTTC AAG	Forward primer for introducing an AgeI site into <i>C(2)M</i> before stop codon
C(2)M8	CGTTCAACCGGTCTCACT CAGCATAAGATTG	Reverse primer for introducing an AgeI site into <i>C(2)M</i> before stop codon
C(2)M9	TCTATCACTAGTACTCAC GTAAGAATTCTCAATTC	Forward primer for introducing a SpeI site into <i>C(2)M</i> at Thr 250 (II)
AF20	ATGAAGCTACTGTCTTCT ATCG	Forward primer, anneals at the start codon of Gal4, was used in combination with AF21 for amplifying mat α - tub Gal4
AF21	GCCAATCTATCTGTGACG GC	Reverse primer, anneals 300 bp downstream of the start codon of Gal4, was used in combination with AF20 for amplifying mat α - tub Gal4
CL18	CGCAGGTACCACCTTATG TTATTTTCATCATG	P-Element specific forward primer for identification of P-Elements, was used to identify the EP(2)2115 insertion in transgenic lines in combination with Mei20, produces a 110 bp product when EP is present.
Mei01	TCAACTTCAGCCACGTGA TGATGTA	Forward primer for DNA sequencing to check insertion of AgeI site at the end of <i>C(2)M</i> coding region.
Mei03	TCTGTATGAAATCGATAT AATTGATTAATGAATTGG	Forward primer for sequencing of the 5'end of <i>C(2)M</i>
Mei11	TTTCTTTACGGCAACATT GGT	Forward primer for sequencing of the 5'end of <i>C(2)M</i> , binds 300 bp upstream of the start codon of <i>C(2)M</i> .
Mei20	GACTGAGTGCAACTCTCG GTTGTGCAATAGACTTTT TGCGAAAA	Reverse Primer, was used for identification of EP (2) 2115 insertion in transgenic lines in combination with CL18 produces a 110 bp product when EP is present
Mei28	CAGGAATCGGATCTATTG GATG	Forward primer for sequencing to check presence of SpeI site at position I and II.
FF05	GGATTGCCATGGGTAAGC CTATCCCTAACC	Amplifies TEV-Protease sequence without NLS (771 bp) in combination with FF06
FF06	CTTAGAGAATTCACCCTT GCGAGTACAC	Amplifies TEV-Protease sequence without NLS (771 bp) in combination with FF05
Pwht1	GTAACGCTAATCACTCCG AACAGGTCACA	Sense amplification primer for the 5' end of P-elements in combination with Plac1.
Plac1	CACCCAAGGCTCTGCTCC CACAAT	Antisense amplification primer for thw 5' end of P-elements in combination with

		Pwht1.
Pry1	CCTTAGCATGTCCGTGGG GTTTGAAT	Antisense amplification primer for the 3' end of P-elements in combination with Pry4.
Pry4	CAATCATATCGCTGTCTC ACTCA	Sense amplification primer for the 3' end of P-elements in combination with Pry1.
Sp1	ACACAACCTTTCCTCTCA ACAA	Antisense sequencing primer for the 5' end of P-elements in combination with Plac1 and Pwht1.
Spep1	GCACTCAGAATACTATT C	Sense sequencing primer for the 3' end of P-elements in combination with Pry1 and Pry4

Chapter V Abbreviations

a.a.	amino acid(s)
AB	activation buffer
ABC	ATP binding cassette
APC	anaphase promoting complex
ARS	autonomously replicating sequence
ATP	adenosine 5'-triphosphate
BACs	bacterial artificial chromosomes
bp	base pairs
BSA	bovine serum albumin
Cdc	cell division cycle
Cdk	cyclin-dependent kinase
C-terminal	carboxy-terminal
C-terminus	carboxy-terminus
C(2)M	crossover suppressor on 2 of Manheim
C(3)G	crossover suppressor on 3 of Gowen
DCC	dosage compensation complex
DMSO	dimethylsulfoxide
DNA	deoxyribonucleic acid
dNTP	deoxynucleotide 5'-triphosphate
dUTP	deoxyuridine 5'-triphosphate
DTT	dithiothreitol

EB	elusion buffer
<i>E. coli</i>	<i>Escherichia coli</i>
EDTA	ethylendiamine tetraacetic acid
EGFP	enhanced green fluorescent protein
EGTA	ethylen glycol tetraacetic acid
FBS	fetal bovine serum
Fig.	Figure
FISH	Fluorescent in situ hybridization
FRAP	Fluorescent Recovery After Photobleaching
Fm	mobile fraction
g	gram or gravitational constant (9.81 m/s ²)
HA	hemagglutinin
HEAT	helical repeat protein domain (<u>H</u> untingtin, <u>e</u> longation factor 3, PP2A- <u>A</u> , <u>T</u> or1)
HEPES	4-(2-hydroxyethyl)-1piperazineethansulfonic acid
ICC	initiation of chromosome condensation
k	kilo
kb	kilo base pairs
kDa	kilo dalton
LB	Luria-Bertani
m	milli
μ	micro
M	molar
MCS	multiple cloning site
M.F.I.	mean fluorescent intensity
mRFP	monomeric red fluorescent protein
MTOC	microtubules organizing centers
min	minute(s)
mRNA	messenger RNA
NEBD	nuclear envelope breakdown
NGS	normal goat serum
N-terminal	amino-terminal
N-terminus	amino-terminus
ORC	origin recognition complex

PAGE	polyacrylamide gel electrophoresis
PBS	phosphate buffered saline
PCR	polymerase chain reaction
PEG	polyethylene glycol
Plk1	Polo-like kinase 1
PP2A	protein phosphatase 2A
RFI	Relative Fluorescent Intensity
RNase	ribonuclease
ROI	region of interest
rpm	revolutions per minute
RT	room temperature
S14	stage 14
SAR	scaffold associated region
Scc	sister-chromatid cohesion
SDS	sodium dodecylsulfate
s	seconds
SMC	structural maintenance of chromosomes
TEMED	N,N,N',N'-tetramethylethylenediamine
Tev	tobacco etch virus
Tris	tris(hydroxymethyl)aminomethane
U	unit
UAS	upstream activating sequence
v/v	volume per volume
Wapl	wings apart-like
w/v	weight per volume
XCAP	<i>Xenopus</i> chromosome associated proteins
ZAB	Zalokar's buffer

Chapter VI References

- Adolph, K.W., Cheng, S.M., and Laemmli, U.K. (1977). Role of nonhistone proteins in metaphase chromosome structure. *Cell* *12*, 805-816.
- Ahmad, K., and Henikoff, S. (2002). Histone H3 variants specify modes of chromatin assembly. *Proc Natl Acad Sci U S A* *99 Suppl 4*, 16477-16484.
- Alexandru, G., Zachariae, W., Schleiffer, A., and Nasmyth, K. (1999). Sister chromatid separation and chromosome re-duplication are regulated by different mechanisms in response to spindle damage. *EMBO J* *18*, 2707-2721.
- Anderson, D.E., Losada, A., Erickson, H.P., and Hirano, T. (2002). Condensin and cohesin display different arm conformations with characteristic hinge angles. *J Cell Biol* *156*, 419-424.
- Aono, N., Sutani, T., Tomonaga, T., Mochida, S., and Yanagida, M. (2002). Cnd2 has dual roles in mitotic condensation and interphase. *Nature* *417*, 197-202.
- Bailey, A. (1999). sevenless-GAL4 transgene.
- Bannister, L.A., Reinholdt, L.G., Munroe, R.J., and Schimenti, J.C. (2004). Positional cloning and characterization of mouse *mei8*, a disrupted allele of the meiotic cohesin *Rec8*. *Genesis* *40*, 184-194.
- Basler, K., and Hafen, E. (1989). Ubiquitous expression of *sevenless*: position-dependent specification of cell fate. *Science* *243*, 931-934.
- Bazett-Jones, D.P., Kimura, K., and Hirano, T. (2002). Efficient supercoiling of DNA by a single condensin complex as revealed by electron spectroscopic imaging. *Mol Cell* *9*, 1183-1190.
- Bell, S.P., and Stillman, B. (1992). ATP-dependent recognition of eukaryotic origins of DNA replication by a multiprotein complex. *Nature* *357*, 128-134.
- Belmont, A.S., and Bruce, K. (1994). Visualization of G1 chromosomes: a folded, twisted, supercoiled chromonema model of interphase chromatid structure. *J Cell Biol* *127*, 287-302.
- Belmont, A.S., Sedat, J.W., and Agard, D.A. (1987). A three-dimensional approach to mitotic chromosome structure: evidence for a complex hierarchical organization. *J Cell Biol* *105*, 77-92.
- Bhalla, N., Biggins, S., and Murray, A.W. (2002). Mutation of *YCS4*, a budding yeast condensin subunit, affects mitotic and nonmitotic chromosome behavior. *Mol Biol Cell* *13*, 632-645.
- Bhat, M.A., Philp, A.V., Glover, D.M., and Bellen, H.J. (1996). Chromatid segregation at anaphase requires the barren product, a novel chromosome-associated protein that interacts with Topoisomerase II. *Cell* *87*, 1103-1114.
- Birkenbihl, R.P., and Subramani, S. (1992). Cloning and characterization of *rad21* an essential gene of *Schizosaccharomyces pombe* involved in DNA double-strand-break repair. *Nucleic Acids Res* *20*, 6605-6611.

- Bischof, J., Maeda, R.K., Hediger, M., Karch, F., and Basler, K. (2007). An optimized transgenesis system for *Drosophila* using germ-line-specific phiC31 integrases. *Proc Natl Acad Sci U S A* *104*, 3312-3317.
- Blat, Y., and Kleckner, N. (1999). Cohesins bind to preferential sites along yeast chromosome III, with differential regulation along arms versus the centric region. *Cell* *98*, 249-259.
- Boggs, B.A., Allis, C.D., and Chinault, A.C. (2000). Immunofluorescent studies of human chromosomes with antibodies against phosphorylated H1 histone. *Chromosoma* *108*, 485-490.
- Bowers, J.L., Randell, J.C., Chen, S., and Bell, S.P. (2004). ATP hydrolysis by ORC catalyzes reiterative Mcm2-7 assembly at a defined origin of replication. *Mol Cell* *16*, 967-978.
- Brand, A.H., and Perrimon, N. (1993). Targeted gene expression as a means of altering cell fates and generating dominant phenotypes. *Development* *118*, 401-415.
- Brewer, B.J., and Fangman, W.L. (1987). The localization of replication origins on ARS plasmids in *S. cerevisiae*. *Cell* *51*, 463-471.
- Buonomo, S.B., Clyne, R.K., Fuchs, J., Loidl, J., Uhlmann, F., and Nasmyth, K. (2000). Disjunction of homologous chromosomes in meiosis I depends on proteolytic cleavage of the meiotic cohesin Rec8 by separin. *Cell* *103*, 387-398.
- Cadoret, J.C., Meisch, F., Hassan-Zadeh, V., Luyten, I., Guillet, C., Duret, L., Quesneville, H., and Prioleau, M.N. (2008). Genome-wide studies highlight indirect links between human replication origins and gene regulation. *Proc Natl Acad Sci U S A* *105*, 15837-15842.
- Cai, X., Dong, F., Edelman, R.E., and Makaroff, C.A. (2003). The Arabidopsis SYN1 cohesin protein is required for sister chromatid arm cohesion and homologous chromosome pairing. *J Cell Sci* *116*, 2999-3007.
- Carpenter, A.J., and Porter, A.C. (2004). Construction, characterization, and complementation of a conditional-lethal DNA topoisomerase IIalpha mutant human cell line. *Mol Biol Cell* *15*, 5700-5711.
- Carramolino, L., Lee, B.C., Zaballos, A., Peled, A., Barthelemy, I., Shav-Tal, Y., Prieto, I., Carmi, P., Gothelf, Y., Gonzalez de Buitrago, G., *et al.* (1997). SA-1, a nuclear protein encoded by one member of a novel gene family: molecular cloning and detection in hemopoietic organs. *Gene* *195*, 151-159.
- Chan, R.C., Severson, A.F., and Meyer, B.J. (2004). Condensin restructures chromosomes in preparation for meiotic divisions. *J Cell Biol* *167*, 613-625.
- Chang, C.R., Wu, C.S., Hom, Y., and Gartenberg, M.R. (2005). Targeting of cohesin by transcriptionally silent chromatin. *Genes Dev* *19*, 3031-3042.
- Chelysheva, L., Diallo, S., Vezon, D., Gendrot, G., Vrielynck, N., Belcram, K., Rocques, N., Marquez-Lema, A., Bhatt, A.M., Horlow, C., *et al.* (2005). AtREC8 and AtSCC3 are essential to the monopolar orientation of the kinetochores during meiosis. *J Cell Sci* *118*, 4621-4632.

- Chuang, P.T., Albertson, D.G., and Meyer, B.J. (1994). DPY-27: a chromosome condensation protein homolog that regulates *C. elegans* dosage compensation through association with the X chromosome. *Cell* *79*, 459-474.
- Ciosk, R., Shirayama, M., Shevchenko, A., Tanaka, T., Toth, A., and Nasmyth, K. (2000). Cohesin's binding to chromosomes depends on a separate complex consisting of Scc2 and Scc4 proteins. *Mol Cell* *5*, 243-254.
- Ciosk, R., Zachariae, W., Michaelis, C., Shevchenko, A., Mann, M., and Nasmyth, K. (1998). An ESP1/PDS1 complex regulates loss of sister chromatid cohesion at the metaphase to anaphase transition in yeast. *Cell* *93*, 1067-1076.
- Cobbe, N., Savvidou, E., and Heck, M.M. (2006). Diverse mitotic and interphase functions of condensins in *Drosophila*. *Genetics* *172*, 991-1008.
- Coelho, P.A., Queiroz-Machado, J., and Sunkel, C.E. (2003). Condensin-dependent localisation of topoisomerase II to an axial chromosomal structure is required for sister chromatid resolution during mitosis. *J Cell Sci* *116*, 4763-4776.
- Cohen-Fix, O., Peters, J.M., Kirschner, M.W., and Koshland, D. (1996). Anaphase initiation in *Saccharomyces cerevisiae* is controlled by the APC-dependent degradation of the anaphase inhibitor Pds1p. *Genes Dev* *10*, 3081-3093.
- Corpet, F. (1988). Multiple sequence alignment with hierarchical clustering. *Nucleic Acids Res* *16*, 10881-10890.
- D'Amours, D., Stegmeier, F., and Amon, A. (2004). Cdc14 and condensin control the dissolution of cohesin-independent chromosome linkages at repeated DNA. *Cell* *117*, 455-469.
- Darwiche, N., Freeman, L.A., and Strunnikov, A. (1999). Characterization of the components of the putative mammalian sister chromatid cohesion complex. *Gene* *233*, 39-47.
- de la Barre, A.E., Gerson, V., Gout, S., Creaven, M., Allis, C.D., and Dimitrov, S. (2000). Core histone N-termini play an essential role in mitotic chromosome condensation. *EMBO J* *19*, 379-391.
- Dej, K.J., Ahn, C., and Orr-Weaver, T.L. (2004). Mutations in the *Drosophila* condensin subunit dCAP-G: defining the role of condensin for chromosome condensation in mitosis and gene expression in interphase. *Genetics* *168*, 895-906.
- Dernburg, A.F., Sedat, J.W., and Hawley, R.S. (1996). Direct evidence of a role for heterochromatin in meiotic chromosome segregation. *Cell* *86*, 135-146.
- DiNardo, S., Voelkel, K., and Sternglanz, R. (1984). DNA topoisomerase II mutant of *Saccharomyces cerevisiae*: topoisomerase II is required for segregation of daughter molecules at the termination of DNA replication. *Proc Natl Acad Sci U S A* *81*, 2616-2620.
- Donovan, S., Harwood, J., Drury, L.S., and Diffley, J.F. (1997). Cdc6p-dependent loading of Mcm proteins onto pre-replicative chromatin in budding yeast. *Proc Natl Acad Sci U S A* *94*, 5611-5616.
- Donze, D., Adams, C.R., Rine, J., and Kamakaka, R.T. (1999). The boundaries of the silenced HMR domain in *Saccharomyces cerevisiae*. *Genes Dev* *13*, 698-708.

- Dougherty, W.G., and Parks, T.D. (1989). Molecular genetic and biochemical evidence for the involvement of the heptapeptide cleavage sequence in determining the reaction profile at two tobacco etch virus cleavage sites in cell-free assays. *Virology* *172*, 145-155.
- Drury, L.S., Perkins, G., and Diffley, J.F. (1997). The Cdc4/34/53 pathway targets Cdc6p for proteolysis in budding yeast. *EMBO J* *16*, 5966-5976.
- Earnshaw, W.C., and Heck, M.M. (1985). Localization of topoisomerase II in mitotic chromosomes. *J Cell Biol* *100*, 1716-1725.
- Edgar, B.A., and O'Farrell, P.H. (1989). Genetic control of cell division patterns in the *Drosophila* embryo. *Cell* *57*, 177-187.
- Egel, R. (1995). The synaptonemal complex and the distribution of meiotic recombination events. *Trends Genet* *11*, 206-208.
- Eickbush, T.H., and Moudrianakis, E.N. (1978). The histone core complex: an octamer assembled by two sets of protein-protein interactions. *Biochemistry* *17*, 4955-4964.
- Eijpe, M., Heyting, C., Gross, B., and Jessberger, R. (2000). Association of mammalian SMC1 and SMC3 proteins with meiotic chromosomes and synaptonemal complexes. *J Cell Sci* *113* (Pt 4), 673-682.
- Eijpe, M., Offenber, H., Jessberger, R., Revenkova, E., and Heyting, C. (2003). Meiotic cohesin REC8 marks the axial elements of rat synaptonemal complexes before cohesins SMC1beta and SMC3. *J Cell Biol* *160*, 657-670.
- Ellermeier, C., and Smith, G.R. (2005). Cohesins are required for meiotic DNA breakage and recombination in *Schizosaccharomyces pombe*. *Proc Natl Acad Sci U S A* *102*, 10952-10957.
- Evan, G.I., Lewis, G.K., Ramsay, G., and Bishop, J.M. (1985). Isolation of monoclonal antibodies specific for human c-myc proto-oncogene product. *Mol Cell Biol* *5*, 3610-3616.
- Fawcett, D.W. (1956). The fine structure of chromosomes in the meiotic prophase of vertebrate spermatocytes. *J Biophys Biochem Cytol* *2*, 403-406.
- Fischer, S.G., and Laemmli, U.K. (1980). Cell cycle changes in *Physarum polycephalum* histone H1 phosphate: relationship to deoxyribonucleic acid binding and chromosome condensation. *Biochemistry* *19*, 2240-2246.
- Freeman, L., Aragon-Alcaide, L., and Strunnikov, A. (2000). The condensin complex governs chromosome condensation and mitotic transmission of rDNA. *J Cell Biol* *149*, 811-824.
- Freeman, M. (1996). Reiterative use of the EGF receptor triggers differentiation of all cell types in the *Drosophila* eye. *Cell* *87*, 651-660.
- Fujimoto, S., Yonemura, M., Matsunaga, S., Nakagawa, T., Uchiyama, S., and Fukui, K. (2005). Characterization and dynamic analysis of *Arabidopsis* condensin subunits, AtCAP-H and AtCAP-H2. *Planta* *222*, 293-300.
- Gandhi, R., Gillespie, P.J., and Hirano, T. (2006). Human Wapl is a cohesin-binding protein that promotes sister-chromatid resolution in mitotic prophase. *Curr Biol* *16*, 2406-2417.

- Gasser, S.M., Laroche, T., Falquet, J., Boy de la Tour, E., and Laemmli, U.K. (1986). Metaphase chromosome structure. Involvement of topoisomerase II. *J Mol Biol* *188*, 613-629.
- Gause, M., Webber, H.A., Misulovin, Z., Haller, G., Rollins, R.A., Eissenberg, J.C., Bickel, S.E., and Dorsett, D. (2008). Functional links between *Drosophila* Nipped-B and cohesin in somatic and meiotic cells. *Chromosoma* *117*, 51-66.
- Gerlich, D., Hirota, T., Koch, B., Peters, J.M., and Ellenberg, J. (2006a). Condensin I stabilizes chromosomes mechanically through a dynamic interaction in live cells. *Curr Biol* *16*, 333-344.
- Gerlich, D., Koch, B., Dupeux, F., Peters, J.M., and Ellenberg, J. (2006b). Live-cell imaging reveals a stable cohesin-chromatin interaction after but not before DNA replication. *Curr Biol* *16*, 1571-1578.
- Giet, R., and Glover, D.M. (2001). *Drosophila* aurora B kinase is required for histone H3 phosphorylation and condensin recruitment during chromosome condensation and to organize the central spindle during cytokinesis. *J Cell Biol* *152*, 669-682.
- Gillespie, P.J., and Hirano, T. (2004). Scc2 couples replication licensing to sister chromatid cohesion in *Xenopus* egg extracts. *Curr Biol* *14*, 1598-1603.
- Gorr, I.H., Boos, D., and Stemmann, O. (2005). Mutual inhibition of separase and Cdk1 by two-step complex formation. *Mol Cell* *19*, 135-141.
- Gorr, I.H., Reis, A., Boos, D., Wuhr, M., Madgwick, S., Jones, K.T., and Stemmann, O. (2006). Essential CDK1-inhibitory role for separase during meiosis I in vertebrate oocytes. *Nat Cell Biol* *8*, 1035-1037.
- Gruber, S., Arumugam, P., Katou, Y., Kuglitsch, D., Helmhart, W., Shirahige, K., and Nasmyth, K. (2006). Evidence that loading of cohesin onto chromosomes involves opening of its SMC hinge. *Cell* *127*, 523-537.
- Gruber, S., Haering, C.H., and Nasmyth, K. (2003). Chromosomal cohesin forms a ring. *Cell* *112*, 765-777.
- Guacci, V., Koshland, D., and Strunnikov, A. (1997). A direct link between sister chromatid cohesion and chromosome condensation revealed through the analysis of MCD1 in *S. cerevisiae*. *Cell* *91*, 47-57.
- Guo, X.W., Th'ng, J.P., Swank, R.A., Anderson, H.J., Tudan, C., Bradbury, E.M., and Roberge, M. (1995). Chromosome condensation induced by fostriecin does not require p34cdc2 kinase activity and histone H1 hyperphosphorylation, but is associated with enhanced histone H2A and H3 phosphorylation. *EMBO J* *14*, 976-985.
- Haering, C.H., Lowe, J., Hochwagen, A., and Nasmyth, K. (2002). Molecular architecture of SMC proteins and the yeast cohesin complex. *Mol Cell* *9*, 773-788.
- Haering, C.H., Schoffnegger, D., Nishino, T., Helmhart, W., Nasmyth, K., and Lowe, J. (2004). Structure and stability of cohesin's Smc1-kleisin interaction. *Mol Cell* *15*, 951-964.
- Hagstrom, K.A., Holmes, V.F., Cozzarelli, N.R., and Meyer, B.J. (2002). *C. elegans* condensin promotes mitotic chromosome architecture, centromere organization, and sister chromatid segregation during mitosis and meiosis. *Genes Dev* *16*, 729-742.

- Harder, B., Schomburg, A., Pflanz, R., Kustner, K., Gerlach, N., and Schuh, R. (2008). TEV protease-mediated cleavage in *Drosophila* as a tool to analyze protein functions in living organisms. *Biotechniques* *44*, 765-772.
- Hartl, T.A., Sweeney, S.J., Knepler, P.J., and Bosco, G. (2008). Condensin II resolves chromosomal associations to enable anaphase I segregation in *Drosophila* male meiosis. *PLoS Genet* *4*, e1000228.
- Hartman, T., Stead, K., Koshland, D., and Guacci, V. (2000). Pds5p is an essential chromosomal protein required for both sister chromatid cohesion and condensation in *Saccharomyces cerevisiae*. *J Cell Biol* *151*, 613-626.
- Hartsuiker, E., Vaessen, E., Carr, A.M., and Kohli, J. (2001). Fission yeast Rad50 stimulates sister chromatid recombination and links cohesion with repair. *EMBO J* *20*, 6660-6671.
- Hauf, S., Roitinger, E., Koch, B., Dittrich, C.M., Mechtler, K., and Peters, J.M. (2005). Dissociation of cohesin from chromosome arms and loss of arm cohesion during early mitosis depends on phosphorylation of SA2. *PLoS Biol* *3*, e69.
- Hauf, S., Waizenegger, I.C., and Peters, J.M. (2001). Cohesin cleavage by separase required for anaphase and cytokinesis in human cells. *Science* *293*, 1320-1323.
- Hazelett, D.J., Bourouis, M., Walldorf, U., and Treisman, J.E. (1998). *decapentaplegic* and *wingless* are regulated by *eyes absent* and *eyegone* and interact to direct the pattern of retinal differentiation in the eye disc. *Development* *125*, 3741-3751.
- Heale, J.T., Ball, A.R., Jr., Schmiesing, J.A., Kim, J.S., Kong, X., Zhou, S., Hudson, D.F., Earnshaw, W.C., and Yokomori, K. (2006). Condensin I interacts with the PARP-1-XRCC1 complex and functions in DNA single-strand break repair. *Mol Cell* *21*, 837-848.
- Heeger, S., Leismann, O., Schittenhelm, R., Schraidt, O., Heidmann, S., and Lehner, C.F. (2005). Genetic interactions of separase regulatory subunits reveal the diverged *Drosophila* Cenp-C homolog. *Genes Dev* *19*, 2041-2053.
- Heidmann, D., Horn, S., Heidmann, S., Schleiffer, A., Nasmyth, K., and Lehner, C.F. (2004). The *Drosophila* meiotic kleisin C(2)M functions before the meiotic divisions. *Chromosoma* *113*, 177-187.
- Hirano, M., and Hirano, T. (2006). Opening closed arms: long-distance activation of SMC ATPase by hinge-DNA interactions. *Mol Cell* *21*, 175-186.
- Hirano, T. (2005). Condensins: organizing and segregating the genome. *Curr Biol* *15*, R265-275.
- Hirano, T. (2006). At the heart of the chromosome: SMC proteins in action. *Nat Rev Mol Cell Biol* *7*, 311-322.
- Hirano, T., Kobayashi, R., and Hirano, M. (1997). Condensins, chromosome condensation protein complexes containing XCAP-C, XCAP-E and a *Xenopus* homolog of the *Drosophila* Barren protein. *Cell* *89*, 511-521.
- Hirano, T., and Mitchison, T.J. (1994). A heterodimeric coiled-coil protein required for mitotic chromosome condensation in vitro. *Cell* *79*, 449-458.

- Hirota, T., Gerlich, D., Koch, B., Ellenberg, J., and Peters, J.M. (2004). Distinct functions of condensin I and II in mitotic chromosome assembly. *J Cell Sci* *117*, 6435-6445.
- Horsfield, J.A., Anagnostou, S.H., Hu, J.K., Cho, K.H., Geisler, R., Lieschke, G., Crosier, K.E., and Crosier, P.S. (2007). Cohesin-dependent regulation of Runx genes. *Development* *134*, 2639-2649.
- Huang, C.E., Milutinovich, M., and Koshland, D. (2005). Rings, bracelet or snaps: fashionable alternatives for Smc complexes. *Philos Trans R Soc Lond B Biol Sci* *360*, 537-542.
- Huang, J., and Moazed, D. (2006). Sister chromatid cohesion in silent chromatin: each sister to her own ring. *Genes Dev* *20*, 132-137.
- Hudson, D.F., Ohta, S., Freisinger, T., Macisaac, F., Sennels, L., Alves, F., Lai, F., Kerr, A., Rappsilber, J., and Earnshaw, W.C. (2008). Molecular and genetic analysis of condensin function in vertebrate cells. *Mol Biol Cell* *19*, 3070-3079.
- Hudson, D.F., Vagnarelli, P., Gassmann, R., and Earnshaw, W.C. (2003). Condensin is required for nonhistone protein assembly and structural integrity of vertebrate mitotic chromosomes. *Dev Cell* *5*, 323-336.
- Ishimi, Y. (1997). A DNA helicase activity is associated with an MCM4, -6, and -7 protein complex. *J Biol Chem* *272*, 24508-24513.
- Ivanov, D., and Nasmyth, K. (2007). A physical assay for sister chromatid cohesion in vitro. *Mol Cell* *27*, 300-310.
- Ivanov, D., Schleiffer, A., Eisenhaber, F., Mechtler, K., Haering, C.H., and Nasmyth, K. (2002). Eco1 is a novel acetyltransferase that can acetylate proteins involved in cohesion. *Curr Biol* *12*, 323-328.
- Ivanovska, I., Khandan, T., Ito, T., and Orr-Weaver, T.L. (2005). A histone code in meiosis: the histone kinase, NHK-1, is required for proper chromosomal architecture in *Drosophila* oocytes. *Genes Dev* *19*, 2571-2582.
- Jager, H., Rauch, M., and Heidmann, S. (2005). The *Drosophila melanogaster* condensin subunit Cap-G interacts with the centromere-specific histone H3 variant CID. *Chromosoma* *113*, 350-361.
- Jallepalli, P.V., Waizenegger, I.C., Bunz, F., Langer, S., Speicher, M.R., Peters, J.M., Kinzler, K.W., Vogelstein, B., and Lengauer, C. (2001). Securin is required for chromosomal stability in human cells. *Cell* *105*, 445-457.
- Kapust, R.B., Tozser, J., Fox, J.D., Anderson, D.E., Cherry, S., Copeland, T.D., and Waugh, D.S. (2001). Tobacco etch virus protease: mechanism of autolysis and rational design of stable mutants with wild-type catalytic proficiency. *Protein Eng* *14*, 993-1000.
- Karr, T.L. (1991). Intracellular sperm/egg interactions in *Drosophila*: a three-dimensional structural analysis of a paternal product in the developing egg. *Mech Dev* *34*, 101-111.
- Katis, V.L., Galova, M., Rabitsch, K.P., Gregan, J., and Nasmyth, K. (2004). Maintenance of cohesin at centromeres after meiosis I in budding yeast requires a kinetochore-associated protein related to MEI-S332. *Curr Biol* *14*, 560-572.

- Kerrebrock, A.W., Moore, D.P., Wu, J.S., and Orr-Weaver, T.L. (1995). Mei-S332, a *Drosophila* protein required for sister-chromatid cohesion, can localize to meiotic centromere regions. *Cell* 83, 247-256.
- Khetani, R.S., and Bickel, S.E. (2007). Regulation of meiotic cohesion and chromosome core morphogenesis during pachytene in *Drosophila* oocytes. *J Cell Sci* 120, 3123-3137.
- Kim, S.T., Xu, B., and Kastan, M.B. (2002). Involvement of the cohesin protein, Smc1, in Atm-dependent and independent responses to DNA damage. *Genes Dev* 16, 560-570.
- Kimura, K., Cuvier, O., and Hirano, T. (2001). Chromosome condensation by a human condensin complex in *Xenopus* egg extracts. *J Biol Chem* 276, 5417-5420.
- Kimura, K., Hirano, M., Kobayashi, R., and Hirano, T. (1998). Phosphorylation and activation of 13S condensin by Cdc2 in vitro. *Science* 282, 487-490.
- Kimura, K., and Hirano, T. (1997). ATP-dependent positive supercoiling of DNA by 13S condensin: a biochemical implication for chromosome condensation. *Cell* 90, 625-634.
- Kimura, K., Rybenkov, V.V., Crisona, N.J., Hirano, T., and Cozzarelli, N.R. (1999). 13S condensin actively reconfigures DNA by introducing global positive writhe: implications for chromosome condensation. *Cell* 98, 239-248.
- King, R.W., Deshaies, R.J., Peters, J.M., and Kirschner, M.W. (1996). How proteolysis drives the cell cycle. *Science* 274, 1652-1659.
- Kireeva, N., Lakonishok, M., Kireev, I., Hirano, T., and Belmont, A.S. (2004). Visualization of early chromosome condensation: a hierarchical folding, axial glue model of chromosome structure. *J Cell Biol* 166, 775-785.
- Kitajima, T.S., Hauf, S., Ohsugi, M., Yamamoto, T., and Watanabe, Y. (2005). Human Bub1 defines the persistent cohesion site along the mitotic chromosome by affecting Shugoshin localization. *Curr Biol* 15, 353-359.
- Kitajima, T.S., Kawashima, S.A., and Watanabe, Y. (2004). The conserved kinetochore protein shugoshin protects centromeric cohesion during meiosis. *Nature* 427, 510-517.
- Kitajima, T.S., Sakuno, T., Ishiguro, K., Iemura, S., Natsume, T., Kawashima, S.A., and Watanabe, Y. (2006). Shugoshin collaborates with protein phosphatase 2A to protect cohesin. *Nature* 441, 46-52.
- Kitajima, T.S., Yokobayashi, S., Yamamoto, M., and Watanabe, Y. (2003). Distinct cohesin complexes organize meiotic chromosome domains. *Science* 300, 1152-1155.
- Klein, F., Mahr, P., Galova, M., Buonomo, S.B., Michaelis, C., Nairz, K., and Nasmyth, K. (1999). A central role for cohesins in sister chromatid cohesion, formation of axial elements, and recombination during yeast meiosis. *Cell* 98, 91-103.
- Koshland, D., and Hartwell, L.H. (1987). The structure of sister minichromosome DNA before anaphase in *Saccharomyces cerevisiae*. *Science* 238, 1713-1716.

- Kudo, N.R., Wassmann, K., Anger, M., Schuh, M., Wirth, K.G., Xu, H., Helmhart, W., Kudo, H., McKay, M., Maro, B., *et al.* (2006). Resolution of chiasmata in oocytes requires separase-mediated proteolysis. *Cell* *126*, 135-146.
- Kueng, S., Hegemann, B., Peters, B.H., Lipp, J.J., Schleiffer, A., Mechtler, K., and Peters, J.M. (2006). Wapl controls the dynamic association of cohesin with chromatin. *Cell* *127*, 955-967.
- Labib, K., Diffley, J.F., and Kearsley, S.E. (1999). G1-phase and B-type cyclins exclude the DNA-replication factor Mcm4 from the nucleus. *Nat Cell Biol* *1*, 415-422.
- Labib, K., Tercero, J.A., and Diffley, J.F. (2000). Uninterrupted MCM2-7 function required for DNA replication fork progression. *Science* *288*, 1643-1647.
- Lara-Pezzi, E., Pezzi, N., Prieto, I., Barthelemy, I., Carreiro, C., Martinez, A., Maldonado-Rodriguez, A., Lopez-Cabrera, M., and Barbero, J.L. (2004). Evidence of a transcriptional co-activator function of cohesin STAG/SA/Scs3. *J Biol Chem* *279*, 6553-6559.
- Lavoie, B.D., Tuffo, K.M., Oh, S., Koshland, D., and Holm, C. (2000). Mitotic chromosome condensation requires Brn1p, the yeast homologue of Barren. *Mol Biol Cell* *11*, 1293-1304.
- Lee, J., Iwai, T., Yokota, T., and Yamashita, M. (2003). Temporally and spatially selective loss of Rec8 protein from meiotic chromosomes during mammalian meiosis. *J Cell Sci* *116*, 2781-2790.
- Leismann, O., Herzig, A., Heidmann, S., and Lehner, C.F. (2000). Degradation of *Drosophila* PIM regulates sister chromatid separation during mitosis. *Genes Dev* *14*, 2192-2205.
- Lenart, P., Petronczki, M., Steegmaier, M., Di Fiore, B., Lipp, J.J., Hoffmann, M., Rettig, W.J., Kraut, N., and Peters, J.M. (2007). The small-molecule inhibitor BI 2536 reveals novel insights into mitotic roles of polo-like kinase 1. *Curr Biol* *17*, 304-315.
- Lengronne, A., McIntyre, J., Katou, Y., Kanoh, Y., Hopfner, K.P., Shirahige, K., and Uhlmann, F. (2006). Establishment of sister chromatid cohesion at the *S. cerevisiae* replication fork. *Mol Cell* *23*, 787-799.
- Lewis, C.D., and Laemmli, U.K. (1982). Higher order metaphase chromosome structure: evidence for metalloprotein interactions. *Cell* *29*, 171-181.
- Li, C.J., Vassilev, A., and DePamphilis, M.L. (2004). Role for Cdk1 (Cdc2)/cyclin A in preventing the mammalian origin recognition complex's largest subunit (Orc1) from binding to chromatin during mitosis. *Mol Cell Biol* *24*, 5875-5886.
- Lieb, J.D., Albrecht, M.R., Chuang, P.T., and Meyer, B.J. (1998). MIX-1: an essential component of the *C. elegans* mitotic machinery executes X chromosome dosage compensation. *Cell* *92*, 265-277.
- Lipp, J.J., Hirota, T., Poser, I., and Peters, J.M. (2007). Aurora B controls the association of condensin I but not condensin II with mitotic chromosomes. *J Cell Sci* *120*, 1245-1255.
- Losada, A., Hirano, M., and Hirano, T. (1998). Identification of *Xenopus* SMC protein complexes required for sister chromatid cohesion. *Genes Dev* *12*, 1986-1997.

- Losada, A., Hirano, M., and Hirano, T. (2002). Cohesin release is required for sister chromatid resolution, but not for condensin-mediated compaction, at the onset of mitosis. *Genes Dev* *16*, 3004-3016.
- Losada, A., and Hirano, T. (2005). Dynamic molecular linkers of the genome: the first decade of SMC proteins. *Genes Dev* *19*, 1269-1287.
- Losada, A., Yokochi, T., Kobayashi, R., and Hirano, T. (2000). Identification and characterization of SA/Scs3p subunits in the *Xenopus* and human cohesin complexes. *J Cell Biol* *150*, 405-416.
- Lowe, J., Cordell, S.C., and van den Ent, F. (2001). Crystal structure of the SMC head domain: an ABC ATPase with 900 residues antiparallel coiled-coil inserted. *J Mol Biol* *306*, 25-35.
- Lupo, R., Breiling, A., Bianchi, M.E., and Orlando, V. (2001). *Drosophila* chromosome condensation proteins Topoisomerase II and Barren colocalize with Polycomb and maintain Fab-7 PRE silencing. *Mol Cell* *7*, 127-136.
- Machin, F., Paschos, K., Jarmuz, A., Torres-Rosell, J., Pade, C., and Aragon, L. (2004). Condensin regulates rDNA silencing by modulating nucleolar Sir2p. *Curr Biol* *14*, 125-130.
- Maeshima, K., and Laemmli, U.K. (2003). A two-step scaffolding model for mitotic chromosome assembly. *Dev Cell* *4*, 467-480.
- Mahowald, A.P., Goralski, T.J., and Caulton, J.H. (1983). In vitro activation of *Drosophila* eggs. *Dev Biol* *98*, 437-445.
- Manheim, E.A., and McKim, K.S. (2003). The Synaptonemal complex component C(2)M regulates meiotic crossing over in *Drosophila*. *Curr Biol* *13*, 276-285.
- Marsden, M.P., and Laemmli, U.K. (1979). Metaphase chromosome structure: evidence for a radial loop model. *Cell* *17*, 849-858.
- McGuinness, B.E., Hirota, T., Kudo, N.R., Peters, J.M., and Nasmyth, K. (2005). Shugoshin prevents dissociation of cohesin from centromeres during mitosis in vertebrate cells. *PLoS Biol* *3*, e86.
- Megee, P.C., and Koshland, D. (1999). A functional assay for centromere-associated sister chromatid cohesion. *Science* *285*, 254-257.
- Mei, J., Huang, X., and Zhang, P. (2001). Securin is not required for cellular viability, but is required for normal growth of mouse embryonic fibroblasts. *Curr Biol* *11*, 1197-1201.
- Melby, T.E., Ciampaglio, C.N., Briscoe, G., and Erickson, H.P. (1998). The symmetrical structure of structural maintenance of chromosomes (SMC) and MukB proteins: long, antiparallel coiled coils, folded at a flexible hinge. *J Cell Biol* *142*, 1595-1604.
- Michaelis, C., Ciosk, R., and Nasmyth, K. (1997). Cohesins: chromosomal proteins that prevent premature separation of sister chromatids. *Cell* *91*, 35-45.
- Micklem, D.R., Dasgupta, R., Elliott, H., Gergely, F., Davidson, C., Brand, A., Gonzalez-Reyes, A., and St Johnston, D. (1997). The mago nashi gene is required for

the polarisation of the oocyte and the formation of perpendicular axes in *Drosophila*. *Curr Biol* 7, 468-478.

Milutinovich, M., and Koshland, D.E. (2003). Molecular biology. SMC complexes--wrapped up in controversy. *Science* 300, 1101-1102.

Mirkovitch, J., Mirault, M.E., and Laemmli, U.K. (1984). Organization of the higher-order chromatin loop: specific DNA attachment sites on nuclear scaffold. *Cell* 39, 223-232.

Moldovan, G.L., Pfander, B., and Jentsch, S. (2006). PCNA controls establishment of sister chromatid cohesion during S phase. *Mol Cell* 23, 723-732.

Molnar, M., Bahler, J., Sipiczki, M., and Kohli, J. (1995). The *rec8* gene of *Schizosaccharomyces pombe* is involved in linear element formation, chromosome pairing and sister-chromatid cohesion during meiosis. *Genetics* 141, 61-73.

Moore, D.P., and Orr-Weaver, T.L. (1998). Chromosome segregation during meiosis: building an unambivalent bivalent. *Curr Top Dev Biol* 37, 263-299.

Moses, M.J. (1956). Studies on nuclei using correlated cytochemical, light, and electron microscope techniques. *J Biophys Biochem Cytol* 2, 397-406.

Murray, A.W., and Szostak, J.W. (1985). Chromosome segregation in mitosis and meiosis. *Annu Rev Cell Biol* 1, 289-315.

Nakaseko, Y., Goshima, G., Morishita, J., and Yanagida, M. (2001). M phase-specific kinetochore proteins in fission yeast: microtubule-associating Dis1 and Mtc1 display rapid separation and segregation during anaphase. *Curr Biol* 11, 537-549.

Nasmyth, K., and Haering, C.H. (2009). Cohesin: its roles and mechanisms. *Annu Rev Genet* 43, 525-558.

Neuwald, A.F., and Hirano, T. (2000). HEAT repeats associated with condensins, cohesins, and other complexes involved in chromosome-related functions. *Genome Res* 10, 1445-1452.

Nguyen, V.Q., Co, C., and Li, J.J. (2001). Cyclin-dependent kinases prevent DNA re-replication through multiple mechanisms. *Nature* 411, 1068-1073.

Niman, H.L., Houghten, R.A., Walker, L.E., Reisfeld, R.A., Wilson, I.A., Hogle, J.M., and Lerner, R.A. (1983). Generation of protein-reactive antibodies by short peptides is an event of high frequency: implications for the structural basis of immune recognition. *Proc Natl Acad Sci U S A* 80, 4949-4953.

Nishitani, H., Lygerou, Z., Nishimoto, T., and Nurse, P. (2000). The Cdt1 protein is required to license DNA for replication in fission yeast. *Nature* 404, 625-628.

Ohsumi, K., Katagiri, C., and Kishimoto, T. (1993). Chromosome condensation in *Xenopus* mitotic extracts without histone H1. *Science* 262, 2033-2035.

Oliveira, R.A., Coelho, P.A., and Sunkel, C.E. (2005). The condensin I subunit Barren/CAP-H is essential for the structural integrity of centromeric heterochromatin during mitosis. *Mol Cell Biol* 25, 8971-8984.

Oliveira, R.A., Heidmann, S., and Sunkel, C.E. (2007). Condensin I binds chromatin early in prophase and displays a highly dynamic association with *Drosophila* mitotic chromosomes. *Chromosoma* 116, 259-274.

- Onn, I., Aono, N., Hirano, M., and Hirano, T. (2007). Reconstitution and subunit geometry of human condensin complexes. *EMBO J* 26, 1024-1034.
- Ono, T., Fang, Y., Spector, D.L., and Hirano, T. (2004). Spatial and temporal regulation of Condensins I and II in mitotic chromosome assembly in human cells. *Mol Biol Cell* 15, 3296-3308.
- Ono, T., Losada, A., Hirano, M., Myers, M.P., Neuwald, A.F., and Hirano, T. (2003). Differential contributions of condensin I and condensin II to mitotic chromosome architecture in vertebrate cells. *Cell* 115, 109-121.
- Oudet, P., Gross-Bellard, M., and Chambon, P. (1975). Electron microscopic and biochemical evidence that chromatin structure is a repeating unit. *Cell* 4, 281-300.
- Page, A.W., and Orr-Weaver, T.L. (1997). Activation of the meiotic divisions in *Drosophila* oocytes. *Dev Biol* 183, 195-207.
- Page, S.L., and Hawley, R.S. (2001). c(3)G encodes a *Drosophila* synaptonemal complex protein. *Genes Dev* 15, 3130-3143.
- Panizza, S., Tanaka, T., Hochwagen, A., Eisenhaber, F., and Nasmyth, K. (2000). Pds5 cooperates with cohesin in maintaining sister chromatid cohesion. *Curr Biol* 10, 1557-1564.
- Parisi, S., McKay, M.J., Molnar, M., Thompson, M.A., van der Spek, P.J., van Drunen-Schoenmaker, E., Kanaar, R., Lehmann, E., Hoeijmakers, J.H., and Kohli, J. (1999). Rec8p, a meiotic recombination and sister chromatid cohesion phosphoprotein of the Rad21p family conserved from fission yeast to humans. *Mol Cell Biol* 19, 3515-3528.
- Parra, M.T., Viera, A., Gomez, R., Page, J., Benavente, R., Santos, J.L., Rufas, J.S., and Suja, J.A. (2004). Involvement of the cohesin Rad21 and SCP3 in monopolar attachment of sister kinetochores during mouse meiosis I. *J Cell Sci* 117, 1221-1234.
- Pasierbek, P., Jantsch, M., Melcher, M., Schleiffer, A., Schweizer, D., and Loidl, J. (2001). A *Caenorhabditis elegans* cohesion protein with functions in meiotic chromosome pairing and disjunction. *Genes Dev* 15, 1349-1360.
- Pauli, A., Althoff, F., Oliveira, R.A., Heidmann, S., Schuldiner, O., Lehner, C.F., Dickson, B.J., and Nasmyth, K. (2008). Cell-type-specific TEV protease cleavage reveals cohesin functions in *Drosophila* neurons. *Dev Cell* 14, 239-251.
- Paulson, J.R., and Laemmli, U.K. (1977). The structure of histone-depleted metaphase chromosomes. *Cell* 12, 817-828.
- Pelttari, J., Hoja, M.R., Yuan, L., Liu, J.G., Brundell, E., Moens, P., Santucci-Darmanin, S., Jessberger, R., Barbero, J.L., Heyting, C., *et al.* (2001). A meiotic chromosomal core consisting of cohesin complex proteins recruits DNA recombination proteins and promotes synapsis in the absence of an axial element in mammalian meiotic cells. *Mol Cell Biol* 21, 5667-5677.
- Pezzi, N., Prieto, I., Kremer, L., Perez Jurado, L.A., Valero, C., Del Mazo, J., Martinez, A.C., and Barbero, J.L. (2000). STAG3, a novel gene encoding a protein involved in meiotic chromosome pairing and location of STAG3-related genes flanking the Williams-Beuren syndrome deletion. *FASEB J* 14, 581-592.

- Pidoux, A.L., and Allshire, R.C. (2004). Kinetochores and heterochromatin domains of the fission yeast centromere. *Chromosome Res* 12, 521-534.
- Prieto, I., Pezzi, N., Buesa, J.M., Kremer, L., Barthelemy, I., Carreiro, C., Roncal, F., Martinez, A., Gomez, L., Fernandez, R., *et al.* (2002). STAG2 and Rad21 mammalian mitotic cohesins are implicated in meiosis. *EMBO Rep* 3, 543-550.
- Randell, J.C., Bowers, J.L., Rodriguez, H.K., and Bell, S.P. (2006). Sequential ATP hydrolysis by Cdc6 and ORC directs loading of the Mcm2-7 helicase. *Mol Cell* 21, 29-39.
- Razin, S.V. (1996). Functional architecture of chromosomal DNA domains. *Crit Rev Eukaryot Gene Expr* 6, 247-269.
- Resnick, T.D., Dej, K.J., Xiang, Y., Hawley, R.S., Ahn, C., and Orr-Weaver, T.L. (2009). Mutations in the chromosomal passenger complex and the condensin complex differentially affect synaptonemal complex disassembly and metaphase I configuration in *Drosophila* female meiosis. *Genetics* 181, 875-887.
- Reuter, G., and Spierer, P. (1992). Position effect variegation and chromatin proteins. *Bioessays* 14, 605-612.
- Revenkova, E., Eijpe, M., Heyting, C., Gross, B., and Jessberger, R. (2001). Novel meiosis-specific isoform of mammalian SMC1. *Mol Cell Biol* 21, 6984-6998.
- Revenkova, E., Eijpe, M., Heyting, C., Hodges, C.A., Hunt, P.A., Liebe, B., Scherthan, H., and Jessberger, R. (2004). Cohesin SMC1 beta is required for meiotic chromosome dynamics, sister chromatid cohesion and DNA recombination. *Nat Cell Biol* 6, 555-562.
- Richmond, T.J., Finch, J.T., Rushton, B., Rhodes, D., and Klug, A. (1984). Structure of the nucleosome core particle at 7 Å resolution. *Nature* 311, 532-537.
- Riedel, C.G., Katis, V.L., Katou, Y., Mori, S., Itoh, T., Helmhart, W., Galova, M., Petronczki, M., Gregan, J., Cetin, B., *et al.* (2006). Protein phosphatase 2A protects centromeric sister chromatid cohesion during meiosis I. *Nature* 441, 53-61.
- Robinson, P.J., Fairall, L., Huynh, V.A., and Rhodes, D. (2006). EM measurements define the dimensions of the "30-nm" chromatin fiber: evidence for a compact, interdigitated structure. *Proc Natl Acad Sci U S A* 103, 6506-6511.
- Rolef Ben-Shahar, T., Heeger, S., Lehane, C., East, P., Flynn, H., Skehel, M., and Uhlmann, F. (2008). Eco1-dependent cohesin acetylation during establishment of sister chromatid cohesion. *Science* 321, 563-566.
- Rorth, P. (1998). Gal4 in the *Drosophila* female germline. *Mech Dev* 78, 113-118.
- Rowland, B.D., Roig, M.B., Nishino, T., Kurze, A., Uluocak, P., Mishra, A., Beckouet, F., Underwood, P., Metson, J., Imre, R., *et al.* (2009). Building sister chromatid cohesion: smc3 acetylation counteracts an antiestablishment activity. *Mol Cell* 33, 763-774.
- Saitoh, N., Goldberg, I.G., Wood, E.R., and Earnshaw, W.C. (1994). ScII: an abundant chromosome scaffold protein is a member of a family of putative ATPases with an unusual predicted tertiary structure. *J Cell Biol* 127, 303-318.

- Saka, Y., Sutani, T., Yamashita, Y., Saitoh, S., Takeuchi, M., Nakaseko, Y., and Yanagida, M. (1994). Fission yeast cut3 and cut14, members of a ubiquitous protein family, are required for chromosome condensation and segregation in mitosis. *EMBO J* 13, 4938-4952.
- Sakaguchi, A., and Kikuchi, A. (2004). Functional compatibility between isoform alpha and beta of type II DNA topoisomerase. *J Cell Sci* 117, 1047-1054.
- Sakuno, T., and Watanabe, Y. (2009). Studies of meiosis disclose distinct roles of cohesion in the core centromere and pericentromeric regions. *Chromosome Res* 17, 239-249.
- Salah, S.M., and Nasmyth, K. (2000). Destruction of the securin Pds1p occurs at the onset of anaphase during both meiotic divisions in yeast. *Chromosoma* 109, 27-34.
- Samoshkin, A., Arnaoutov, A., Jansen, L.E., Ouspenski, I., Dye, L., Karpova, T., McNally, J., Dasso, M., Cleveland, D.W., and Strunnikov, A. (2009). Human condensin function is essential for centromeric chromatin assembly and proper sister kinetochore orientation. *PLoS One* 4, e6831.
- Sauer, K., Knoblich, J.A., Richardson, H., and Lehner, C.F. (1995). Distinct modes of cyclin E/cdc2c kinase regulation and S-phase control in mitotic and endoreduplication cycles of *Drosophila* embryogenesis. *Genes Dev* 9, 1327-1339.
- Savvidou, E., Cobbe, N., Steffensen, S., Cotterill, S., and Heck, M.M. (2005). *Drosophila* CAP-D2 is required for condensin complex stability and resolution of sister chromatids. *J Cell Sci* 118, 2529-2543.
- Schar, P., Fasi, M., and Jessberger, R. (2004). SMC1 coordinates DNA double-strand break repair pathways. *Nucleic Acids Res* 32, 3921-3929.
- Schleiffer, A., Kaitna, S., Maurer-Stroh, S., Glotzer, M., Nasmyth, K., and Eisenhaber, F. (2003). Kleisins: a superfamily of bacterial and eukaryotic SMC protein partners. *Mol Cell* 11, 571-575.
- Schmekel, K., Wahrman, J., Skoglund, U., and Daneholt, B. (1993). The central region of the synaptonemal complex in *Blaps cribrosa* studied by electron microscope tomography. *Chromosoma* 102, 669-681.
- Schuh, M., Lehner, C.F., and Heidmann, S. (2007). Incorporation of *Drosophila* CID/CENP-A and CENP-C into centromeres during early embryonic anaphase. *Curr Biol* 17, 237-243.
- Sedat, J., and Manuelidis, L. (1978). A direct approach to the structure of eukaryotic chromosomes. *Cold Spring Harb Symp Quant Biol* 42 Pt 1, 331-350.
- Sequeira-Mendes, J., Diaz-Uriarte, R., Apedaile, A., Huntley, D., Brockdorff, N., and Gomez, M. (2009). Transcription initiation activity sets replication origin efficiency in mammalian cells. *PLoS Genet* 5, e1000446.
- Shen, X., Yu, L., Weir, J.W., and Gorovsky, M.A. (1995). Linker histones are not essential and affect chromatin condensation in vivo. *Cell* 82, 47-56.
- Shintomi, K., and Hirano, T. (2009). Releasing cohesin from chromosome arms in early mitosis: opposing actions of Wapl-Pds5 and Sgo1. *Genes Dev* 23, 2224-2236.

- Siddiqui, N.U., Stronghill, P.E., Dengler, R.E., Hasenkampf, C.A., and Riggs, C.D. (2003). Mutations in Arabidopsis condensin genes disrupt embryogenesis, meristem organization and segregation of homologous chromosomes during meiosis. *Development* *130*, 3283-3295.
- Sjogren, C., and Nasmyth, K. (2001). Sister chromatid cohesion is required for postreplicative double-strand break repair in *Saccharomyces cerevisiae*. *Curr Biol* *11*, 991-995.
- Sonoda, E., Matsusaka, T., Morrison, C., Vagnarelli, P., Hoshi, O., Ushiki, T., Nojima, K., Fukagawa, T., Waizenegger, I.C., Peters, J.M., *et al.* (2001). *Scc1/Rad21/Mcd1* is required for sister chromatid cohesion and kinetochore function in vertebrate cells. *Dev Cell* *1*, 759-770.
- Soppa, J. (2001). Prokaryotic structural maintenance of chromosomes (SMC) proteins: distribution, phylogeny, and comparison with MukBs and additional prokaryotic and eukaryotic coiled-coil proteins. *Gene* *278*, 253-264.
- Steffensen, S., Coelho, P.A., Cobbe, N., Vass, S., Costa, M., Hassan, B., Prokopenko, S.N., Bellen, H., Heck, M.M., and Sunkel, C.E. (2001). A role for *Drosophila* SMC4 in the resolution of sister chromatids in mitosis. *Curr Biol* *11*, 295-307.
- Stemmann, O., Zou, H., Gerber, S.A., Gygi, S.P., and Kirschner, M.W. (2001). Dual inhibition of sister chromatid separation at metaphase. *Cell* *107*, 715-726.
- Stinchcomb, D.T., Struhl, K., and Davis, R.W. (1979). Isolation and characterisation of a yeast chromosomal replicator. *Nature* *282*, 39-43.
- Stray, J.E., and Lindsley, J.E. (2003). Biochemical analysis of the yeast condensin Smc2/4 complex: an ATPase that promotes knotting of circular DNA. *J Biol Chem* *278*, 26238-26248.
- Strom, L., Lindroos, H.B., Shirahige, K., and Sjogren, C. (2004). Postreplicative recruitment of cohesin to double-strand breaks is required for DNA repair. *Mol Cell* *16*, 1003-1015.
- Strunnikov, A.V., Hogan, E., and Koshland, D. (1995). SMC2, a *Saccharomyces cerevisiae* gene essential for chromosome segregation and condensation, defines a subgroup within the SMC family. *Genes Dev* *9*, 587-599.
- Strunnikov, A.V., Larionov, V.L., and Koshland, D. (1993). SMC1: an essential yeast gene encoding a putative head-rod-tail protein is required for nuclear division and defines a new ubiquitous protein family. *J Cell Biol* *123*, 1635-1648.
- Suau, P., Bradbury, E.M., and Baldwin, J.P. (1979). Higher-order structures of chromatin in solution. *Eur J Biochem* *97*, 593-602.
- Sullivan, M., Higuchi, T., Katis, V.L., and Uhlmann, F. (2004a). Cdc14 phosphatase induces rDNA condensation and resolves cohesin-independent cohesion during budding yeast anaphase. *Cell* *117*, 471-482.
- Sullivan, M., Hornig, N.C., Porstmann, T., and Uhlmann, F. (2004b). Studies on substrate recognition by the budding yeast separase. *J Biol Chem* *279*, 1191-1196.
- Sumara, I., Vorlaufer, E., Gieffers, C., Peters, B.H., and Peters, J.M. (2000). Characterization of vertebrate cohesin complexes and their regulation in prophase. *J Cell Biol* *151*, 749-762.

- Sundin, O., and Varshavsky, A. (1980). Terminal stages of SV40 DNA replication proceed via multiply intertwined catenated dimers. *Cell* 21, 103-114.
- Sutani, T., Yuasa, T., Tomonaga, T., Dohmae, N., Takio, K., and Yanagida, M. (1999). Fission yeast condensin complex: essential roles of non-SMC subunits for condensation and Cdc2 phosphorylation of Cut3/SMC4. *Genes Dev* 13, 2271-2283.
- Sym, M., and Roeder, G.S. (1994). Crossover interference is abolished in the absence of a synaptonemal complex protein. *Cell* 79, 283-292.
- Takahashi, T.S., Basu, A., Bermudez, V., Hurwitz, J., and Walter, J.C. (2008). Cdc7-Drf1 kinase links chromosome cohesion to the initiation of DNA replication in *Xenopus* egg extracts. *Genes Dev* 22, 1894-1905.
- Takahashi, T.S., Yiu, P., Chou, M.F., Gygi, S., and Walter, J.C. (2004). Recruitment of *Xenopus* Scc2 and cohesin to chromatin requires the pre-replication complex. *Nat Cell Biol* 6, 991-996.
- Takemoto, A., Kimura, K., Yanagisawa, J., Yokoyama, S., and Hanaoka, F. (2006). Negative regulation of condensin I by CK2-mediated phosphorylation. *EMBO J* 25, 5339-5348.
- Takemoto, A., Kimura, K., Yokoyama, S., and Hanaoka, F. (2004). Cell cycle-dependent phosphorylation, nuclear localization, and activation of human condensin. *J Biol Chem* 279, 4551-4559.
- Takemoto, A., Maeshima, K., Ikehara, T., Yamaguchi, K., Murayama, A., Imamura, S., Imamoto, N., Yokoyama, S., Hirano, T., Watanabe, Y., *et al.* (2009). The chromosomal association of condensin II is regulated by a noncatalytic function of PP2A. *Nat Struct Mol Biol* 16, 1302-1308.
- Tanaka, S., and Diffley, J.F. (2002). Interdependent nuclear accumulation of budding yeast Cdt1 and Mcm2-7 during G1 phase. *Nat Cell Biol* 4, 198-207.
- Tanaka, T., Cosma, M.P., Wirth, K., and Nasmyth, K. (1999). Identification of cohesin association sites at centromeres and along chromosome arms. *Cell* 98, 847-858.
- Tanaka, T., Knapp, D., and Nasmyth, K. (1997). Loading of an Mcm protein onto DNA replication origins is regulated by Cdc6p and CDKs. *Cell* 90, 649-660.
- Tang, T.T., Bickel, S.E., Young, L.M., and Orr-Weaver, T.L. (1998). Maintenance of sister-chromatid cohesion at the centromere by the *Drosophila* MEI-S332 protein. *Genes Dev* 12, 3843-3856.
- Tang, Z., Shu, H., Qi, W., Mahmood, N.A., Mumby, M.C., and Yu, H. (2006). PP2A is required for centromeric localization of Sgo1 and proper chromosome segregation. *Dev Cell* 10, 575-585.
- Terret, M.E., Wassmann, K., Waizenegger, I., Maro, B., Peters, J.M., and Verlhac, M.H. (2003). The meiosis I-to-meiosis II transition in mouse oocytes requires separase activity. *Curr Biol* 13, 1797-1802.
- Theurkauf, W.E., and Hawley, R.S. (1992). Meiotic spindle assembly in *Drosophila* females: behavior of nonexchange chromosomes and the effects of mutations in the nod kinesin-like protein. *J Cell Biol* 116, 1167-1180.

- Toth, A., Ciosk, R., Uhlmann, F., Galova, M., Schleiffer, A., and Nasmyth, K. (1999). Yeast cohesin complex requires a conserved protein, Eco1p(Ctf7), to establish cohesion between sister chromatids during DNA replication. *Genes Dev* *13*, 320-333.
- Uhlmann, F., Lottspeich, F., and Nasmyth, K. (1999). Sister-chromatid separation at anaphase onset is promoted by cleavage of the cohesin subunit Scc1. *Nature* *400*, 37-42.
- Uhlmann, F., and Nasmyth, K. (1998). Cohesion between sister chromatids must be established during DNA replication. *Curr Biol* *8*, 1095-1101.
- Unal, E., Arbel-Eden, A., Sattler, U., Shroff, R., Lichten, M., Haber, J.E., and Koshland, D. (2004). DNA damage response pathway uses histone modification to assemble a double-strand break-specific cohesin domain. *Mol Cell* *16*, 991-1002.
- Unal, E., Heidinger-Pauli, J.M., Kim, W., Guacci, V., Onn, I., Gygi, S.P., and Koshland, D.E. (2008). A molecular determinant for the establishment of sister chromatid cohesion. *Science* *321*, 566-569.
- Unal, E., Heidinger-Pauli, J.M., and Koshland, D. (2007). DNA double-strand breaks trigger genome-wide sister-chromatid cohesion through Eco1 (Ctf7). *Science* *317*, 245-248.
- Vagnarelli, P., Hudson, D.F., Ribeiro, S.A., Trinkle-Mulcahy, L., Spence, J.M., Lai, F., Farr, C.J., Lamond, A.I., and Earnshaw, W.C. (2006). Condensin and Repo-Man-PP1 co-operate in the regulation of chromosome architecture during mitosis. *Nat Cell Biol* *8*, 1133-1142.
- van Heemst, D., and Heyting, C. (2000). Sister chromatid cohesion and recombination in meiosis. *Chromosoma* *109*, 10-26.
- van Holde, K., and Zlatanova, J. (1995). Chromatin higher order structure: chasing a mirage? *J Biol Chem* *270*, 8373-8376.
- von Wettstein, D. (1984). The synaptonemal complex and genetic segregation. *Symp Soc Exp Biol* *38*, 195-231.
- Waizenegger, I.C., Hauf, S., Meinke, A., and Peters, J.M. (2000). Two distinct pathways remove mammalian cohesin from chromosome arms in prophase and from centromeres in anaphase. *Cell* *103*, 399-410.
- Watanabe, Y., and Nurse, P. (1999). Cohesin Rec8 is required for reductional chromosome segregation at meiosis. *Nature* *400*, 461-464.
- Watrin, E., Schleiffer, A., Tanaka, K., Eisenhaber, F., Nasmyth, K., and Peters, J.M. (2006). Human Scc4 is required for cohesin binding to chromatin, sister-chromatid cohesion, and mitotic progression. *Curr Biol* *16*, 863-874.
- Weinreich, M., Liang, C., Chen, H.H., and Stillman, B. (2001). Binding of cyclin-dependent kinases to ORC and Cdc6p regulates the chromosome replication cycle. *Proc Natl Acad Sci U S A* *98*, 11211-11217.
- Wignall, S.M., Deehan, R., Maresca, T.J., and Heald, R. (2003). The condensin complex is required for proper spindle assembly and chromosome segregation in *Xenopus* egg extracts. *J Cell Biol* *161*, 1041-1051.

- Wodarz, A., Hinz, U., Engelbert, M., and Knust, E. (1995). Expression of crumbs confers apical character on plasma membrane domains of ectodermal epithelia of *Drosophila*. *Cell* 82, 67-76.
- Xu, H., Beasley, M., Verschoor, S., Inselman, A., Handel, M.A., and McKay, M.J. (2004). A new role for the mitotic RAD21/SCC1 cohesin in meiotic chromosome cohesion and segregation in the mouse. *EMBO Rep* 5, 378-384.
- Xu, H., Beasley, M.D., Warren, W.D., van der Horst, G.T., and McKay, M.J. (2005). Absence of mouse REC8 cohesin promotes synapsis of sister chromatids in meiosis. *Dev Cell* 8, 949-961.
- Yamamoto, A., Guacci, V., and Koshland, D. (1996). Pds1p, an inhibitor of anaphase in budding yeast, plays a critical role in the APC and checkpoint pathway(s). *J Cell Biol* 133, 99-110.
- Yan R, Thomas SE, Tsai JH, Yamada Y, and McKee BD. (2010). SOLO: a meiotic protein required for centromere cohesion, coorientation, and SMC1 localization in *Drosophila melanogaster*. *J Cell Biol* 188, 335-49.
- Yeong, F.M., Hombauer, H., Wendt, K.S., Hirota, T., Mudrak, I., Mechtler, K., Loregger, T., Marchler-Bauer, A., Tanaka, K., Peters, J.M., *et al.* (2003). Identification of a subunit of a novel Kleisin-beta/SMC complex as a potential substrate of protein phosphatase 2A. *Curr Biol* 13, 2058-2064.
- Yong-Gonzalez, V., Wang, B.D., Butylin, P., Ouspenski, I., and Strunnikov, A. (2007). Condensin function at centromere chromatin facilitates proper kinetochore tension and ensures correct mitotic segregation of sister chromatids. *Genes Cells* 12, 1075-1090.
- Yoshimura, S.H., Hizume, K., Murakami, A., Sutani, T., Takeyasu, K., and Yanagida, M. (2002). Condensin architecture and interaction with DNA: regulatory non-SMC subunits bind to the head of SMC heterodimer. *Curr Biol* 12, 508-513.
- Yu, H.G., and Dawe, R.K. (2000). Functional redundancy in the maize meiotic kinetochore. *J Cell Biol* 151, 131-142.
- Yu, H.G., and Koshland, D. (2005). Chromosome morphogenesis: condensin-dependent cohesin removal during meiosis. *Cell* 123, 397-407.
- Yu, H.G., and Koshland, D.E. (2003). Meiotic condensin is required for proper chromosome compaction, SC assembly, and resolution of recombination-dependent chromosome linkages. *J Cell Biol* 163, 937-947.
- Zatsepina, O.V., Poliakov, V., and Chentsov Iu, S. (1983). [Electron microscopic study of the chromonema and chromomeres in mitotic and interphase chromosomes]. *Tsitologiya* 25, 123-129.
- Zhang, J., Shi, X., Li, Y., Kim, B.J., Jia, J., Huang, Z., Yang, T., Fu, X., Jung, S.Y., Wang, Y., *et al.* (2008a). Acetylation of Smc3 by Eco1 is required for S phase sister chromatid cohesion in both human and yeast. *Mol Cell* 31, 143-151.
- Zhang, N., Kuznetsov, S.G., Sharan, S.K., Li, K., Rao, P.H., and Pati, D. (2008b). A handcuff model for the cohesin complex. *J Cell Biol* 183, 1019-1031.

Zou, H., McGarry, T.J., Bernal, T., and Kirschner, M.W. (1999). Identification of a vertebrate sister-chromatid separation inhibitor involved in transformation and tumorigenesis. *Science* 285, 418-422.

Curriculum vitae

Sonal Nagarkar

8055, Cambridge street, Cambridge court

Houston-77054, Texas, USA

email : snagarka@bcm.edu

sonal.nagarkar@gmail.com

Phone: 001-8326133773

Personal Profile

Date of birth: 1st August 1979

Nationality: Indian

Marital status: Married

Academic Qualifications:

Masters of Science (M.Sc.) in Industrial Microbiology (July 2001 - July 2003), Devi Ahilya University, Indore, India (79.5%)

Dissertation title: “Analysis of role of Intraflagellar Transport (IFT) particles in *Drosophila melanogaster*”. (Done in the laboratory of Dr. Krishanu Ray at Dept of Biological Sciences, Tata Institute of Fundamental Research, Mumbai, India.)

Bachelor of Science (B.Sc.) in Micro-biology (July 1998 - July 2001), Devi Ahilya University, Indore, India (65%)

Higher Secondary (July 1996) from Madhya Pradesh Board, India with percentage 71%

High School (July 1994) from Madhya Pradesh Board, India with percentage 64%

Research Experience

Feb 2006 till June 2010: Ph.D. Thesis at Department of Genetics, University of Bayreuth, Germany.

Thesis title: “Chromosome dynamics during cell divisions in *Drosophila melanogaster*: The role of Rad21 in meiotic cohesion and dynamic analysis of the condensin subunit CapG in early embryonic mitotic divisions.”

May-Dec. 2005: Project work at Prof. E. Mandelkow's lab, Max-Planck-Unit for Structural Molecular Biology, Hamburg, Germany.

Project title: "Establishment of the Tet-off gene inducible adenoviral vector system for primary mouse neuronal cells."

July 2003 - May 2005: Worked as Junior Research Fellow in the laboratory of Dr. Krishanu Ray at Dept of Biological Sciences, Tata Institute of Fundamental Research, Mumbai, India.

Project title: "Analysis of molecular interaction between Kinesin II subunits of *Drosophila melanogaster*.",

Awards and scholarships:

- July 2003 – May 2005 Junior research fellowship by Department of Science and Technology (DST), Govt. of India.
- Qualified Graduate Aptitude Test in Engineering examination (GATE) -percentile 81.68 (2003)
- Qualified National Eligibility Test conducted by University Grants Commission, India for recruitment of Lecturers in Universities and colleges. (Dec 2002).